Psychological Review
2008, Vol. 115, No. 4, 913–954

0033-295X/08/$12.00 DOI: 10.1037/a0013123

Queuing Network Modeling of the Psychological Refractory Period (PRP)

Changxu Wu and Yili Liu
University of Michigan

The psychological refractory period (PRP) is a basic but important form of dual-task information processing. Existing serial or parallel processing models of PRP have successfully accounted for a variety of PRP phenomena; however, each also encounters at least 1 experimental counterexample to its predictions or modeling mechanisms. This article describes a queuing network-based mathematical model of PRP that is able to model various experimental findings in PRP with closed-form equations including all of the major counterexamples encountered by the existing models with fewer or equal numbers of free parameters. This modeling work also offers an alternative theoretical account for PRP and demonstrates the importance of the theoretical concepts of "queuing" and "hybrid cognitive networks" in understanding cognitive architecture and multitask performance.

Keywords: psychological refractory period (PRP), cognitive architecture, queuing network, multitask performance, serial and parallel processing

Performing multiple tasks at the same time is common in daily life; for example, drivers can steer a car and at the same time talk with friends in the car, and telephone operators can answer customer phone calls and type textual information into a computer. Among the wide range of multiple task situations, the psychological refractory period (PRP) is one of the most basic and simplest forms of a dual-task situation. In a PRP experiment, two reaction-time (RT) tasks are presented close together in time, and participants are asked to perform the two tasks as quickly as possible. Typically, participants' response to the second of the two RT tasks is performed more slowly than to the first when the interval between the presentation times of these two tasks is short. PRP has been studied in laboratories over 100 years, from the behavioral (Creamer, 1963; Kantowitz, 1974; Oberauer & Kliegl, 2004; Pashler, 1984, 1994b; Schumacher et al., 1999; Solomons & Stein, 1896; Welch, 1898; Welford, 1952) to the neurological level (Jiang, Saxe, & Kanwisher, 2004; Sommer, Leuthold, & Schubert, 2001). It is also the subject of extensive theoretical work and the focal point of an important theoretical controversy between several computational models of cognition. There are several important cognitive models of PRP, including the response-selection bottleneck (RSB) or central bottleneck model proposed by Pashler (1984, 1990, 1994a, 1994b, 1994c), the executive-process interactive control (EPIC) model proposed by Meyer and Kieras (1997a, 1997b), and the model based on the ACT-R/perceptual-motor system (ACT-R/PM) proposed by Byrne and Anderson (2001). Each of these models is able to account for some of the important aspects of PRP; however, each appears to encounter at least one experimental counterexample to its predictions (Jiang et al., 2004; Meyer & Kieras, 1997a, 1997b; Oberauer & Kliegl, 2004; Ruthruff, Pashler, & Klaassen, 2001). Therefore, the questions remain about how to model these experimental results, provide a unified account of the discoveries in behavioral and neuroscience studies, and gain further insights into the mechanisms of dual-task performance.

This article takes further steps toward addressing these important questions with a queuing network-based computational cognitive architecture (Liu, 1996, 1997; Liu, Feyen, & Tsimhoni, 2006; Wu & Liu, 2007a, 2007b, 2008; Wu, Liu, & Walsh, in press; Wu, Tsimhoni, & Liu, in press). First, we introduce the major experimental results in PRP studies and the major PRP effects. Second, the major existing models of PRP are described, including their advantages and their counterexamples. Third, we describe the queuing network model, including its major assumptions and components. In the fourth section, we describe how the queuing network model mathematically accounts for and theoretically explains the PRP phenomena. Finally, we discuss the implications of the model, as well as its extension in future research.

EXPERIMENTAL STUDIES IN PRP

In the following section, we introduce the major findings in experimental studies of PRP, including the basic PRP experiment paradigm and the major PRP effects that have been the subject of theoretical controversy—the subadditive difficulty effect, the response grouping effect, the practice effect, and brain imaging patterns in PRP.

Basic PRP Experiment Paradigm

The basic PRP experiment paradigm requires the participants to perform two tasks called Task 1 (T1) and Task 2 (T2) concur-

Changxu Wu and Yili Liu, Department of Industrial and Operations Engineering, University of Michigan.

Changxu Wu is now at the Department of Industrial and Systems Engineering, State University of New York at Buffalo.

We appreciate the support from the National Science Foundation (NSF) for this work (NSF Grant 0308000).

Correspondence concerning this article should be addressed to Changxu Wu, State University of New York (SUNY)—Buffalo, 414 Bell Hall, Buffalo, NY 14260-2050, or to Yili Liu, Department of Industrial and Operations Engineering, University of Michigan, 1205 Beal Avenue, Ann Arbor, MI 48109. E-mail: changxu@buffalo.edu or yililiu@umich.edu

rently. The delay between the presentation of the stimuli of T1 and T2 is called the stimulus onset asynchrony (SOA). Two stimuli (S1 and S2) are presented to the participants in rapid succession, and each requires a quick response (R1 and R2). RT of each task (RT1 and RT2) is measured from the time when the stimulus is presented to the time when the corresponding response is made. In the basic PRP paradigm in which the tasks are choice RT tasks and participants do not receive extensive practice on the dual task, responses to S1 typically are unimpaired, but responses to S2 are slowed by 200–300 ms or more in the short SOA conditions. For instance, Figure 1 shows the experimental results of the basic PRP paradigm in Schumacher et al. (1999).

Schumacher et al.'s (1999) study consisted of a series of PRP experiments, of which their Experiments 3 and 4 are described here for illustration and modeling purposes. T1 was an auditory–manual task in Experiment 3 but an auditory–vocal task in Experiment 4. Participants heard either a low- or a high-pitched tone and responded by pressing the left middle or the left index finger on a keypad, respectively (Experiment 3), or making a corresponding vocal response (Experiment 4). T2 was always a visual–manual task involving compatible or incompatible situations. In each trial of T2, an *O* replaced one of four dashes in a horizontal row centered on the display monitor. In the compatible situation of T2, participants pressed the right-hand index, middle, ring, or little finger keys when the *O* appeared in the far left, middle left, middle right, or far right spatial positions, respectively. In the incompatible situation of T2, participants pressed the right-hand index, middle, ring, or little finger keys when the *O* appeared in the middle left, far right, far left, or middle right positions, respectively. The stimuli for T1 and T2 were separated by one of five SOAs: 50, 150, 250, 500, or 1,000 ms. The compatible situation of T2 in Experiment 4 is an example of the basic PRP experimental paradigm, whose results are shown in Figure 1: RT1 was not affected by T2, but RT2 was longer in the short SOA conditions than in the long SOA conditions. Similar experimental results can be found in many other PRP studies (e.g., Karlin & Kestenbaum, 1968). The importance of the other experimental conditions of Schumacher et al.'s study is described below.

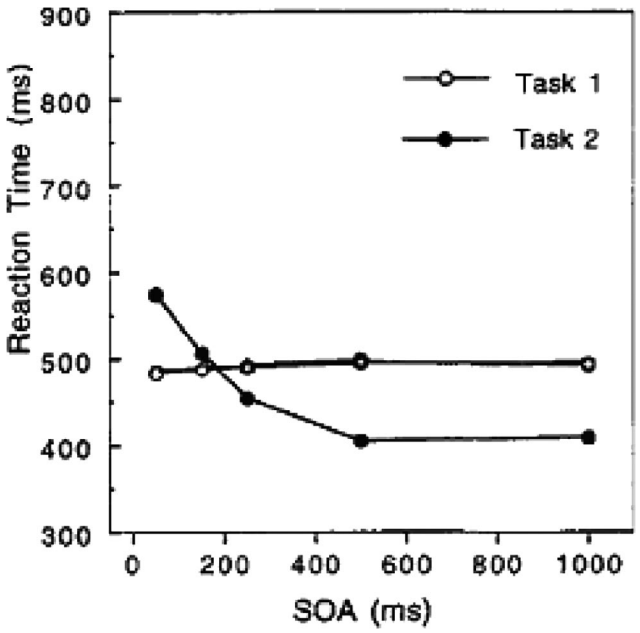

Figure 1. Typical experimental results in the basic psychological refractory period experiment paradigm. Adapted from "Concurrent Response-Selection Processes in Dual-Task Performance: Evidence for Adaptive Executive Control of Task Scheduling," by E. H. Schumacher et al., 1999, *Journal of Experimental Psychology: Human Perception and Performance, 25,* p. 809. Copyright 1999 by the American Psychological Association. SOA = stimulus onset asynchrony.

Subadditive Difficulty Effect

Several PRP experiments (Hawkins, Rodriguez, & Reicher, 1979; Karlin & Kestenbaum, 1968; Schumacher et al., 1999; Sommer et al., 2001) have found that if the difficulty level of T2 at its central processing stage (i.e., at the response-selection stage occurring after the perceptual stage and before the motor stage) is manipulated, the difference of RT2 between the easy and the hard T2s in the short SOA conditions is smaller than that in the long SOA conditions. This pattern or effect is called the subadditive difficulty effect.

Schumacher et al.'s (1999) Study

The subadditive difficulty effect appeared in Experiments 3 and 4 of Schumacher et al.'s (1999) study described above, in which the level of difficulty of T2 was manipulated via the degree of stimulus–response compatibility in T2. In both experiments, Schumacher et al. found a subadditive interaction between the SOA and the response-selection difficulty on the mean RTs of T2, showing the subadditive difficulty effect.

Hawkins, Rodriguez, and Reicher's (1979) Study

The subadditive difficulty effect can also be found in the experimental results of Hawkins et al.'s (1979) study, in which the difficulty level of T2 was manipulated by changing the number of stimuli in a category for making the same response. In the easy T2 condition, the stimuli were the digits *2* and *3,* and the responses were keypresses with the right-hand index and middle fingers, respectively. In the hard T2 condition, the stimuli were the digits *2–9*—four of them (*2, 5, 6,* and *9*) belonged to the first category, the other four digits belonged to the second category, and the participants were asked to press with the right-hand index or middle finger after they saw one of the four digits in the first or the second category.

Karlin and Kestenbaum's (1968) Study

Karlin and Kestenbaum (1968) found the subadditive difficulty effect by manipulating the difficulty level of T2 via changing the number of stimulus–response pairs—one was a simple reaction task, and the other was a two-choice reaction task. In their experiment, T1 was a visual–manual task: Participants were asked to respond to the digits (*1–5*) on a visual display by pressing their left-hand fingers corresponding to the digits. T2 was an auditory–manual task where participants used their right-hand index and middle fingers to respond to high- and low-pitched tones, respectively. Their experimental results clearly demonstrated the pattern of the subadditive difficulty effect: The difference of RT2 between the easy and the hard T2s in the short SOA condition is smaller than that in the long SOA conditions (see Figure 2).

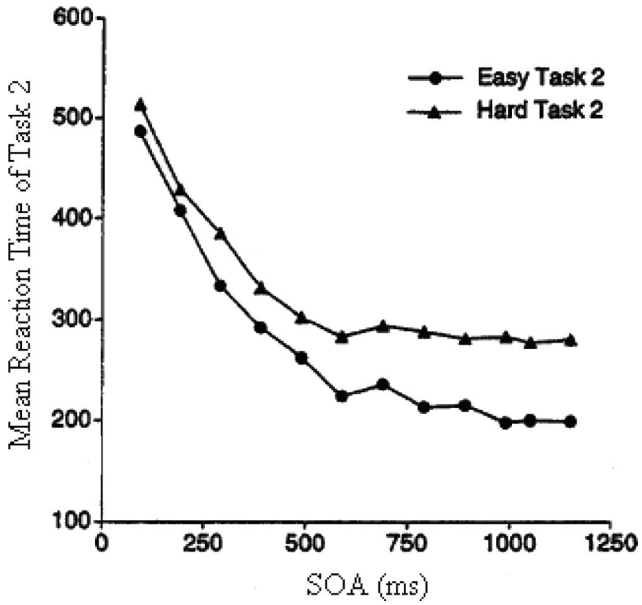

Figure 2. Experimental results showing the subadditive difficulty effect. Adapted from "Effects of Number of Alternatives on the Psychological Refractory Period," by L. Karlin and R. Kestenbaum, 1968, *Quarterly Journal of Experimental Psychology, 20,* p. 175. Copyright 1968 by Taylor & Francis Ltd. (Web site: http://www.informaworld.com). Adapted with permission. SOA = stimulus onset asynchrony.

Sommer et al.'s (2001) Study

Sommer et al. (2001) replicated Karlin and Kestenbaum's (1968) experiment and used one of the electrophysiological measurements—the event-related potential (ERP) techniques—to measure stimulus-lateralized readiness potential (S-LRP), which is a measure of response preparation or activation at the cerebral motor cortex, including the premotor cortex (Sommer et al., 2001; Wildgruber, Ackermann, & Grodd, 2001). They not only found the subadditive difficulty results in RT but also found that when T2 was a simple reaction task, there was an early onset of S-LRP before S2 was presented (its onset time was 15 ms before S2 was presented), which meant that the motor component of the cognitive system started to prepare the processing of S2 before it was presented. Moreover, their results showed that the percentage of negative RT2s (RT2 $<$ 0 ms) increased with an increase in the SOA, which was consistent with the results of another study (Van Selst & Jolicoeur, 1997) that showed the same pattern of result.

Brain Imaging Patterns (Jiang et al., 2004)

Jiang et al. (2004) conducted the first functional magnetic resonance imaging (fMRI) study that followed the experimental paradigm of PRP and tested a large number of participants in an effort to find neural correlates of the basic PRP with fMRI techniques. They did not find any increase in activation in the brain regions corresponding to executive control in the short SOA conditions compared with the long SOA conditions. In their experiment, both T1 and T2 were visual–manual two-choice reaction tasks. In T1, squares or circles were presented on a display, and participants pressed with the left hand *1* for a square and *2* for a circle. T2 involved two groups of participants. Participants responded to a letter *A* or *B* (for the first group) or to a red or green cross (for the second group) by pressing the number *3* or *4* on a keypad, respectively. Jiang et al. measured the activation of all of the brain areas related to the possible executive control, including the dorsal lateral prefrontal cortex (DLPFC), the anterior cingulate cortex (ACC), the inferior frontal gyrus (GFi), the anterior-dorsal prefrontal cortex (ADPFC), the superior parietal lobule, and the middle frontal gyrus (GFm). However, they found virtually no increase in activation in these brain regions in the short SOA conditions compared with the long SOA conditions.

Response Grouping Effect (Ruthruff, Pashler, & Klaassen 2001)

Ruthruff, Pashler, and Klaassen (2001) designed a new PRP experiment paradigm in which the stimuli of T1 and T2 were presented at the same time (SOA = 0) with equal emphasis and the participants were asked to emit both responses at the same time (i.e., grouping the responses; the corresponding finding is called the response grouping effect in this article). They found that RT1 and RT2 in the dual-task situations were significantly longer than those in the single-task situations. In their experiment, one of the two tasks was a tone-counting task—participants were asked to count the number of tones (one or two). In the easy version, the participants vocally reported this number aloud; in the hard version, they vocalized the opposite number aloud (i.e., they reported "two" if they heard one tone and "one" if they heard two tones). The other task was a spatial working memory task—participants responded whether upside-down letter stimuli were normal or mirror images by pressing the *J* and *K* keys, respectively. In the single-task blocks, either a tone or a letter appeared (chosen at random). In the dual-task blocks, the tone and the letter always appeared simultaneously. The participants were instructed to emit both responses at the same time. To test the cost of response grouping, Ruthruff et al. also conducted several control experiments in which they found that the cost of response grouping was only 21 ms.[1] The participants in Ruthruff et al.'s experiment received relatively extensive practice in both the single- and dual-task situations (two blocks of single-task practice and two blocks of dual-task practice, each block including 20 warm-up trials and 80 practice trails).

Practice Effect on PRP (Oberauer & Kliegl, 2004)

In Oberauer and Kliegl's (2004) experimental study, one experimental task was a spatial working memory task. Spatial operations were indicated by red arrows with a length of 2.5 cm, displayed in the central cell of a 5 $\times$ 5 grid and pointing in one of eight possible directions horizontally, vertically, or diagonally. Participants were asked to mentally shift a dot from its current location (Cell 1) to another location (Cell 2) in the indicated direction. Another task

[1] To provide a more precise estimate, Ruthruff, Pashler, and Klaassen (2001) ran a control experiment (N = 6) in which they manipulated whether or not the participants grouped responses. The tone always preceded the letter by 1.5 s, effectively eliminating central interference. RT in the grouped response condition was only 21 ms longer than that in the nongrouped condition.

was a numerical operations task in which a given digit from *1* to *9* was presented at the center of the grid. The task was indicated by tones with a 50-ms duration—a high-pitched tone (800 Hz) requiring an addition of two and a low-pitched tone (200 Hz) requiring a subtraction of one from the current value of the digit. In each trial, after the participants completed seven to nine spatial and/or numerical operations, they were asked to hit the space bar, and the stimuli of the next operation (or pair of operations) were displayed immediately. At the end of the trials, the participants were asked about the final digit value and the final spatial position in a random order.

Participants were divided into two practice groups—a single-task and a dual-task practice group. In the single-task practice group, participants practiced only one task at a time, and the two stimuli of the two tasks were never presented at the same time. In the dual-task practice group, the two stimuli of the two tasks were always presented at the same time (SOA = 0). Participants in the single-task and the dual-task groups went through the same number of trials and operations for T1 and T2. Each group received a pretest and a posttest of their performance before and after extensive practice (12 sessions). There were two conditions in each test—a sequential and a simultaneous condition. In the sequential condition, the test started with a complete sequence of operations of one kind (either spatial or numerical, selected at random from trial to trial), followed by the same number of successive operations of the other kind. The maximum RT of the numerical and the spatial tasks was regarded as the RT of the two tasks in this sequential condition. In the simultaneous condition, one numerical operation and one spatial operation were displayed at the same time. RT in the two tasks was the duration between the time when the stimuli of the two tasks appeared on the display and the time when the space bar was hit in each operation. After extensive practice, the PRP effect in the dual-task practice group was much smaller than that in the single-task practice group.

Summary of Experimental Results

As a basic form of multitasking, PRP has received extensive attention in experimental psychology because of the vital role it plays in understanding multitasking performance and related cognitive mechanisms. To explore the processing mechanisms underlying the various PRP effects summarized above, one may ask how well these PRP effects can be accounted for by existing cognitive models. After reviewing all of these major PRP effects, we now turn to a review of existing models of PRP, including their assumptions.

EXISTING MODELS OF PRP

Over the past decades, several computational models have been developed to model the experimental results in PRP, including the RSB model or central bottleneck model (Pashler, 1984, 1990, 1994a, 1994b, 1994c), the EPIC-strategic response deferment (EPIC-SRD) model (Meyer & Kieras, 1997a, 1997b), and the PRP model based on the ACT-R/PM system (Byrne & Anderson, 2001). Among these representative models, RSB and ACT-R/PM assume serial processing at the cognitive stage, while EPIC-SRD assumes that cognitive processing is parallel. Each of these models has successfully accounted for a number of experimental studies reviewed above; however, it appears that each of them also encounters at least one experimental study as a counterexample to their predictions or modeling mechanisms (see Table 1).

Response-Selection Bottleneck Model

The RSB model was developed by Pashler (1984, 1990, 1994a, 1994b, 1994c). The basic assumption of the RSB model is that multiple stimuli may be identified simultaneously and stored in short-term memory but that the process of response selection (i.e., converting symbolic stimulus codes to symbolic response codes, also called the central process, cognitive process, or central stage) is able to accommodate only one task at a time.

Overall, the RSB model is a very parsimonious model, and its serial processing assumption at the central stage of cognition is able to explain the experimental result of the basic PRP paradigm (Pashler, 1984a, 1984b, 1989, 1990, 1994a, 1994b, 1994c; Pashler, Johnston, & Ruthruff, 2001; Pashler et al., 1994). According to the RSB model, when the interval between the times when the two tasks reach the central cognition stage is very short, T1 is processed first without affecting its RT, and T2 has to wait for the completion of T1 in the cognition stage. As this time interval increases, the chance that T2 has to wait for the completion of T1 at the cognition stage decreases, producing the basic PRP effect

Table 1
Coverage of PRP Experimental Studies and Effects by the Existing Models

	Coverage of existing cognitive models		
	Serial cognitive process		Parallel cognitive process
Experimental results	RSB	ACT-R/PM	EPIC-SRD
Basic PRP	Math	Simulation	Math[a]
Subadditive difficulty effect			
Schumacher et al. (1999)	CR	Simulation	—
Hawkins et al. (1979)	CR	—	Simulation
Karlin & Kestenbaum (1968)	CR	—	Simulation[b]
Sommer et al. (2001)	—	—	CR
Brain imaging pattern			
Jiang et al. (2004)	—	—	CR
Response grouping effect			
Ruthruff, Pashler, & Klaassen (2001)	—	—	CR
Practice effect on PRP			
Oberauer & Kliegl (2004)	CR	CR	—

Note. Math: experimental results are modeled with closed-form mathematical equations, which are regarded as a more rigorous form of reasoning than simulation. Simulation: experimental results are modeled with simulation. CR: experimental results are contradictory to the prediction or basic assumptions of the model. Dash indicates that the experimental results are not modeled. PRP = psychological refractory period; RSB = response-selection bottleneck; ACT-R/PM = ACT-R/perceptual-motor; EPIC-SRD = executive-process interactive control-strategic response deferment. [a]Based on a strategic scheduling mechanism that appears to be contradictory to the related fMRI findings (Jiang et al., 2004). [b]Based on a post-RSB mechanism that appears to be contradictory to the related findings in the event-related potential study of Sommer et al. (2001).

(i.e., RT1 remains as a constant, while RT2 decreases as the SOA increases from 0 and then becomes a constant in the long SOA conditions).

However, two major PRP effects appear to be contradictory to the predictions or assumptions of the RSB model.

First, the subadditive difficulty effect reviewed in the earlier section indicates that if we manipulate the difficulty level of T2 at its central processing stage, the difference of RT2 between the easy and the hard T2s under the short SOA conditions is smaller than that under the long SOA conditions. However, according to the prediction of the RSB model, if the duration of the cognitive process of T2 increases, the difference between the easy and hard T2s under the short SOA conditions should be the same as that under the long SOA conditions (see the detailed description in Byrne & Anderson, 1998).

Second, the practice effect of PRP reported in Oberauer and Kliegl (2004) demonstrates that the dual-task practice group produces smaller PRP effect than the single-task practice group. In Oberauer and Kliegl's study, the dual- and single-task practice groups went through the same number of trials for T1 and T2. Since the PRP effect in the RSB model equals $1A + 1B - 2A - SOA$ (Pashler & Johnston, 1989)[2] and the improvement of each single processing stage (1A, 1B, and 2A) is solely determined by the amount of practice of each task (there should be no interaction between any of the terms), each of these terms (1A, 1B, and 2A) decreases with the same magnitude in both the dual- and single-task practice groups. Therefore, on the basis of this prediction of the RSB model, there is no difference in the PRP effect between the dual- and the single-task practice groups after extensive practice. However, Oberauer and Kliegl's study found that the PRP effect in the dual-task practice group was around only 59 ms, which was much smaller than the PRP effect in the single-task practice group (409 ms). The RSB model might have difficulty explaining this relatively large difference (350 ms) in the mean PRP effect between these two groups.

ACT-R/PM was developed by Byrne and Anderson (2001) on the basis of the original structure of ACT-R (Anderson & Lebiere, 1998) and the perceptual and motor part of EPIC. At the central processing stage, ACT-R/PM assumes that cognition is serial. To support this assumption, Byrne and Anderson (2001) conducted a series of experiments that provided evidence that people cannot perform two complex cognitive tasks at the same time. Because the motor part of ACT-R/PM is adapted from EPIC, which assumes serial processing at each motor module, a second serial processing or bottleneck in ACT-R/PM is located at its motor module (movement feature preparation; Byrne & Anderson, 1998).

As one of the major cognitive architectures with applications in various basic and real-world task settings, ACT-P/PM offers an accurate quantification of the basic PRP paradigm and the subadditive difficulty effect in PRP. First, ACT-R/PM simulates the result of the basic PRP paradigm in Karlin and Kestenbaum's (1968) experiment with the bottleneck at the motor module (Byrne & Anderson, 1998). In this simulation, ACT-R/PM acts as the RSB model but with a structural bottleneck in the motor module (motor feature preparation), producing the experimental results in the basic PRP paradigm. Furthermore, the multiple-bottleneck assumption enables ACT-R/PM to model the subadditive difficulty effect in Experiment 3 of Schumacher et al.'s (1999) study with the same multiple-bottleneck mechanism originally proposed by Dejong (1993). ACT-R/PM simulates the subadditive difficultly effect found in Experiment 4 of Schumacher et al.'s study with a scheduling strategy similar to that used in EPIC-SRD (Meyer & Kieras, 1997a, 1997b).[3]

In Oberauer and Kliegl's (2004) study, within each trial, participants went through a sequence of seven to nine dual-task operations (the stimuli of the dual tasks were presented in the visual and auditory modalities, respectively); however, participants were asked to make one manual response at the end of each trial by hitting the space bar. Therefore, this experiment eliminates the second bottleneck in ACT-R in the motor module, which suggests that ACT-R works in a single bottleneck format like the RSB model in this case. As we described in our discussion of the RSB model's limitation, ACT-R may also have difficulty in accounting for Oberauer and Kliegl's results (a relatively large difference [350 ms] in the mean PRP effect between the single-practice and the dual-practice groups).

EPIC-SRD

In contrast to the RSB model, EPIC does not assume a hardware bottleneck in the cognitive process and regards the observed bottleneck in PRP as the result of strategic or voluntary control in the cognitive process as well as serial processing in peripheral motor output processes (i.e., each motor processor processes information in a serial manner; Meyer & Kieras, 1997a, 1997b, 1999). With this architecture, Meyer and Kieras (1997a, 1997b) developed the strategic response deferment (SRD) model (called executive control) to model the PRP phenomena—the executive control in EPIC needs to monitor the progress of both T1 and T2, using scheduling strategies to lock and unlock T1 and T2 in certain processing stages to produce the PRP effects. The strategic scheduling methods of the EPIC-SRD model provide great flexibility and allow the model to simulate several major effects in PRP, for example, the basic PRP and the subadditive difficulty effect as introduced in the previous section. Moreover, EPIC itself is a comprehensive architecture that unifies many findings in psychological studies, and it has been employed to model dual-task performance in both theoretical (Meyer & Kieras, 1997a, 1997b) and applied research (Kieras & Meyer, 1997).

In comparing the EPIC-SRD's basic assumption with the major effects reviewed in the introductory section, it appears that EPIC-SRD also encounters several counterexamples found in the existing experimental studies.

First, the response grouping effect reviewed above (Ruthruff, Pashler, & Klaassen, 2001) might contradict EPIC's prediction. Ruthruff, Pashler, and Klaassen (2001) eliminated the potential strategic postponement bottleneck by emphasizing the two tasks

[2] 1A indicates processing time of T1 at the perceptual stage; 1B is the processing time of T1 at the cognitive stage; 2A indicates the processing time of T2 at the perceptual stage.

[3] ACT-R/PM uses an objective and systematic method to set the values of free parameters: Free parameters are adjusted in the long SOA conditions to fit the simulation results with the experimental results, and then, without changing their values, these parameters are used in the model in the short SOA conditions to generate the simulation results. Therefore, in this parameter-setting method, no free parameter is used to fit the experiment results of the short SOA conditions.

equally, using a 0-ms SOA, and urging participants to emit both responses at the same time. They also eliminated potential perceptual bottleneck by using different perceptual modalities. If there is no strategic bottleneck at the central processing stage, then according to the assumption of EPIC, the central processor should be able to process the information of the two tasks at the same time; furthermore, since there is no other noncentral interference (interferences in perceptual or motor process), dual-task performance should be similar to single-task performance. However, they still found that RT1 and RT2 in the dual-task condition were significantly longer than in the single-task situations. This experimental result appears to be contradictory to the prediction of EPIC in central processing.

Second, according to the assumptions of EPIC, dual-task interference arises when the SOA becomes shorter, since participants need to monitor the progress of T1, halt T2, resume T1, and so on. Therefore, the brain areas corresponding to the central executive should increase their activation level in the short SOA conditions compared with the long SOA conditions. However, the fMRI study of Jiang et al. (2004) found virtually no increase in these brain regions in the short SOA conditions compared with the long SOA conditions. "These data suggest that passive queueing, rather than active monitoring, occurs during the PRP" (Jiang et al., 2004, p. 390).

Third, Sommer et al. (2001) replicated Karlin and Kestenbaum's (1968) experiment with ERP techniques and measured the RT, percentage of negative RT2s, and lateralized readiness potential (LRP). Ample research in ERP studies found that the onset time of LRP reflects the starting stage of motor preparation in the cognitive system (Leuthold & Jentzsch, 2001; Ulrich, Leuthold, & Sommer, 1998). When T2 was a simple RT (SRT) task, Sommer et al. found two phenomena: First, the average onset time of LRP occurred before S2 was presented, which indicated that the cognitive system started to prepare the processing of S2 before it was presented. Second, the percentage of negative RT2s (RT2 $<$ 0 ms) increased as the SOA increased. However, according to the EPIC-SRD model, S2 is processed by the model after it is presented (Meyer & Kieras, 1997b, p. 756: "When Task 2 involves just one S–R pair (i.e., it is a simple-reaction task), detection of the auditory stimulus triggers the SRD model's Task 2 production rules"), so the onset time of LRP in this simple reaction condition should be after the arrival of S2, and RT2 at the behavioral level should be positive. On the basis of these two contradictions, Sommer et al. believed that their experimental results might reject the modeling mechanism of EPIC-SRD (a post-RSB) in generating the RT of Karlin and Kestenbaum's experiment with some confidence (Sommer et al., 2001, p. 87).

In summary, each existing PRP model encounters at least one experimental study that can be regarded as a counterexample to its predictions. Moreover, closed-form equations are regarded as a more rigorous form of reasoning and modeling than simulation, and most PRP experimental findings summarized in Table 1 have not been modeled by closed-form mathematical models yet. In the following, we describe our queuing network-based architecture and how it is used to develop closed-form mathematical equations to quantify various PRP phenomena summarized in Table 1.

QUEUING NETWORK ARCHITECTURE

To model human performance and electrophysiological activities of the brain, the current modeling approach represents the human cognition system as a queuing network-based on several similarities between them. First, ample research evidence has shown that major brain areas with certain information-processing functions are localized and connected with each other in the brain cortex via neural pathways (Bear, Connors, & Paradiso, 2001; Faw, 2003; Kaufer & Lewis, 1999; Roland, 1993; Smith & Jonides, 1998; Zysset, Muller, Lehmann, Thone-Otto, & von Cramon, 2001), which is highly similar to a queuing network of servers (information-processing units) that can process entities (to-be-processed pieces of information) traveling through the routes serially or/and in parallel depending on specific network arrangements. Therefore, brain regions with similar functions can be represented as servers and neural pathways connecting them as routes in the queuing network. Second, for different tasks and learning stages, the to-be-processed information sometimes is processed by the related brain regions (servers) immediately; sometimes, information has to be maintained in certain regions, to wait while some other information is being processed (Braus, 2004; Bullock, 1968; Chklovskii, Mel, & Svoboda, 2004; Eagleman, Jacobson, & Sejnowski, 2004; Habib, 2003; Rieke, Warland, van Steveninck, & Bialek, 1997; Smith & Jonides, 1998; Taylor et al., 2000). Hence, these to-be-processed pieces of information are represented as entities in the queuing network, and entities are processed in the network through certain queuing processes, which represent the waiting and servicing processes of the information entities.

The servers in the queuing network model are defined as the information-processing units in the brain, which includes both the related brain regions and the connections among them. Servers are not passive storage for information but active processing units that perform their functions in the psychological process of transforming stimulus into response.

There are several similarities between the queuing network model and the brain itself. First, both are structures that are composed of multiple servers (in the model) or modules (in the brain). Second, in both structures, servers or modules are connected to, rather than isolated from, each other, and behavior emerges from the coordinated activities of the connected servers/modules. Third, both queuing network servers and brain modules take a certain amount of time to perform their respective information-processing functions. Fourth, both structures contain a processing aspect and a waiting (or queuing) aspect (information being maintained in the brain for processing), which correspond to the situations when information is being processed and when it is waiting for a processing unit to be available.

The difference between the queuing network model and the brain comes from the fact that the model is an abstraction or representation of the brain rather than the brain itself. The brain is composed of billions of neurons, which form an extremely complex network. There are different ways to represent the brain, at different levels of granularity. For example, neural network models represent and analyze the brain at the level of neurons, while the RSB model represents the brain activities as three stages (perception, cognition, and motor stages). This three-stage architecture is also assumed in a human performance model called the

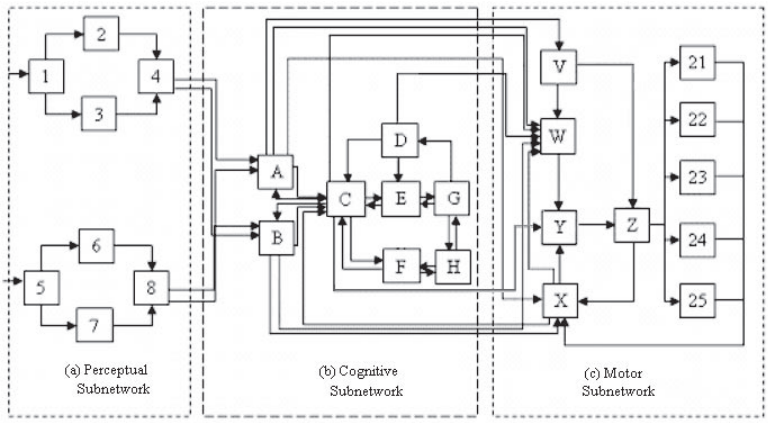

Perceptual Subnetwork	Cognitive Subnetwork	Motor Subnetwork
1. Common visual processing	A. Visuospatial sketchpad	V. Sensorimotor integration
2. Visual recognition	B. Phonological loop	W. Motor program retrieval
3. Visual location	C. Central executive	X. Feedback information collection
4. Visual recognition and location integration	D. Long-term procedural memory	Y. Motor program assembling and error detecting
5. Common auditory processing	E. Performance monitor	Z. Sending information to body parts
6. Auditory recognition	F. Complex cognitive function	21-25: Body parts: eye, mouth, left hand, right hand, foot
7. Auditory location	G. Goal initiation	
8. Auditory recognition and location integration	H. Long-term declarative & spatial memory	

Figure 3. The general structure of the queuing network-model human processor (further developed from Liu, Feyen, & Tsimhoni, 2006; Wu & Liu, 2007a).

model human processor (MHP), which is widely adopted in the field of human–computer interaction (Card, Moran, & Newell, 1983). The queuing network model divides each stage into a subnetwork of a small number of servers and thus has a level of granularity that falls between the neural network and the RSB and MHP models.

In modeling human performance, mathematical models based on queuing networks have successfully integrated a large number of mathematical models in response time (Liu, 1996) and in multitask performance (Liu, 1997) as special cases of queuing networks. A computational cognitive architecture called the queuing network-MHP (QN-MHP; see Figures 3 and 4) has been developed as an integration of queuing networks and MHP for both mathematical modeling and real-time generation of psychological behavior (Liu et al., 2006). QN-MHP has been successfully used to generate human performance and mental workload in real time, including driver performance (Liu et al., 2006) and driver workload (Wu & Liu, 2007a, 2007b; Wu, Tsimhoni, & Liu, in press), transcription typing (Wu & Liu, 2008), and visual–manual tracking performance and mental workload measured by ERP techniques (Wu & Liu, 2008).

QN-MHP consists of three subnetworks: perceptual, cognitive, and motor subnetworks, as described in the following sections.

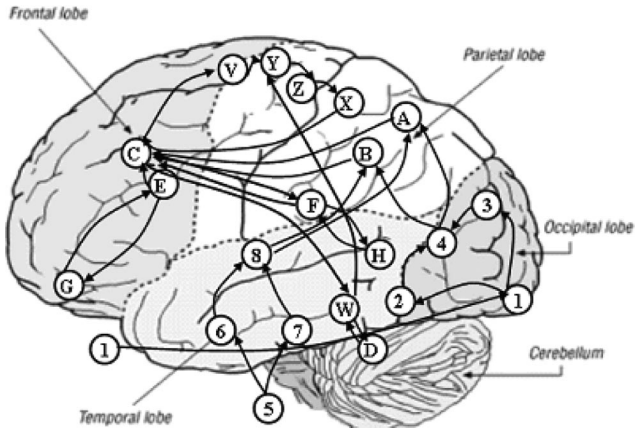

Figure 4. Approximate mapping of servers in the queuing network model onto human brain (Wu & Liu, 2007a). Letters and numbers in illustration correspond to the key in Figure 3.

Perceptual Subnetwork

The perceptual subnetwork includes a visual and an auditory perceptual subnetwork, each of which is composed of four servers. In the visual perceptual subnetwork, visual entities enter the network at Server 1, representing the eye, the lateral geniculate nucleus, the superior colliculus, the primary visual cortex, and the secondary visual cortex (Bear et al., 2001). Then, these entities are transmitted in parallel visual pathways—the parvocellular stream (represented by Server 2) and the magnocellular stream (Server 3)—where the object content features (e.g., color, shape, labeling, etc.) and location features (e.g., spatial coordinates, speed, etc.) are processed (Bear, et al., 2001; Smith & Jonides, 1998; Ungerleider & Haxby, 1994). The distributed parallel area (represented by Server 4)—including the neuron connections between V3 and V4 as well as V4 and V5, the superior frontal sulcus, and the GFi—integrate the information of these features from the two visual pathways and generate integrated perception of the objects (Bear et al., 2001). These brain regions also serve as the visual sensory memory storage for the visual information (Bear et al., 2001;

Simon et al., 2002). On the basis of the mechanism of working memory of Baddeley (1992) and the functions of these brain regions (Ohbayashi, Ohki, & Miyashita, 2003; Smith & Jonides, 1998), the majority of the graphical visual information is transmitted to the left and right hemisphere posterior parietal cortex (Server B and Server A, respectively; Bear et al., 2001; Smith & Jonides, 1998).

The auditory perceptual subnetwork also contains four servers: The middle and inner ear (represented by Server 5) transmit auditory information to the parallel auditory pathways, including the neuron pathway from the ventral cochlear nucleus to the superior olivary complex (represented by Server 7) and the neuron pathway from the dorsal and ventral cochlear nuclei to the inferior colliculus (Server 6), where location, pattern, and other aspects of the sound are processed (Bear et al., 2001). The auditory information in the auditory pathways is integrated at the primary auditory cortex and the planum temporale (represented by Server 8; Mustovic et al., 2003). These brain regions also serve as the auditory sensory memory storage place for the auditory information (Mustovic et al., 2003). On the basis of the mechanism of working memory of Baddeley (1992) and functions of multimodal areas (neuron pathways between the primary auditory cortex and the posterior parietal cortex and the angular and supramarginal gyri), the auditory information is transmitted to the left-hemisphere posterior parietal cortex (Server B) as well as the right-hemisphere posterior parietal cortex (Server A; Faw, 2003).

Cognitive Subnetwork

The cognitive subnetwork includes a working memory system, a goal execution system, a long-term memory system, and a complex cognitive processing system. An important feature of QN-MHP, compared with EPIC and ACT-R, is its hybrid structure of the cognitive subnetwork, and it includes both serial processing at Server F and parallel processing in the other servers in the cognitive subnetwork.

Following Baddeley's (1992) working memory model, QN-MHP contains four components in the working memory system: a visuospatial sketchpad (Server A), representing the right-hemisphere posterior parietal cortex; a phonological loop (Server B), standing for the left-hemisphere posterior parietal cortex; a central executor (Server C), representing the DLPFCs, the ADPFCs, the right ventral frontal cortex, and the GFm; and a performance monitor (Server E), standing for the ACC. The visuospatial sketchpad and the phonological loop store and maintain visuospatial and phonological information in working memory (Smith & Jonides, 1998). The brain regions represented by Server C play a crucial role in suppressing automatic responses (Burle, Vidal, Tandonnet, & Hasbroucq, 2004; Koski & Paus, 2000; Smith & Jonides, 1998) and categorization information (Grossman et al., 2002; Shafritz, Kartheiser, & Belger, 2005; Vartanian & Goel, 2005). In the model, it is assumed that suppressing an automatic response takes one additional cycle (18 ms; Liu et al., 2006) at Server C; the number of cycles to search for a target stimulus is proportional to the size of a search category, that is, if one category is composed of n stimuli, it takes n cycles to search one stimulus in that category. The ACC (Server E) is responsible for performance monitoring and error detection (Smith & Jonides, 1998).

The goal execution system (Server G) represents the orbitofrontal region and the amygdala complex, which are typically involved in goal initiation and motivation (Rolls, 2000).

The long-term memory system represents two types of long-term memory in the human brain: (a) declarative (facts and events) and spatial memory (Server H), standing for the medial temporal lobe, including the hippocampus and the diencephalons (these brain areas store various kinds of production rules in choice reaction, long-term spatial information, perceptual judgment, decision making, and problem solving), and (b) nondeclarative memory (procedural memory and motor program; Server D), representing the striatal and the cerebellar systems, which store all of the steps in task procedure and motor programs related to motor execution (Bear et al., 2001).

On the basis of Byrne and Anderson's (2001) experimental finding that humans cannot perform two arithmetic operations at once, the complex cognitive processing system (Server F) is assumed to perform complex cognitive functions in a serial manner. Such functions include multiple-choice decision, phonological judgment, anticipation of stimuli in simple reaction tasks, spatial working memory operations, visuomotor choices, and mental calculation (excluding the functions of Server C, e.g., information categorization and suppression of automatic responses). Correspondingly, Server F represents brain areas responsible for these functions, and these areas include the intraparietal sulcus (IPS), the superior frontal gyrus (SFS), the GFi, the inferior parietal cortex, the ventrolateral frontal cortex, and the superior parietal gyrus (Fletcher & Henson, 2001; Kazui, Kitagaki, & Mori, 2000; Manoach et al., 1997; Smith & Jonides, 1998).

Motor Subnetwork

The motor subnetwork includes five servers corresponding to the major brain areas in retrieval, assembly, and execution of motor commands, as well as sensory information feedback. First, Server V represents the premotor cortex in Brodmann Area 6, which plays an important role in sensorimotor and sensory cue detection, especially in a single RT task (Kansaku, Hanakawa, Wu, & Hallett, 2004; Mitz, Godschalk, & Wise, 1991; Roland, 1993); moreover, the premotor cortex is one of the generators of LRP (Leuthold & Jentzsch, 2001, 2002; Ulrich et al., 1998), and it also has the function in processing spatial working memory information after practice (Mitz et al., 1991). Second, the basal ganglia (Server W) retrieve motor programs and long-term procedural information from long-term procedural memory (Server D; Bear et al., 2001; Cook & Woollacott, 1995; Gilbert, 2001). Third, the supplementary motor area (SMA) and the pre-SMA (Server Y) have the major function of assembling motor programs and ensuring movement accuracy (Gordon & Soechting, 1995). Fourth, the function of the primary motor cortex (Server Z) is to address the spinal and bulbar motorneurons and transmit the neural signals to different body parts as motor actuators (mouth, left and right hands, left and right feet server, etc.; Roland, 1993). In addition, the primary motor cortex is also one of the origins of LRP (Leuthold & Jentzsch, 2001, 2002; Ulrich et al., 1998). Fifth, S1 (the somosensory cortex, Server X) collects motor information of efference copies from the primary motor cortex (Server Z) and sensory information from body parts and then relays them to the

prefrontal cortex (Server C) as well as the SMA (Server Y; Roland, 1993).

MODELING MECHANISMS AND RESULTS

On the basis of the major assumptions of QN-MHP, in the following section, we describe how a queuing network model is able to mathematically model a wide range of PRP effects, including all of the counterexamples to the existing models reviewed above. For each PRP effect, we introduce the experimental results, the route of entities in the network, the corresponding mathematical modeling mechanism, and a comparison between the modeling and experimental results.

Basic PRP

Modeling the experimental results in the basic PRP paradigm provides an introduction to the modeling approach of the queuing network model in this article, including how the routes of entities in the network are selected, how the mathematical models are developed, how the parameters in the model are set, and how the modeling results are validated with the experimental results.

Routes of Entities

The route of entities in the queuing network is determined on the basis of the previous queuing network modeling work in modeling the connectivity of brain regions (Wu & Liu, 2004a, 2004b): In general, depending on the task to be performed, the servers whose functions are related to the target task are included in the route of entities, which is consistent with the concept of *functional connectivity* employed in neuroscience—a functional network for a particular cognitive task is defined by specifying the brain regions composing the network as well as the anatomical links between these regions (Horwitz, Tagamets, & McIntosh, 1999; McIntosh, 1999, 2000; Sporns, Tononi, & Edelman, 2000; Taylor, 2003; Taylor et al., 2000).

In T1, entities representing the auditory stimulus enter the auditory perceptual subnetwork first (Server 5→6/7→8); then, they are transmitted to the cognitive subnetwork, including Servers B, C, and F, responsible for making the phonological judgment. After that, since T1 involves vocalization (produces vocal response to the tones), Servers Y, Z, and Mouth are in the route of entities according to the neuron pathways among the brain regions represented by these servers (as described in the introductory section of this article). Therefore, according to the connection between these brain regions, the route of T1 is

T1: 5→6/7→8→B→C→F→C→Y→Z→Mouth.

For T2, entities representing the visual stimulus enter the visual perceptual subnetwork first (Servers 1→2/3→4). Via Server 4, the entities are transmitted to the cognitive subnetwork, including Servers A, C, and F, in which the judgment is made. After that, they travel to the motor subnetwork (Servers W, Y, and Z and the hand server), which retrieves motor programs, assembles the motor programs, and initiates the motor response. As a result, according to the connection between these brain regions, the route of T2 is

T2: 1→2/3→4→A→C→F→C→W→Y→Z→Hand.

Modeling Mechanisms

Entities of both tasks travel through Server F, which works as a structural bottleneck based on the assumption of QN-MHP about the cognitive subnetwork. Accordingly, for the task situation in Experiment 4 of Schumacher et al. (1999), entities of T1 are not delayed in receiving processing, but entities of T2 have to wait for the entities of T1 to leave Server F before they can be processed at Server F (see the short SOA condition compared with the long SOA condition in Figure 5).

Mathematical Modeling of the Expected Reaction Time

The expected RT of T1—$E(RT1)$—can be predicted by the sum of the servers' processing times along the route of entities of T1, since no previous entities occupy any of the servers in the route (see T1 in Figure 5 and Equation 1).

$$E(RT1) = T_{1,AP} + T_{1,B} + T_{1,C} + T_{1,F} + T_{1,C} + T_{1,Y} + T_{1,Z} + T_{1,VO}, \quad (1)$$

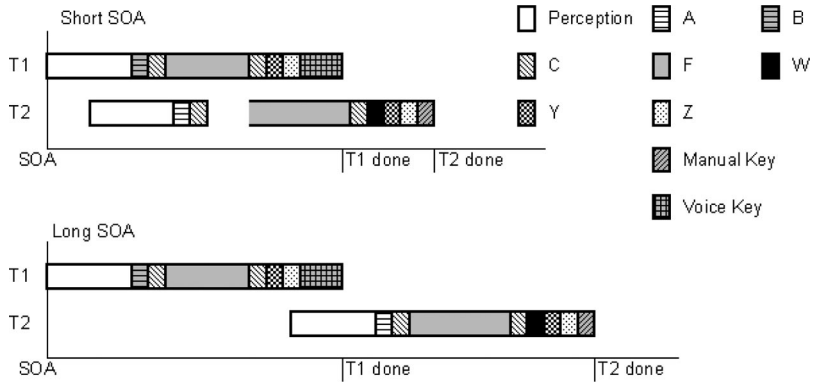

Figure 5. Mechanisms for modeling the basic psychological refractory period with the queuing network-model human processor. SOA = stimulus onset asynchrony; T1 = Task 1; T2 = Task 2.

where $T_{1,AP}$ is the processing time of the auditory perceptual subnetwork and $T_{1,B}$, $T_{1,C}$, $T_{1,F}$, $T_{1,Y}$, $T_{1,Z}$, and $T_{1,VO}$ represent the processing time of Servers B, C, F, Y, Z, and Mouth, respectively.

The expected RT of T2—$E(RT2)$—depends on a comparison between (a) the difference between the SOA and the time at which entities of T1 exit Server F ($T_{1,AP} + T_{1,B} + T_{1,C} + T_{1,F} - SOA$) and (b) the duration of the processing time before entities of T2 enter Server F (the sum of the processing times in the visual perceptual subnetwork and Servers A and C; i.e., $T_{2,VP} + T_{2,A} + T_{2,C}$; see Equation 2): If Part a is longer than Part b (the short SOA conditions), entities of T2 have to wait for the entities of T1 to finish their processing at Server F (the short SOA conditions in Figure 5); hence, the waiting time of T2's entities is the difference between SOA and the time at which entities of T1 exit Server F ($T_{1,AP} + T_{1,B} + T_{1,C} + T_{1,F} - SOA$). The duration of time that entities of T1 spend in the perceptual subnetwork as well as at Servers A and C is absorbed during this waiting process, since other servers in the network can process the entities of T1 and T2 at the same time. As a result, the total processing time of T2's entities in this condition is the waiting time ($T_{1,AP} + T_{1,B} + T_{1,C} + T_{1,F} - SOA$) plus the sum of the processing time of Server F and the following servers. Conversely, if Part a is shorter or equal to Part b (the long SOA conditions), entities of T2 enter the vacant Server F immediately, and the RT of T2 is the sum of the processing time of T2's entities at the perceptual subnetwork and at Servers A and C ($T_{2,VP} + T_{2,A} + T_{2,C}$) as well as the processing time in the servers that follow Server C.

$$E(RT2) = \max(T_{1,AP} + T_{1,B} + T_{1,C} + T_{1,F} - SOA, T_{2,VP} + T_{2,A} + T_{2,C}) + T_{2,F} + T_{2,C} + T_{2,W} + T_{2,Y} + T_{2,Z} + T_{2,K}. \quad (2)$$

Equation 2 above can be rewritten as Equation 3, shown at the bottom of this page.

Figure 6 shows the expected pattern of RT1 and RT2 as the SOA increases. Equation 1 for RT1 shows that the expected RT1 is a constant and its value is independent of the SOA. Equation 3 of RT2 shows that when $SOA < T_{1,AP} + T_{1,B} + T_{1,C} + T_{1,F} - (T_{2,VP} + T_{2,A} + T_{2,C})$, a negative linear relationship between SOA and RT2 is expected (slope = −1; see the first part of Equation 3), but when $SOA \geq T_{1,AP} + T_{1,B} + T_{1,C} + T_{1,F} - (T_{2,VP} + T_{2,A} + T_{2,C})$, the expected RT2 remains as a constant and its value is independent of SOA.

Parameter Setting

The expected pattern of RT in the basic PRP conditions shown above (Equations 1 and 3 and Figure 6) is consistent with the pattern of data observed in basic PRP experiments. To fit particular data, we need to set the parameters on the right hand side of the equations. In modeling all of the experimental studies, we follow the same parameter-setting method used in ACT-R/PM (Byrne & Anderson, 2001; see the introduction of ACT-R/PM in this article). For example, in modeling the basic PRP, two free parameters in QN-MHP (the processing times of Server F in T1 and T2) are set to fit the experimental data in the long SOA conditions. The same values of these parameters are used for the short SOA conditions to predict the RT1 and RT2. Therefore, for the short SOA conditions, there are no free parameters to fit the experimental results. Moreover, the values of these two free parameters set for the long SOA conditions are not set arbitrarily but are constrained by the tasks in the experiment: The processing times of T1 and T2 at Server F are close to each other (the difference between these two processing times is less than 120 ms) since the difficulty levels of T1 and T2 in the experiment are similar (see Appendix A, Table A1).

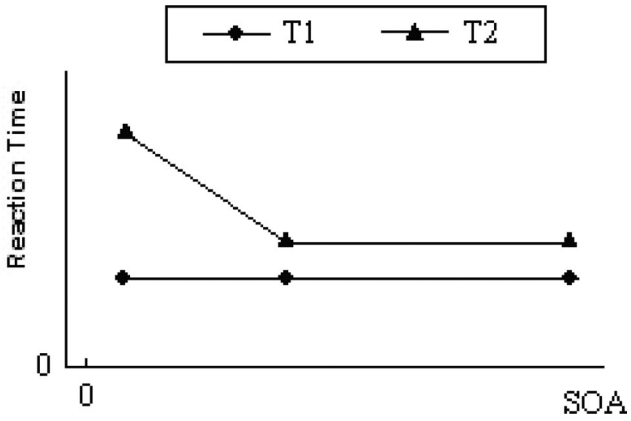

Figure 6. The expected pattern of reaction time in the basic psychological refractory period based on the queuing network-model human processor's mathematical prediction. SOA = stimulus onset asynchrony; T1 = Task 1; T2 = Task 2.

The other processing times adopt the same values in the original version of QN-MHP, which has been used to model a wide range of human performance in various tasks (Liu et al., 2006; Wu & Liu, 2007a, 2007b, 2008; Wu, Liu, & Walsh, in press). In addition, the setting of the key closure time and voice key closure time is directly based on the study of Byrne and Anderson (2001).

Modeling Results and Their Validation

Figure 7 shows the modeling results compared with the basic PRP experimental results. The R^2 of the model is .91 (T2), and the root–mean–square (RMS) = 22 ms.

Subadditive Difficulty Effect

Modeling of the subadditive difficulty effect includes quantifications of the four experimental studies described above, in which

$$E(RT2) = \begin{cases} T_{1,AP} + T_{1,B} + T_{1,C} + T_{1,F} - SOA + T_{2,F} + T_{2,C} + T_{2,W} + T_{2,Y} + T_{2,Z} + T_{2,K} & \text{If } SOA < T_{1,AP} + T_{1,B} + T_{1,C} + T_{1,F} - (T_{2,VP} + T_{2,A} + T_{2,C}) \\ T_{2,VP} + T_{2,A} + T_{2,C} + T_{2,F} + T_{2,C} + T_{2,W} + T_{2,Y} + T_{2,Z} + T_{2,K} & \text{If } SOA \geq T_{1,AP} + T_{1,B} + T_{1,C} + T_{1,F} - (T_{2,VP} + T_{2,A} + T_{2,C}) \end{cases}. \quad (3)$$

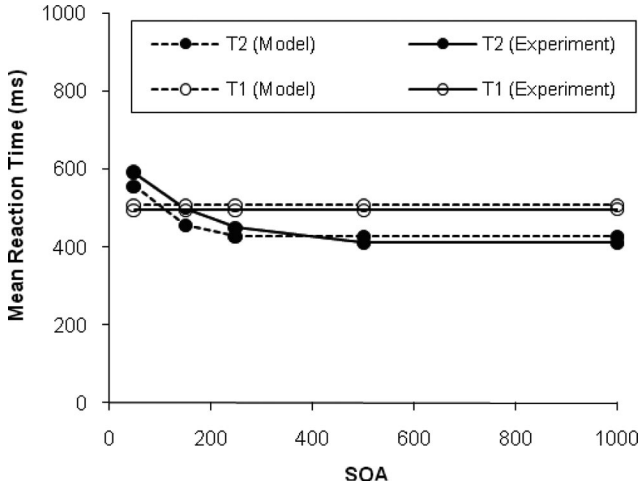

Figure 7. Mean reaction time in the basic psychological refractory period effect in Experiment 4 of Schumacher et al. (1999; compatible T2 condition, solid lines) compared with modeling results (dashed lines). Experiment 4 data adapted from "Concurrent Response-Selection Processes in Dual-Task Performance: Evidence for Adaptive Executive Control of Task Scheduling," by E. H. Schumacher et al., 1999, *Journal of Experimental Psychology: Human Perception and Performance, 25,* p. 809. Copyright 1999 by the American Psychological Association. SOA = stimulus onset asynchrony; T1 = Task 1; T2 = Task 2.

the difficulty level of T2 was manipulated by the degree of compatibility (Schumacher et al., 1999), the number of stimuli in a category in making the same response (Hawkins et al., 1979), or the number of stimulus–response pairs (Karlin & Kestenbaum, 1968; Sommer et al., 2001).

Schumacher et al.'s (1999) Study

As described earlier in this article, through changing the degree of compatibility of T2. Schumacher et al. (1999) found subadditive difficulty effects, which can be modeled by the queuing network model in the following manner.

Routes of Entities

Routes of Entities in Experiment 3

Similar to the routes in the modeling mechanism of the basic PRP paradigm of Schumacher et al. (1999), as described in the basis PRP modeling section above, based on the task and corresponding functions of the brain areas, the routes of T1 and T2 (both compatible and incompatible conditions) are

T1: 5→6/7→8→B→C→F→C→W→Y→Z→Hand

and

T2: 1→2/3→4→A→C→F→C→W→Y→Z→Hand.

Routes of Entities in Experiment 4

Following the same route-setting logic, the routes of entities in Experiment 4 are

T1: 5→6/7→8→B→C→F→C→Y→Z→Mouth

and

T2: 1→2/3→4→A→C→F→C→W→Y→Z→Hand.

Modeling Mechanisms

The queuing network model is able to account for the subadditive difficulty effect without using scheduling or lock/unlock strategies. In the short SOA conditions, entities in both compatible and incompatible conditions of T2 have to wait in front of Server F until entities of T1 complete the processing at Server F. On the basis of the function of Server C in inhibiting incompatible responses, it takes Server C one additional cycle to inhibit the incompatible responses. Server C takes less time to process the entities of compatible T2 than those of incompatible T2; as a result, entities of compatible T2 wait a longer time than entities of incompatible T2. However, since this extra waiting time of compatible T2 in front of Server F is absorbed in Server F's processing time in the short SOA conditions, the difference between RTs in the compatible and incompatible conditions is smaller than that in the long SOA conditions, in which this extra waiting time of the compatible T2 is not absorbed (see Figures 8 and 9). Therefore, it is predicted that the difference between RTs in the compatible and incompatible tasks in the short SOA conditions is smaller than that in the long SOA conditions, which is consistent with the subadditive difficulty effect. The same mechanism can also be applied to explain the experimental results of Experiment 4, in which different motor output modalities were used. Therefore, the subadditive difficulty effect can be modeled as a natural outcome of the interactions of the servers providing service to entities in the queuing network without using any lock/unlock strategies or executive control processes.

Mathematical Modeling of the Expected Reaction Time

Similar to the equations in quantifying RT in the basic PRP, the mathematical quantification of the expected RT1 and RT2 in Experiment 3 is

$$E(RT1) = T_{1,AP} + T_{1,B} + T_{1,C} + T_{1,F} + T_{1,C} + T_{1,W} + T_{1,Y} + T_{1,Z} + T_{1,K}, \quad (4)$$

$$E(RT2_{comp}) = \max(T_{1,AP} + T_{1,B} + T_{1,C} + T_{1,F} - SOA, T_{2,VP} + T_{2,A} + T_{2,C\text{-}comp}) + T_{2,F\text{-}comp} + T_{2,C\text{-}comp} + T_{2,W} + T_{1,Y} + T_{2,Z} + T_{2,K}, \quad (5)$$

and

$$E(RT2_{incomp}) = \max(T_{1,AP} + T_{1,B} + T_{1,C} + T_{1,F} - SOA, T_{2,VP} + T_{2,A} + T_{2,C\text{-}incomp}) + T_{2,F\text{-}incomp} + T_{2,C\text{-}incomp} + T_{2,W} + T_{1,Y} + T_{2,Z} + T_{2,K}. \quad (6)$$

The mathematical quantification of the expected RT1 and RT2 in Experiment 4 is

$$E(RT1) = T_{1,AP} + T_{1,B} + T_{1,C} + T_{1,F} + T_{1,C} + T_{1,Y} + T_{1,Z} + T_{1,VO}, \quad (7)$$

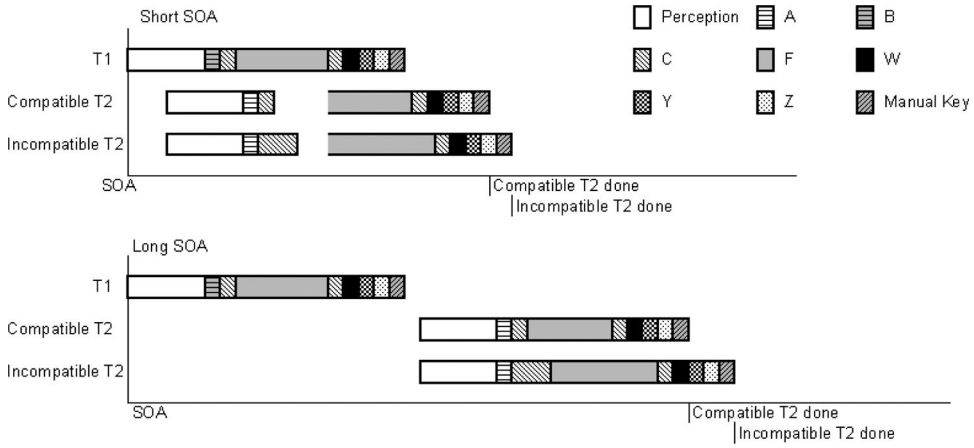

Figure 8. Mechanisms for modeling Experiment 3 of Schumacher et al. (1999). SOA = stimulus onset asynchrony; T1 = Task 1; T2 = Task 2.

$$E(RT2_{comp}) = \max(T_{1,AP} + T_{1,B} + T_{1,C} + T_{1,F} - SOA, T_{2,VP} + T_{2,A} + T_{2,C\text{-}comp}) + T_{2,F\text{-}comp} + T_{2,C\text{-}comp} + T_{2,W} + T_{2,Y} + T_{2,Z} + T_{2,K}, \quad (8)$$

and

$$E(RT2_{incomp}) = \max(T_{1,AP} + T_{1,B} + T_{1,C} + T_{1,F} - SOA, T_{2,VP} + T_{2,A} + T_{2,C\text{-}incomp}) + T_{2,F\text{-}incomp} + T_{2,C\text{-}incomp} + T_{2,W} + T_{2,Y} + T_{2,Z} + T_{2,K}, \quad (9)$$

where $T_{2,C\text{-}comp}$, $T_{2,C\text{-}incomp}$, $T_{2,F\text{-}comp}$, and $T_{2,F\text{-}incomp}$ are the processing times of Server C and F in the compatible and incompatible conditions of T2, respectively.

On the basis of the equations developed above, the expected pattern of RTs in the compatible and incompatible conditions of T2 in Schumacher et al. (1999) is shown in Figure 10. The difference of RT2 between the compatible and incompatible conditions is larger in the long SOA conditions ($2T_{2,C\text{-}incomp} - 2T_{2,C\text{-}comp}$) than in the short SOA conditions ($T_{2,C\text{-}incomp} - T_{2,C\text{-}comp}$), and the slope of T2 in short SOA conditions is -1.

Parameter Setting

ACT-R/PM uses three free parameters to model the experimental results in the long SOA conditions (tone recording time and activation of stimulus–response mapping chunks in the easy and hard T2 conditions in Experiments 3 and 4; see Byrne & Anderson, 2001, Table 1; in addition, any free parameters adjusted can be regarded as task-specific assumption in general). Using the same parameter-setting method as in ACT-R/PM, QN-MHP also uses three free parameters to model the experimental results in the long SOA conditions. Except for the 3 free parameters, the values of the other parameters are the same as those in Table A1 (see Appendix A). Moreover, the values of these free parameters in the long SOA conditions are constrained by the task properties: Within each experiment, the processing time of entities at Server F in the compatible condition is shorter than that in the incompatible condition. Across different experiments, in the two compatible con-

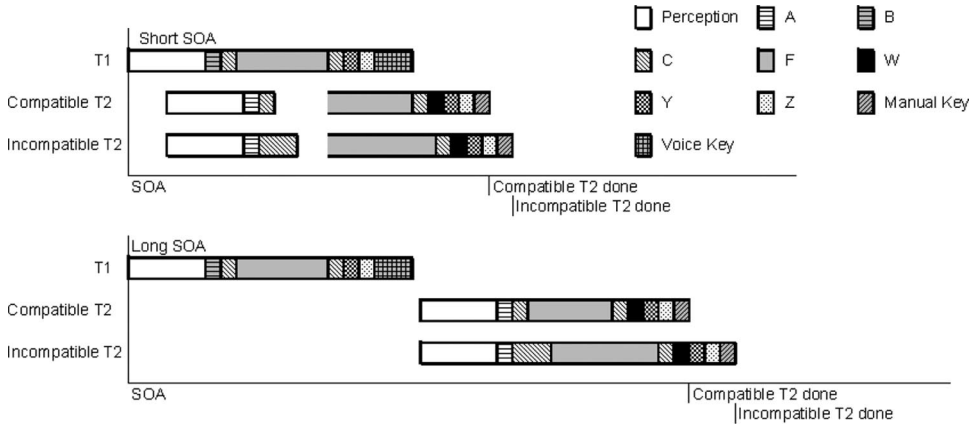

Figure 9. Mechanisms for modeling Experiment 4 of Schumacher et al. (1999). SOA = stimulus onset asynchrony; T1 = Task 1; T2 = Task 2.

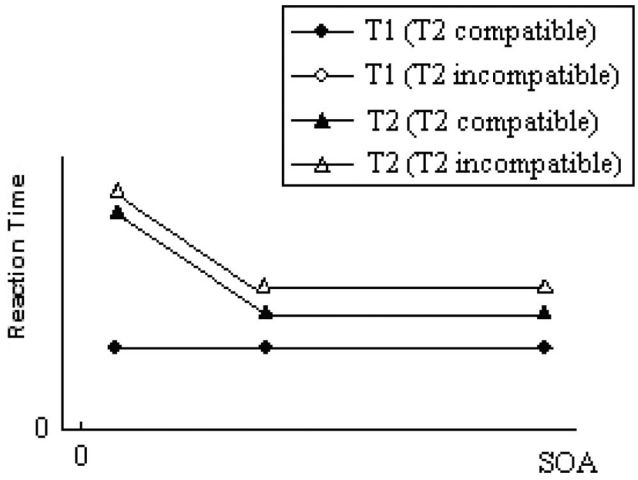

Figure 10. The expected pattern of reaction time in Schumacher et al.'s (1999) study. SOA = stimulus onset asynchrony; T1 = Task 1; T2 = Task 2.

ditions of T2 in Experiments 3 and 4, the processing times of entities at Server F are close to each other since the difficulty level of T1 in Experiment 3 is similar to that in Experiment 4 (the difference between these two processing times is less than 120 ms); this constraint also applies to the processing time of T2 at Server F in the incompatible condition in Experiments 3 and 4 (see Appendix A, Table A2).

Modeling Results and Their Validation

Figures 11 and 12 show the modeling results compared with the experimental results in Experiments 3 and 4: In Experiment 3, the

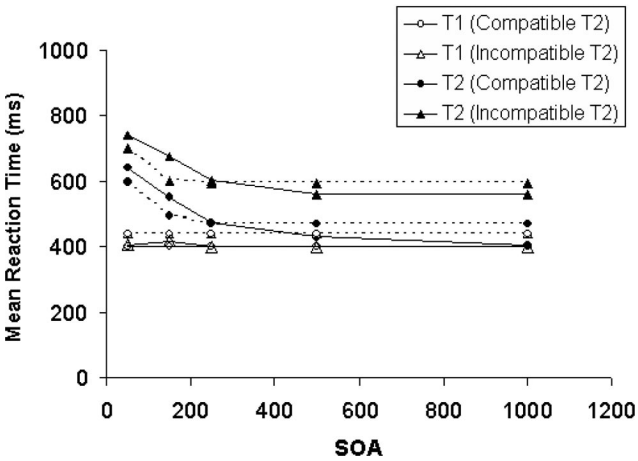

Figure 11. Mean reaction time of Experiment 3 in Schumacher et al. (1999; solid lines) compared with modeling results (dashed lines). Experiment 3 data adapted from "Concurrent Response-Selection Processes in Dual-Task Performance: Evidence for Adaptive Executive Control of Task Scheduling," by E. H. Schumacher et al., 1999, *Journal of Experimental Psychology: Human Perception and Performance, 25,* p. 805. Copyright 1999 by the American Psychological Association. SOA = stimulus onset asynchrony; T1 = Task 1; T2 = Task 2.

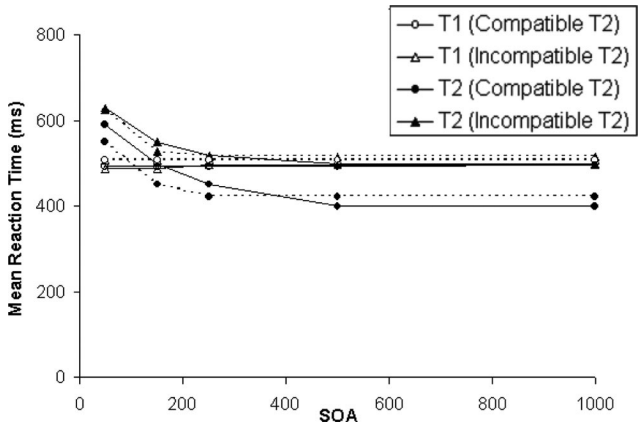

Figure 12. Mean reaction time of Experiment 4 in Schumacher et al. (1999; solid lines) compared with modeling results (dashed lines). Experiment 4 data adapted from "Concurrent Response-Selection Processes in Dual-Task Performance: Evidence for Adaptive Executive Control of Task Scheduling," by E. H. Schumacher et al., 1999, *Journal of Experimental Psychology: Human Perception and Performance, 25,* p. 809. Copyright 1999 by the American Psychological Association. SOA = stimulus onset asynchrony; T1 = Task 1; T2 = Task 2.

R^2 of the model (T2) is .85, and the RMS = 40.9 ms; in Experiment 4, the R^2 of the model is .90 (T2), and the RMS = 18.7 ms.

Hawkins et al.'s (1979) Study

The difficulty level of T2 in Hawkins et al. (1979) was manipulated by changing the number of stimuli in a category for making the same response (for a detailed description of their experimental setting and findings, see the introductory section of this article).

Routes of Entities

The four experiments in Hawkins et al.'s (1979) study included four different combinations of the perceptual and motor modalities of T1: auditory stimulus–manual response, auditory stimulus–vocal response, visual stimulus–vocal response, and visual stimulus–manual response. Following the same route-selection method in modeling the basic PRP, the routes of the entities in these four experiments are

1. Auditory–manual response:

T1: 5 → 6/7 → 8 → B → C → F → C → W → Y → Z → Hand.

2. Auditory–vocal response:

T1: 5 → 6/7 → 8 → B → C → F → C → Y → Z → Mouth.

3. Visual–vocal response:

T1: 1 → 2/3 → 4 → A → C → F → C → Y → Z → Mouth.

4. Visual–manual response:

T1: 1 → 2/3 → 4 → A → C → F → C → W → Y → Z → Hand.

In all four of the experiments, T2 was a visual stimulus–manual response task. Hence, the route of entities of T2 in these four experiments is

T2: 1→2/3→4→A→C→F→C→W→Y→Z→Hand.

Modeling Mechanisms

Similar to the mechanisms of modeling Schumacher et al.'s (1999) experiments, based on the function of Server C in categorizing the stimuli, Server C takes additional cycles to locate the target stimulus into the right category (in the easy condition of T2 in Hawkins et al.'s, 1979, experiment, one cycle time is needed since the category size is one; in the difficult condition of T2, four cycle times are needed because the category size is four); hence, Server C takes a longer time to process the entities of T2 that require this categorization process than entities of T1 without the categorization process. However, since this extra waiting time of compatible T2 in front of Server F is absorbed in Server F's processing time in the short SOA conditions, the difference between the easy and hard RTs is smaller than that in the long SOA conditions.

Mathematical Modeling of the Expected Reaction Time

Similar to mathematical modeling of the basic PRP, the equations quantifying the expected RT in the four experiments in Hawkins et al.'s (1979) experiment are developed as follows:

1. Auditory–manual response: $$E(RT1) = T_{1,AP} + T_{1,B} + T_{1,C} + T_{1,F} + T_{1,C} + T_{1,W} + T_{1,Y} + T_{1,Z} + T_{1,K}. \quad (10)$$

2. Auditory–vocal response: $$E(RT1) = T_{1,AP} + T_{1,B} + T_{1,C} + T_{1,F} + T_{1,C} + T_{1,Y} + T_{1,Z} + T_{1,VO}. \quad (11)$$

3. Visual–vocal response: $$E(RT1) = T_{1,VP} + T_{1,A} + T_{1,C} + T_{1,F} + T_{1,C} + T_{1,Y} + T_{1,Z} + T_{1,VO}. \quad (12)$$

4. Visual–manual response: $$E(RT1) = T_{1,VP} + T_{1,A} + T_{1,C} + T_{1,F} + T_{1,C} + T_{1,W} + T_{1,Y} + T_{1,Z} + T_{1,K}. \quad (13)$$

In all four of the experiments, T2 is a visual stimulus–manual response task; hence, the expected RT2 in these four experiments is

$$E(RT2_{easy}) = \max(T_{1,P} + T_{1,A\backslash B} + T_{1,C} + T_{1,F} - SOA, T_{2,VP} + T_{2,A} + T_{2,C\text{-}easy}) + T_{2,F\text{-}easy} + T_{2,C\text{-}easy} + T_{2,W} + T_{2,Y} + T_{2,Z} + T_{2,K}, \quad (14)$$

and

$$E(RT2_{diff}) = \max(T_{1,P} + T_{1,A\backslash B} + T_{1,C} + T_{1,F} - SOA, T_{2,VP} + T_{2,A} + T_{2,C\text{-}diff}) + T_{2,F\text{-}diff} + T_{2,C\text{-}diff} + T_{2,W} + T_{2,Y} + T_{2,Z} + T_{2,K}, \quad (15)$$

where $T_{1,P}$ is the processing time of the perceptual subnetwork corresponding to the parameter in RT1's equations; $T_{1,A\backslash B}$ is the processing time of Server A or B corresponding to the parameter in RT1's equations; and $T_{2,C\text{-}easy}$, $T_{2,C\text{-}diff}$, $T_{2,F\text{-}easy}$, and $T_{2,F\text{-}diff}$ are the processing times of Servers C and F in the easy and difficult T2 conditions, respectively.

Since the mechanisms of modeling RT and the equations of RT1 and RT2 in Hawkins et al.'s (1979) experimental study are similar to those of Schumacher et al.'s (1999) experimental study, the expected pattern of RT in Hawkins et al.'s experiment is similar to Schumacher et al.'s experimental study except that the difficulty level of T2 includes easy and hard conditions rather than compatible and incompatible conditions.

Parameter Setting

In modeling the four experiments of Hawkins et al. (1979), compared with EPIC, which uses five free parameters (unlocking onset latency, suspension waiting times under the easy and difficult conditions, preparation waiting time, and ocular orientation time; Meyer & Kieras, 1997a, p. 45), QN-MHP uses three free parameters ($T_{1,F}$, $T_{2,F\text{-}easy}$, and $T_{2,F\text{-}diff}$) with the same parameter-setting method as in ACT-R/PM mentioned above. Except for the three free parameters, the values of the other parameters are the same as those in Tables A1 and A2 in Appendix A. Moreover, the values of these free parameters set for the long SOA conditions are constrained by the task properties: Within each experiment, processing time of entities at Server F in the easy condition is shorter than that in the hard condition; across different experiments, in the four easy conditions of T2 in Experiments 1–4, the processing times of T2 at Server F in Experiments 1–4 are close to each other (the difference between these two processing times is less than 120 ms) since the difficulty levels of T2 are similar in these four experiments. This constraint also applies to the processing time of Server F in the four hard conditions of T2 and T1 in Experiments 1–4 (see Appendix A, Table A3).

Modeling Results and Their Validation

Figure 13 shows the modeling results compared with experimental results in Experiments 1–4: In Experiment 1, the R^2 of the model is .929 (T2), and the RMS = 57 ms (EPIC's modeling results: R^2 [T2] = .997, RMS = 14 ms); in Experiment 2, the R^2 of the model is .964 (T2), and the RMS = 28 ms (EPIC's modeling results: R^2 = .976, RMS = [34 + 21]/2 = 27.5 ms); in Experiment 3, the R^2 of the model is .928 (T2), and the RMS = 45 ms (EPIC: R^2 = .984, RMS = 24 ms); and in Experiment 4, the R^2 (T2) of the model is .951, and the RMS = 33 ms (EPIC: R^2 = .975, RMS = [11 + 31]/2 = 21 ms).

Karlin and Kestenbaum's (1968) Study

As described earlier in this article, in Karlin and Kestenbaum's (1968) study, T1 was a visual–manual choice reaction task, and T2

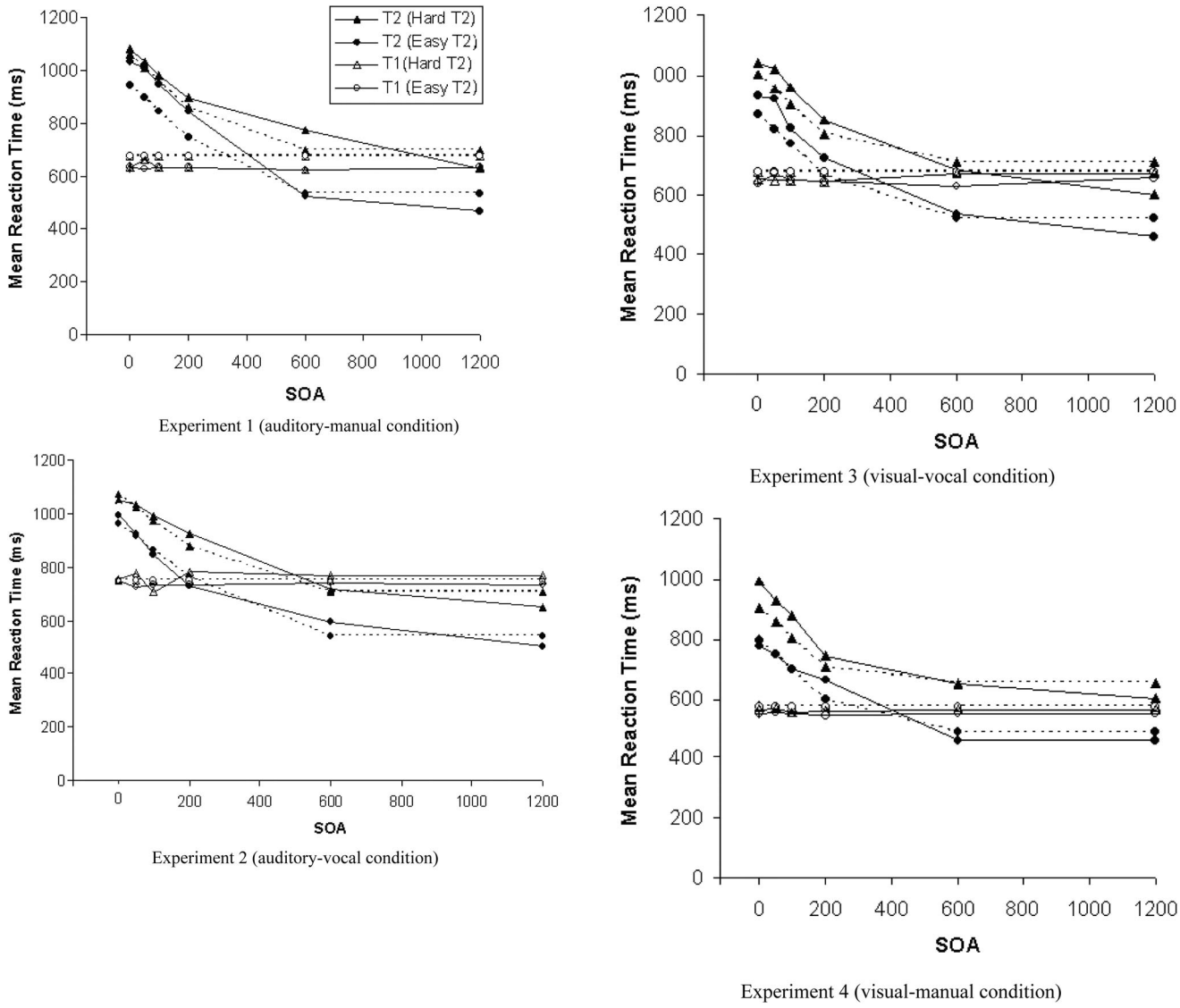

Figure 13. Mean reaction time in Experiments 1–4 of Hawkins, Rodriguez, and Reicher (1979; solid lines) compared with modeling results (dashed lines). SOA = stimulus onset asynchrony; T1 = Task 1; T2 = Task 2.

was an auditory–manual reaction task including two difficulty levels: One was a simple reaction task, and the other was a two-choice reaction task.

Routes of Entities

Similar to the routes in modeling the basic PRP, based on the task and the corresponding functions of the brain areas, the routes of T1 and T2 (choice reaction condition) are

T1: 1→2/3→4→A→C→F→C→W→Y→Z→Hand

and

T2 (choice reaction):

5→6/7→8→B→C→F→C→W→Y→Z→Hand.

Kansaku et al. (2004) found a specific neural network that characterizes simple reaction tasks irrespective of the input modalities and output effectors. This network includes the premotor cortex (Server V) and the right posterior superior temporal cortex (Server F). This is also consistent with the functions of the premotor cortex (included in Server V) and right posterior superior temporal cortex (included in Server F) since a simple reaction task involves sensorimotor processing/integration (Server V), sensory cue detection (Server V), and working memory (phonological) information processing and judgment (Server F). On the basis of the connection between these brain regions, the route of entities in T2 under the simple reaction task condition is

T2 (simple reaction):

5→6/7→8→B→C→F→C→V→Z→Hand.

Modeling of the Expected Reaction Time

The expected RT in T1 and T2 (choice reaction condition) can be derived on the basis of the same mechanism as in the basic PRP (see Equations 16 and 17).

$$E(RT1) = T_{1,VP} + T_{1,A} + T_{1,C} + T_{1,F} + T_{1,C} + T_{1,Y} + T_{1,W} + T_{1,Z} + T_{1,K}, \quad (16)$$

and

$$E(RT2)\ (\text{choice reaction}) = \max(T_{1,VP} + T_{1,A} + T_{1,C} + T_{1,F} - SOA, T_{2,AP} + T_{2,B} + T_{2,C}) + T_{2,F} + T_{2,C} + T_{2,Y} + T_{2,W} + T_{2,Z} + T_{2,K}. \quad (17)$$

The expected RT2 in the simple reaction condition is shown at the bottom of the page in Equation 18, whose derivation is shown in Appendix B (see Equation B15 in Appendix B), where $RT_{2,ANTI}$ is the expected RT of T2 when participants are anticipating the arrival of stimuli and $RT_{2,NOAN}$ is the expected RT of T2 when no anticipation is involved.

On the basis of the equations developed above, the expected pattern of the RT in Karlin and Kestenbaum's (1968) experiment is shown in Figure 14. On the basis of Equation 18, in the short SOA conditions, RT2 (simple reaction) shows the same pattern as RT2 in the choice reaction condition; meanwhile, in the long SOA conditions, according to Equation B16 in Appendix B, there is a nonlinear negative relationship between RT2 (simple reaction) and SOA.

This mechanism of modeling the subadditive difficulty effect described above is consistent with the findings from several behavioral and physiological studies of the same task. In the studies of Karlin and Kestenbaum (1968) and De Jong (1993), the stimulus of the second task was always presented after the first stimulus, increasing the conditional probability of the presentation of the second stimulus with an increase of the SOA (Luce, 1986; Naatanen, 1971; Niemi & Naatanen, 1981). Other behavioral studies (Nickerson, 1965, 1967) also found an increased probability of anticipatory reactions in a simple reaction task in the long SOA conditions under such experimental conditions. The result of these behavioral studies was also confirmed in an ERP study (Sommer et al., 2001) in which the LRP provided direct evidence that the subadditive difficulty

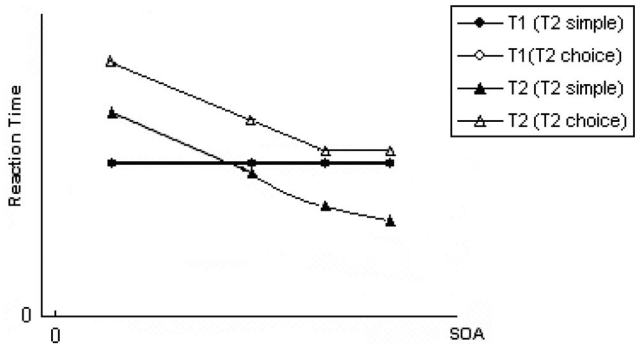

Figure 14. The expected pattern of reaction time in the simple and choice reaction conditions in Karlin and Kestenbaum's (1968) experiment. SOA = stimulus onset asynchrony.

effect is due to an increase of response anticipation in the simple response condition if the secondary task is a simple reaction task. In addition, fMRI studies (Brass & Cramon, 2002) also found that the frontolateral frontal cortex at the junction of the precentral sulcus and the inferior frontal sulcus (represented by Server F) is the crucial frontal component in task preparation.

QN-MHP is able to model the subadditive difficulty effect found in Karlin and Kestenbaum's (1968) experiment without using task-specific scheduling assumptions. When the SOA is longer than certain durations, before S1 appears, Server F starts the anticipation process and prepares its response selection (see Appendix B for the modeling mechanism in detail). The response selection might occur earlier than the actual presentation of stimulus, which also allows QN-MHP to model the other dependent variables in Sommer et al.'s (2001) experiment—percentage of negative responses and onset time of the brain waves of LRP (see the modeling of Sommer et al.'s, 2001, experimental results in Appendix C in detail). This modeling mechanism in stimulus anticipation is a component of the QN-MHP and has been successfully implemented in modeling a driving task (Liu et al., 2006); it is not an additional task-specific assumption added for the current study.

Parameter Setting

All of the parameters used in the model are listed in Table A4 in Appendix A. Compared with EPIC, which uses nine free

$$E(RT2)\ (\text{simple reaction}) = \begin{cases} pRT_{2,ANTI} + (1-p)RT_{2,NOAN} & \text{If } t_a > 0 \text{ (long SOA conditions)} \\ \max(T_{1,VP} + T_{1,A} + T_{1,C} + T_{1,F} - SOA, T_{2,AP} + T_{1,B} + T_{2,C}) & \\ \quad + T_{2,F} + T_{2,C} + T_{2,V} + T_{2,Z} + T_{2,K} & \text{If } t_a = 0 \text{ (short SOA conditions)} \end{cases}. \quad (18)$$

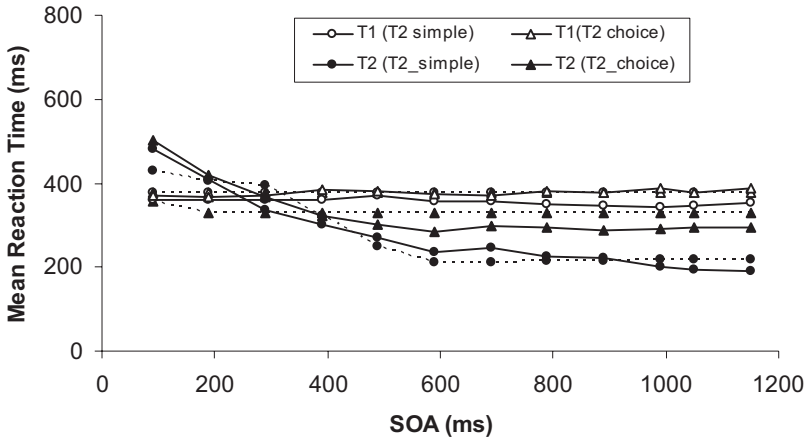

Figure 15. Mean reaction time in experimental results of Karlin and Kestenbaum (1968; solid lines) compared with modeling results (dashed lines). Experimental data adapted from "Effects of Number of Alternatives on the Psychological Refractory Period," by L. Karlin and R. Kestenbaum, 1968, *Quarterly Journal of Experimental Psychology, 20,* p. 175. Copyright 1968 by Taylor & Francis Ltd. (Web site: http://www.informaworld.com). Adapted with permission. SOA = stimulus onset asynchrony; T1 = Task 1; T2 = Task 2.

parameters[4] in simulating the experiment of Karlin and Kestenbaum (1968; see Meyer & Kieras, 1997b, Table 1), QN-MHP uses five free parameters with the same parameter-setting method as in ACT-R/PM. The values of the other parameters are the same as those in Tables A1–A3 in Appendix A. The two parameters in Equation B4 in Appendix B are directly based on a psychophysical study ($k = 2$, $\beta = 0.9$; Wearden, Edwards, Fakhri, & Percival, 1998), and they are not free parameters in this modeling process. Moreover, the values of the free parameters set for the long SOA conditions are constrained by the task properties: The processing time at Server F in the simple reaction condition is at least 18 ms (one cycle time) less than that in the choice reaction condition (see Appendix A, Table A4).

Modeling Results and Their Validation

Figure 15 shows the modeling results compared with experimental results. The R^2 of the model is .73 (both T1 and T2), and the RMS = 41.8 ms (EPIC's modeling results: $R^2 = .985$, RMS = 11 ms).

Van Selst and Jolicoeur (1997) conducted a behavioral experiment to replicate Karlin and Kestenbaum's (1968) experiment. Van Selst and Jolicoeur's experiment had three conditions: SRT, two-alternative forced choice (2AFC), and three-alternative forced choice (3AFC). They found that (a) the difference of RTs between 2AFC and 3AFC remains a constant across the SOAs (Van Selst & Jolicoeur, 1997, regarded this result as one that did not replicate the results of Karlin & Kestenbaum's, 1968, experiment; this additive effect can also be found in McCann & Johnston, 1992; Ruthruff, Miller, & Lachmann, 1995) and (b) the difference of RTs between 2AFC and SRT decreases as the SOA decreases (this is consistent with Karlin & Kestenbaum's, 1968, experimental results). Their finding related to the additive effect can also be explained by the queuing network model: (a) When RT in the 2AFC condition is compared with that in the 3AFC condition, the only difference is the prolonging of service time at Server F in the 3AFC condition, and the whole model is simplified into a single bottleneck, producing the same results as the RSB model (the difference of RTs between 2AFC and 3AFC keeps constant across the SOAs); (b) in the SRT versus 2AFC situation, the anticipation process facilitates the simple response task, which is exactly the same modeling mechanism used in modeling Karlin and Kestenbaum's experiment, as described above in this section.

Sommer et al.'s (2001) Study

Sommer et al. (2001) replicated Karlin and Kestenbaum's (1968) experiment with the ERP techniques, and they measured RT, percentage of negative RT2s, and LRP, as described in detail in the introductory section of this article. Their experimental setting was the same as that in Karlin and Kestenbaum's experiment except that T1 in Sommer et al.'s experiment was an auditory–manual task and T2 was a visual–manual task. Therefore, the same modeling mechanisms were used in our study to model Sommer et al.'s experiment.

Routes of Entities

Similar to the routes of entities in modeling Karlin and Kestenbaum's (1968) experiment, according to the functions and connections of the related brain regions, the routes of task entities in modeling Sommer et al.'s experiment are

T1: 5 →6/7→8→B→C→F→C→W→Y→Z→Hand,

T2 (choice reaction condition):

[4] The nine free parameters used by EPIC are auditory identification time, auditory detection time, visual identification time, number of selection cycles of T1 and T2, ocular orientation time, unlocking onset latency, suspension waiting time, and preparation waiting time.

$$E(RT2)(\text{simple reaction}) = \begin{cases} pRT_{2,ANTI} + (1-p)RT_{2,NOAN} & \text{If } t_a > 0 \text{ (long SOA conditions)} \\ \max(T_{1,AP} + T_{1,B} + T_{1,C} + T_{1,F} - SOA, T_{2,VP} + T_{1,A} + T_{2,C}) & \\ \quad + T_{2,F} + T_{2,C} + T_{2,V} + T_{2,Z} + T_{2,K} & \text{If } t_a = 0 \text{ (short SOA conditions)} \end{cases}. \quad (21)$$

1→2/3→4→A→C→F→C→W→Y→Z→Hand,

and

T2 (simple reaction condition):

1→2/3→4→A→C→F→C→V→Z→Hand.

Modeling of the Expected Reaction Time, Percentage of Negative Responses, and S-LRP

The expected RTs in Sommer et al.'s (2001) experiment were modeled with the same formula as in modeling Karlin and Kestenbaum's (1968) experiment except for the processing time of Server A, Server B, and the perceptual subnetwork (see Equations 19–21).

$$E(RT1) = T_{1,AP} + T_{1,B} + T_{1,C} + T_{1,F} + T_{1,C} + T_{1,Y} + T_{1,W} + T_{1,Z} + T_{1,K}. \quad (19)$$

$$E(RT2)\ (\text{choice reaction}) = \max(T_{1,AP} + T_{1,B} + T_{1,C} + T_{1,F} - SOA, T_{2,VP} + T_{2,A} + T_{2,C}) + T_{2,F} + T_{2,C} + T_{2,Y} + T_{2,W} + T_{2,Z} + T_{2,K}. \quad (20)$$

See top of page for Equation 21.

In the simple reaction condition of T2, the expected percentage of negative responses (P_n) is estimated according to the difference between the SOA and the sum of $T_{2,C}$, $T_{2,V}$, $T_{2,Z}$, $T_{2,K}$, and T_{Fst} (see Equations 22 and C3, including their derivations in Appendix C).

$$P_n = \begin{cases} 1 - \dfrac{T_{2,C} + T_{2,V} + T_{2,Z} + T_{2,K}}{SOA - T_{Fst}} & \text{If } SOA \geq u + T_{Fst} \\ 0 & \text{If } SOA < u + T_{Fst} \end{cases}. \quad (22)$$

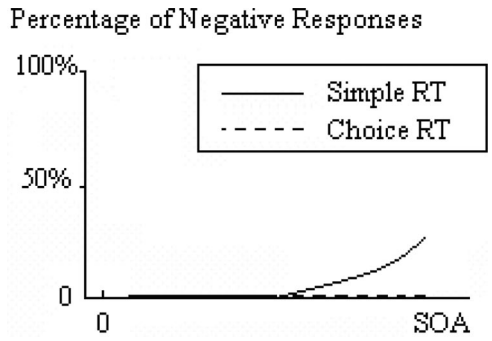

Figure 16. The expected pattern of the percentage of negative responses in Sommer, Leuthold, and Schubert's (2001) experiment. RT = reaction time; SOA = stimulus onset asynchrony.

The expected pattern of the percentage of negative responses is shown in Figure 16. In the simple reaction condition, in the short SOA conditions ($SOA < T_{2,C} + T_{2,V} + T_{2,Z} + T_{2,K} + T_{Fst}$), the expected percentage of negative responses is 0; in the long SOA conditions, the expected percentage of negative responses increases as the SOA increases following the inverse function in Equation 22. In T1 (choice RT) and the choice reaction condition of T2, the expected percentage of negative responses is 0.

Since the LRP reflects motor preparation taking place within the premotor area (Server V) or the primary motor cortex (Server Z; H. Leuthold & Jentzsch, 2001, 2002; Ulrich et al., 1998) and Server V is located before Server Z in the route of the simple reaction task, the arrival time of entities at Server V is regarded as the LRP onset time in this simple reactionsituation.[5] Equation 23, shown at the top of the next page, quantifies the onset time of S-LRP (see Appendix F for its development), which is shown in Figure 17 as the expected pattern of S-LRP with an increase of SOA.

LRP reflects motor preparation taking place within the premotor area (Server V) or the primary motor cortex (Server Z). Hence, in the choice reaction condition of T2, the premotor area (Server V) is not in the route of entities; therefore, the arrival time of entities at Server Z is the expected S-LRP onset time (see Equation 24 and Figure 17). The expected pattern of S-LRP is similar to the expected pattern of RT in this condition (see Figure 6).

$$S\text{-}LRP = \max(T_{1,AP} + T_{1,B} + T_{1,C} + T_{1,F} - SOA, T_{2,VP} + T_{2,A} + T_{2,C}) + T_{2,F} + T_{2,C} + T_{2,Y} + T_{2,W}. \quad (24)$$

Parameter Setting

All of the parameters used in the model are listed in Table A5 in Appendix A. Except for the four4 free parameters set for the

[5] Because of the high temporary accuracy of the ERP techniques (1 ms), the conduction time from the activation of brain regions to the instant when the S-LRP is observed can be ignored (Ilvonen et al., 2003).

$$S\text{-}LRP = \begin{cases} T_{1,AP} + T_{1,B} + T_{1,C} + T_{1,F} + T_{2,F} + T_{2,C} - SOA & \text{If } SOA < T_{1,AP} + T_{1,B} + T_{1,C} + T_{1,F} - (T_{2,VP} + T_{2,A} + T_{2,C}) \\ T_{2,VP} + T_{2,A} + 2T_{2,C} + T_{2,F} & \text{If } T_{1,AP} + T_{1,B} + T_{1,C} + T_{1,F} - (T_{2,VP} + T_{2,A} + T_{2,C}) \le SOA \le T_{Fst} \\ T_{Fst} + (SOA^{\beta} - T_{Fst}{}^{\beta})^{1/\beta} + T_{2,C} - SOA & \text{If } SOA > T_{Fst} \end{cases}. \quad (23)$$

long SOA conditions following ACT-R/PM's parameter-setting method, all of the values of the other parameters are the same as those in Tables A1–A4. The three dependent variables, including RT, ratio of correct response and S-LRP onset time, are modeled on the basis of the same set of parameters shown in Table A5. Moreover, the values of these free parameters set for long SOA conditions are constrained by the task properties: The processing time at Server F in the simple reaction condition is at least 18 ms (one cycle time) less than that in the choice reaction condition.

Modeling Results and Their Validation

Figure 18 shows the modeling results in comparison with experimental results. The R^2 of the model is .84, and the RMS = 53.9 ms.

The modeling results of the percentage of negative responses in comparison with the experiment result are shown in Figure 19. The R^2 of the model is .99 (SRT condition), with RMS = .025 (SRT condition) and RMS = .05 (choice RT condition). Moreover, it is found that at SOA = 700 ms, the percentage of negative RT2s is 15%, which is consistent with Sommer et al.'s (2001) experimental results (16%).

In addition, the modeling result of S-LRP exhibits a pattern similar to the experimental results (see Figure 20 for the comparison of the S-LRP onset time between the prediction of the model and the experimental results; SRT condition: R^2 = .96, RMS = 127.5 ms; choice RT condition: R^2 = .82, RMS = 229.37 ms).

The predicted S-LRP shows the same pattern as the experimental results, especially for the negative and close-to-zero S-LRP values in the SRT condition (SOA = 700 ms). The large RMS in predicting S-LRP in this experimental study might be due to two reasons: First, the majority of the QN-MHP parameters are based on MHP parameters, which are derived from behavioral rather than neurological experiments (Card et al., 1983). Second, the free parameters are set corresponding to RT data in the long SOA condition rather than the S-LRP results.

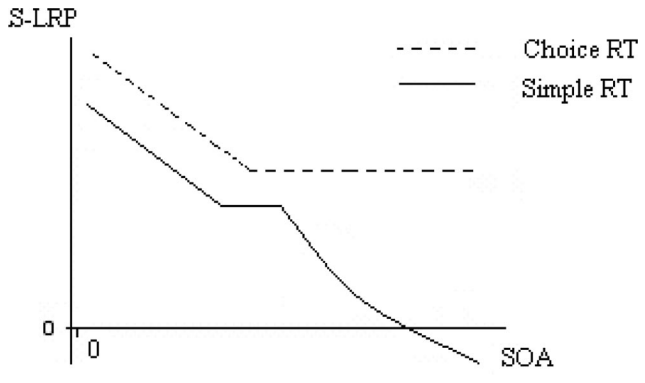

Figure 17. The expected pattern of S-LRP with an increase of SOA in T2. RT = reaction time; S-LRP = stimulus-lateralized readiness potential; SOA = stimulus onset asynchrony; T1 = Task 1; T2 = Task 2.

Brian Imaging Pattern (Jiang et al., 2004)

Jiang et al.'s (2004) experiment provides another challenging counterexample to the strategic scheduling mechanism in EPIC. In their experiment, both Tasks 1 and 2 were visual–manual choice reaction tasks (see the detailed experiment description in the introductory section of this article).

Routes of Entities

Similar to the routes in modeling the basic PRP, on the basis of the task and the corresponding functions of the brain areas, the routes of T1 and T2 are

T1: 1→2/3→4→A→C→F→C→W→Y→Z→Hand

and

T2: 1→2/3→4→A→C→F→C→W→Y→Z→Hand.

Modeling of the Expected Reaction Time

Experiment 1 in Jiang et al.'s (2004) study can be modeled by the queuing mechanism in the basic PRP directly: In the short SOA conditions, entities of T2 will not be able to enter Server F until entities of T1 leave Server F. In this process, Server F processes only the entities of individual tasks rather than scheduling the entities of two tasks actively. The mathematical equations of behavioral performance in this experiment are the same as those formulas used in modeling the basic PRP effect except for the change of the perceptual and motor subnetworks to correspond to Jiang et al.'s experimental setting (see Equations 25 and 26). The expected pattern of RT is the same as that in the basic PRP effect.

$$E(RT1) = T_{1,VP} + T_{1,A} + T_{1,C} + T_{1,F} + T_{1,C} + T_{1,Y} + T_{1,W} + T_{1,Z} + T_{1,K}, \quad (25)$$

and

$$E(RT2) = \max(T_{1,VP} + T_{1,A} + T_{1,C} + T_{1,F} - SOA, T_{2,VP} + T_{2,A} + T_{2,C}) + T_{2,F} + T_{2,C} + T_{2,Y} + T_{2,W} + T_{2,Z} + T_{2,K}. \quad (26)$$

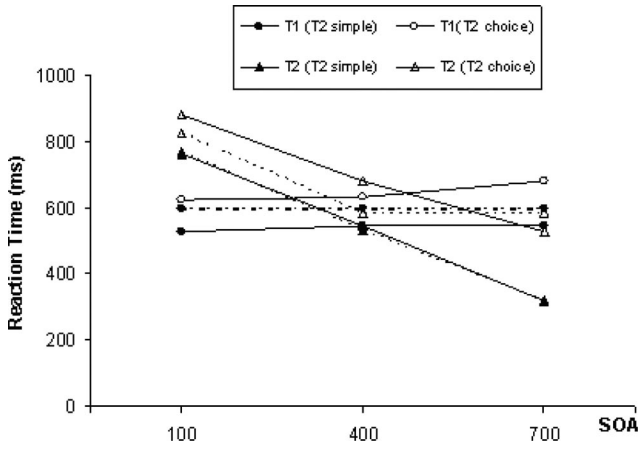

Figure 18. Reaction time in the study of Sommer, Leuthold, and Schubert (2001; solid lines) in comparison with the queuing network modeling results (dashed lines). Study data adapted from "Multiple Bottlenecks in Information Processing? An Electrophysiological Examination," by W. Sommer, H. Leuthold, and T. Schubert, 2001, *Psychonomic Bulletin & Review, 8,* p. 85. Copyright 2001 by the Psychonomic Society. SOA = stimulus onset asynchrony; T1 = Task 1; T2 = Task 2.

Modeling of BOLD Signal and Its Percentage of Change

The integrated BOLD (blood oxygen level dependent) signal—*CB*(*t*)—in the queuing network model is modeled based on the prior fMRI signal modeling work of Cohen (1997) and Anderson, Qin, Sohn, Stenger, and Carter (2003). (See Equation 27 and Appendix D for its development.)

$$CB(t) = \begin{cases} skM \int_{\frac{t-\eta}{s}}^{\frac{t}{s}} Y^a e^{-Y/b} dY & \frac{t-\eta}{s} \le Y \le \frac{t}{s} \\ 0 & \frac{t-\eta}{s} > Y \text{ or } Y > \frac{t}{s} \end{cases}, \quad (27)$$

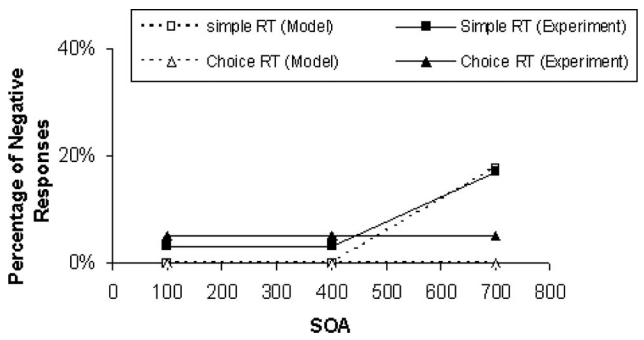

Figure 19. The percentage of negative responses in the study of Sommer, Leuthold, and Schubert (2001; solid lines) compared with the modeling results (dashed lines). Study data adapted from "Multiple Bottlenecks in Information Processing? An Electrophysiological Examination," by W. Sommer, H. Leuthold, and T. Schubert, 2001, *Psychonomic Bulletin & Review, 8,* p. 85. Copyright 2001 by the Psychonomic Society. RT = reaction time; SOA = stimulus onset asynchrony.

where *s, k, M, a,* and *b* come from the equations of Cohen (1997) and Anderson et al. (2003), determined by the properties of the brain regions with certain fMRI measurement techniques; *t* is the duration of each trial; and η in queuing networks can be quantified by Equation 28 (Gross & Harris, 1998):

$$\eta = \rho_i t = \frac{\lambda_i T_i}{Cap_i} t, \quad (28)$$

where ρ_i is Server *i*'s utilization (the fraction of time a server is busy in the total time of each trial), λ_i is the arrival rate (the number of arrivals into Server *i* during *t*), and T_i and Cap_i are the processing time and capacity of Server *i,* respectively.

For the same brain region, the percentage signal change (fMRI *PSC*) is the *CB*(*t*) of the experimental condition compared with the *CB*(*t*) of the baseline condition, $CB(t_0)$: for example, fixation condition in Jiang et al. (2004; see Equation 29); Ben-Shachar, Hendler, Kahn, Ben-Bashat, and Grodzinsky (2003).

$$PSC = \frac{CB(t) - CB(t_0)}{CB(t_0)}. \quad (29)$$

Therefore, according to Equations 27–29, *PSC* in the short and long SOA conditions (PSC_{long}, PSC_{short}) can be calculated if T_i, Cap_i, λ_i, *k, M, s, b, a,* and *t* in these conditions are given.

For the same brain regions measured by the same fMRI techniques, *s, k, M, a,* T_i, Cap_i, and *b* are expected to remain the same in the short and long SOA conditions. Furthermore, since the length of each trial is fixed either in the short or the long SOA conditions, the value of *t* also remains the same in the short and long SOA conditions. During each trial, the same amount of information arrives at the cognitive system during *t*; therefore, λ_i remains the same in the short and long SOA conditions. Therefore, according to Equations 27–29 above, for the same brain region, the

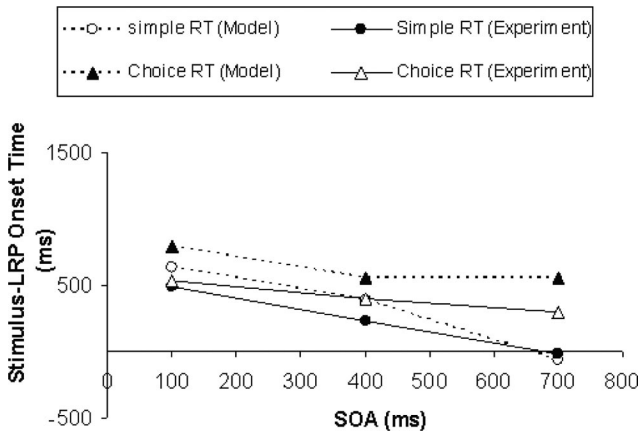

Figure 20. The S-LRP onset time in the study of Sommer, Leuthold, and Schubert (2001; solid lines) compared with the queuing network modeling results (dashed lines). Study data adapted from "Multiple Bottlenecks in Information Processing? An Electrophysiological Examination," by W. Sommer, H. Leuthold, and T. Schubert, 2001, *Psychonomic Bulletin & Review, 8,* p. 85. Copyright 2001 by the Psychonomic Society. LRP = lateralized readiness potential; RT = reaction time; S-LRP = stimulus-lateralized readiness potential; SOA = stimulus onset asynchrony.

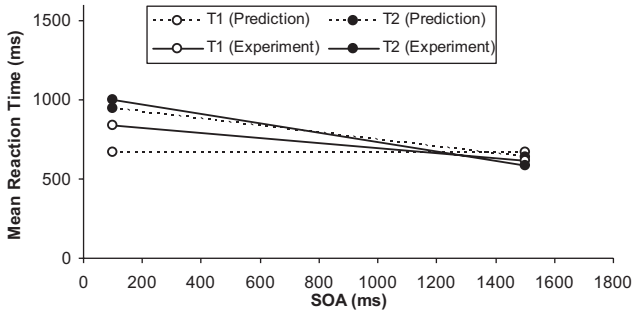

Figure 21. Reaction time in the study of Jiang, Saxe, and Kanwisher (2004; solid lines), along with the queuing network modeling results (dashed lines). SOA = stimulus onset asynchrony; T1 = Task 1; T2 = Task 2.

expected percentage of change of $CB(t)$ keeps constant across the different SOA conditions, that is,

$$\therefore CB(t)_{long} = CB(t)_{short},$$

$$\because PSC_{long} - PSC_{short} = \frac{CB(t)_{long} - CB(t_0)}{CB(t_0)} - \left[\frac{CB(t)_{short} - CB(t_0)}{CB(t_0)}\right] = \frac{CB(t)_{long} - CB(t)_{short}}{CB(t_0)},$$

and

$$\therefore PSC_{long} - PSC_{short} = 0.$$

In other words, in this queuing process, since the amount of information processed by each brain region remains the same in the short and long SOA conditions, the integrated BOLD signal remains the same in the short and long SOA conditions.

Parameter Setting

Except for the two free parameters set for the long SOA condition, the values of the other parameters are the same as in those in Tables A1–A5 in Appendix A. Moreover, the values of the free parameters set for the long SOA conditions are constrained by the nature of the tasks: The processing times of entities at Server F in both T1 and T2 are close to each other (the difference between these two processing times is less than 120 ms) since the difficulty levels of the two choice reaction tasks are similar (see Appendix A, Table A6).

Modeling Results and Their Validation

Using the equations derived in the previous sections, the predicted results of both RT and the percentage of change of fMRI signal are presented and validated with the target experiment results.

Reaction Time

Figure 21 shows the modeling results in comparison with experimental results in RT: The R^2 of the model is .73 (both T1 and T2), and the RMS = 95.9 ms.

fMRI Signal

Figure 22 shows the modeling results in comparison with experimental results of the fMRI signal (RMS = 0.03).

For both RT and brain imaging data ($PSC_{long} - PSC_{short}$), the current model's prediction captures the major patterns of Jiang et al.'s (2004) experimental findings. The relatively large RMS in predicting the brain imaging signals might still be due to the behavioral rather than neurological basis of MHP parameters.

Response Grouping Effect

The experimental study of Ruthruff, Pashler, and Klaassen (2001) found the response grouping effect by asking the participants to emit the responses of two tasks at the same time. The two tasks in their experiment were a tone-counting task and a spatial working memory task (see the detailed experiment description in the introductory part of this article).

Routes of Entities

Considering the experimental task and the corresponding functions of the brain areas, it is possible that the lateral BA 6 (represented by Server V), the SFS (represented by Server F), or both can be involved in processing the spatial working memory task (see the introductory section of this article). According to the neuron pathways and connections between these two brain regions

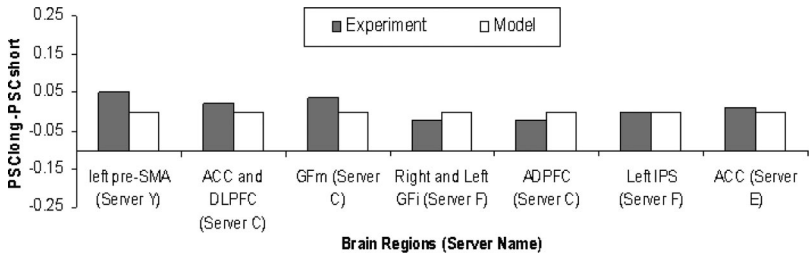

Figure 22. Difference of PSC between the long and short SOA conditions ($PSC_{long} - PSC_{short}$) in the study of Jiang, Saxe, and Kanwisher (2004), along with the queuing network modeling results. ACC= anterior cingulate cortex; ADPFC = anterior-dorsal prefrontal cortex; DLPFC = dorsal lateral prefrontal cortex; GFi = inferior frontal gyrus; GFm = middle frontal gyrus; IPS = intraparietal sulcus; PSC = percentage signal change; SMA = supplementary motor area.

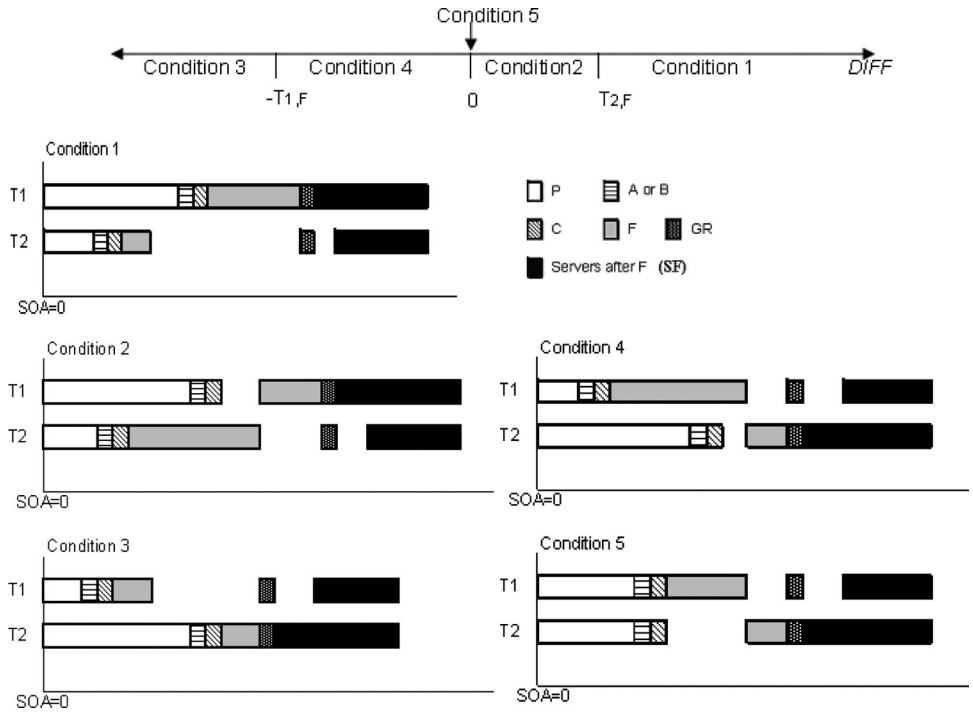

Figure 23. Five possible conditions in estimating the $RT_{1\text{-}route}$ in modeling the response grouping effect. $DIFF = T_{1,P} + T_{1,A\backslash B} + T_{1,C} - (T_{2,P} + T_{2,A\backslash B} + T_{2,C})$; RT = reaction time; SOA = stimulus onset asynchrony; T1 = Task 1; T2 = Task 2.

and other regions, the two possible routes to process the spatial working memory task are as follows:

1. 1→2/3→4→A→C→F→C→W→Y→Z→Hand.

2. 1→2/3→4→A→V→W→Y→Z→Hand.

According to the function of Server F (IPS in Server F is active for the mental calculation and numerical operation task), the route for the numerical operations (i.e., tone-counting) task is

5→6/7→8→B→C→F→C→W→Y→Z→Hand.

Two modeling methods have been used to quantify the response grouping effect. In this section, we introduce the first method, considering only the route without the practice effect on performance (1→2/3→4→A→C→F→C→W→→Y→Z→Hand). In modeling the practice effect of PRP, we introduce the second method, which considers the practice effect on performance as well as the two possible routes in this spatial working memory task.

Modeling of the Expected Reaction Time

If the practice effect is not considered in Ruthruff, Pashler, and Klaassen's (2001) experiment, entities of the spatial working memory task and the tone-counting task both pass through the bottleneck server (Server F), which is similar to the basic PRP situation. In general, there are five possible conditions of the expected RT—$E(RT_{1\text{-}route})$—depending on the different values of *DIFF* (assuming $T_{1,P} + T_{1,A\backslash B} + T_{1,C} - [T_{2,P} + T_{2,A\backslash B} + T_{2,C}] =$ *DIFF*). (Because SOA = 0 and the responses of the two tasks are emitted at the same time, the expected RTs for the two tasks are equal; see Figure 23). A set of five equations corresponding to these five possible conditions of the expected RT—$E(RT_{1\text{-}route})$—is developed in Appendix G.

On the basis of the equations developed in Appendix G and the modeling mechanism above, the expected patterns of RT in these five conditions are shown in Figure 24. The expected RT in the dual-task condition is longer than that in the single reaction condition, and the expected RT in Conditions 1 and 3 is shorter than that in Conditions 2, 4, and 5.

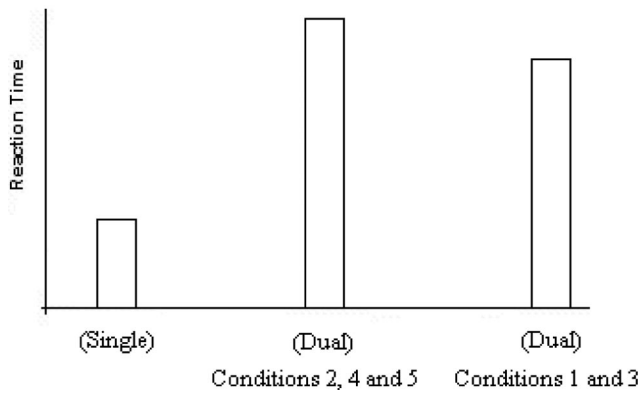

Figure 24. The expected patterns of reaction time in the single- and dual-task conditions in Ruthruff, Johnston, and Van Selst's (2001) experiment (without considering the practice effect).

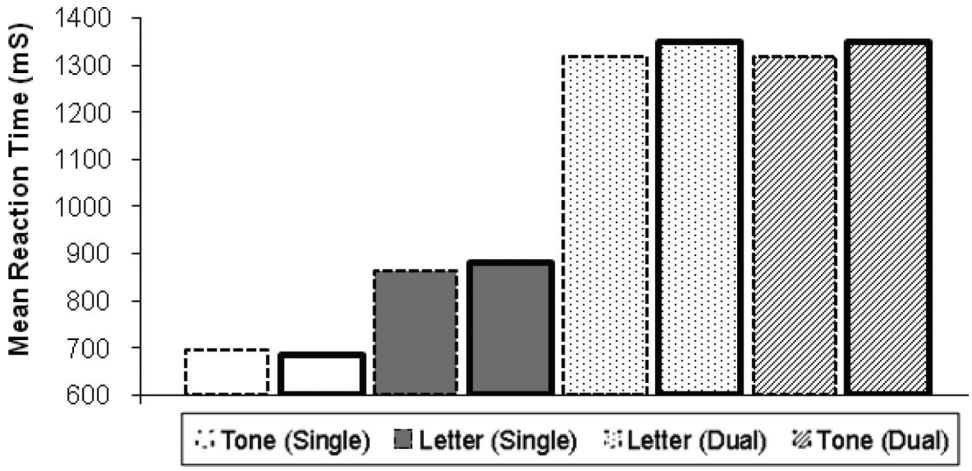

Figure 25. Mean reaction time in Ruthruff, Pashler, and Klaassen's (2001) experiment compared with modeling results (practice effect is not considered). (Modeling results: columns with dashed line borders; experimental results: columns with solid line borders.)

Parameter Setting

Only two free parameters (F_{Tone} and F_{Letter}) are used, and they are set on the basis of the RT in the single-task condition (see Appendix A, Table A7). Moreover, the values of these free parameters set at the long SOA conditions are constrained by the task properties: The spatial working memory task involving mental rotations and the tone-counting task involving mathematical addition are more complex than the choice reaction task in the previous experimental studies in PRP, thus increasing the number of processing cycles at Server F compared with the processing times in the regular choice reaction conditions.

Modeling Results and Their Validation

Figure 25 shows the modeling results compared with experimental results: Without considering the practice effect, the R^2 of the model is .99, and the RMS = 18 ms.

Practice Effect

In the experimental studies of Ruthruff, Johnston, and Van Selst (2001) and Oberauer and Kliegl (2004), participants received relatively extensive practice, and there are two possible routes of the spatial working memory task in the cognitive system (see the two routes in modeling Ruthruff, Pashler, & Klaassen's, 2001, study in the previous section). To model the practice effect in general, QN-MHP makes two task-independent assumptions, which have been used in our work on modeling the practice effect in transcription typing (Wu, Liu, & Walsh, in press). The first assumption quantifies the change of routing probability of entities in the network during the practice process, and the second assumption quantifies the increase of servers' processing speed via practice.

Routes Rewiring Via Practice

It is well recognized that the human brain is not only a network of brain regions but also a system that is able to change itself dynamically in the process of development and learning (Chklovskii et al., 2004; Habib, 2003). On the one hand, the brain traffic concept in neuroscience suggests that information flow (possibly represented by spike trains) in the brain also exhibits features of traffic flow in the network. On the other hand, different brain areas are activated during the visual–motor practice process (Aizawa et al., 1991; Petersen, van Mier, Fiez, & Raichle, 1998; van Mier, Tempel, Perlmutter, Raichle, & Petersen, 1998). This plasticity aspect of the human brain concerns the change of synaptic connection strengths between neurons and rewiring among neural pathways—information flow changes from one neuron pathway to another, with a stronger synaptic connection strength and a higher efficiency in information processing. This rapid regulation is related to a brain-derived neurotrophic factor regarded as a signal of synaptic plasticity in adults (Black, 1999; Braus, 2004).

The routing probability equation (see Equation 30) in the queuing network is developed on the basis of the brain traffic concept above (see Appendix E for its derivation) and Black's (1999) study, where the routing probability (P_i) stands for the probability that information flow (represented by entities) passes through a certain neuron pathway (Route i) in a total of U multiple routes; additionally, sojourn time (S_i) is defined as the sum of waiting time (W_i) and processing time (T_i) of these information entities along that neuron pathway, which is a standard definition in the queuing network literature:

$$P_i = \frac{1/S_i}{\sum_{j=1}^{U} \frac{1}{S_j}}. \tag{30}$$

In other words, the synaptic connection strength, which depends on the practice processes that improve the effectiveness of information processing in the brain regions along the neuron pathway (route), determines the probability that the information entities enter one of multiple neuron pathways (routes). If the majority of

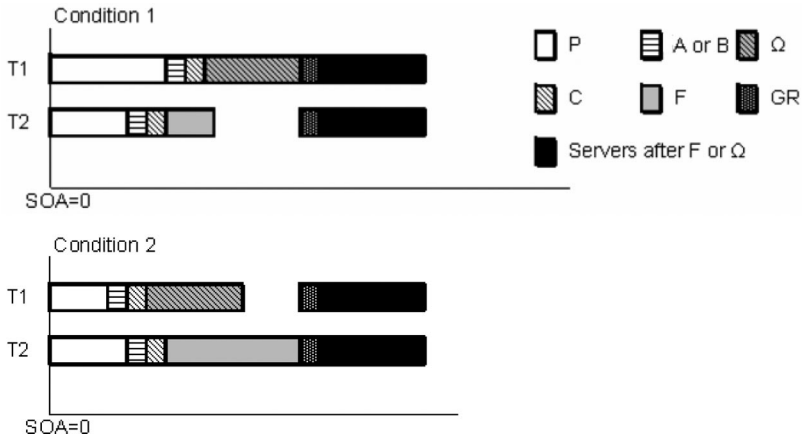

Figure 26. Two possible conditions in estimating the $RT_{2\text{-}route}$. RT = reaction time; SOA = stimulus onset asynchrony; T1 = Task 1; T2 = Task 2.

entities change their route from one to another, rewiring of routes (neuron pathways) occurs.

Reduction of Processing Time at Individual Servers Via Practice

Because the exponential function fits the practice processes in various tasks, including memory search, motor learning, visual search, and mathematical operations, better than the power law (Heathcote, Brown, & Mewhort, 2000), it is applied to model the practice process in each server (see Equation 31).

$$T_i = A_i + B_i \operatorname{Exp}(-\alpha_i N_i), \tag{31}$$

where A_i is the minimal processing time of Server i after intensive practice, B_i represents the change of expected value of processing time of Server i from the beginning to the end of practice, α_i is the learning rate of Server i, and N_i is the number of entities processed by Server i.

Modeling Ruthruff, Johnston, and Van Selst's (2001) Experiment Considering the Practice Effect

In Ruthruff, Johnston, and Van Selst's (2001) experiment, participants received extensive single- and dual-task practices; hence, there are two routes of entities in performing the same spatial working memory task (see the description above of the two routes in modeling of Ruthruff, Johnston, & Van Selst's, 2001, experiment). In the dual-task practice condition,[6] sojourn time at Server C increased from the processing time only to the sum of waiting time (entities maintained at Server C to wait for the previous entities finished processing at Server F) and processing time. Therefore, according to Equation 30 in the route rewiring, the probability of entities entering Server C decreases and the probability of entering Server V increases because of the increased sojourn time, which causes the processing time at Server V to decrease further. As a result, entities take two routes in the dual-task practice condition: A→V or A→C→F. The higher the probability of entities taking the route from Server A to V, the higher the probability that the Server F bottleneck is bypassed and the PRP effect disappears. Therefore, QN-MHP is able to model the disappearance of the PRP effect in dual-task practice based on the queue network architecture.

In the situation in which entities of the two tasks take the two separate routes without any conflict with each other, the expected RT of both tasks—$E(RT_{2\text{-}route})$—can be estimated on the basis of Figure 26 and Equation 32. Since the entities of T1 and T2 take two independent routes at the cognitive subnetwork and entities of T2 are never blocked by the entities of T1 in their route (see Figure 26), in general, the expected mean of RT of both tasks—$E(RT_{2\text{-}route})$—is quantified in Equation 33 (assuming Ω represents any server that can also have the function of Server F in the target task after practice).

$$E(RT_{2\text{-}route}) = \max(T_{1,P} + T_{1,A\backslash B} + T_{1,\Omega}, T_{2,P} + T_{2,A\backslash B} + T_{2,C} + T_{2,F}) + GR + \max(SF_1, SF_2), \tag{32}$$

where $T_{1,\Omega}$ stands for the current processing time of Server Ω, $T_{1,A\backslash B}$ is the current processing time at Server A or B (depends on T1's route), GR refers to the time in grouping the two responses together, and SF_1 and SF_2 are the sum of current processing time of servers after Server F (e.g., Servers Y, W, and Z) of T1 and T2, respectively.

Specifically, $E(RT_{2\text{-}route})$ in Ruthruff, Johnston, and Van Selst's (2001) experiment can be estimated in Equation 33 in which V represents Ω.

$$E(RT_{2\text{-}route}) = \max(T_{S,P} + T_{S,A} + T_{S,VS}, T_{T,P} + T_{T,B} + T_{T,C} + T_{T,F}) + GR + \max(T_{S,C} + T_{S,W} + T_{S,Y} + T_{S,Z} + T_{S,K}, T_{T,C} + T_{T,Y} + T_{T,Z} + T_{T,VO}). \tag{33}$$

Suppose $P_{2\text{-}route}$ is the possibility that the entities take the second route (A→V→Z) in the practice situation, that is, the possibility

[6] The modeling mechanism of Oberauer and Kliegl's (2004) experiment explains why only dual-task practice forms the two routes in processing the spatial working memory task.

that the entities of the two tasks take two routes (see Equation 34); therefore, the expected RT—$E(RT_{practice})$—in the practice situation is

$$E(RT_{practice}) = P_{2\text{-}route}\, E(RT_{2\text{-}route}) + (1 - P_{2\text{-}route})\, E(RT_{1\text{-}route}). \quad (34)$$

On the basis of the equations developed above, Figure 27 shows the expected pattern of RT in the single- and dual-task conditions (the expected RTs of Conditions 1 and 2 in Figure 26 in the modeling mechanism overlap in Figure 27).

Parameter Setting

Only three free parameters are used when the practice effect is taken into consideration (see Appendix A, Table A8). The values of these free parameters set for the long SOA conditions are also constrained by the task properties: The spatial working memory task involving mental rotations and the tone-counting task involving mathematical addition are more complex than the choice reaction task in the previous experimental studies in PRP, increasing the number of cycles at Server F compared with the processing times at regular choice reaction conditions; since Server V processes spatial working memory information after extensive practice (Mitz et al., 1991; see the introductory section of this article), the processing time of Server V without extensive practice is longer than that after extensive practice.

Modeling Results and Their Validation

Figure 28 shows the modeling results compared with the experimental results considering the practice effect: The R^2 of the model is .99, and RMS = 0.1 ms.

Modeling Oberauer and Kliegl's (2004) Study

As described earlier in this article, Oberauer and Kliegl's (2004) experimental study found that the dual-task practice group produced a smaller PRP effect than the single-task practice group (Oberauer & Kliegl, 2004).

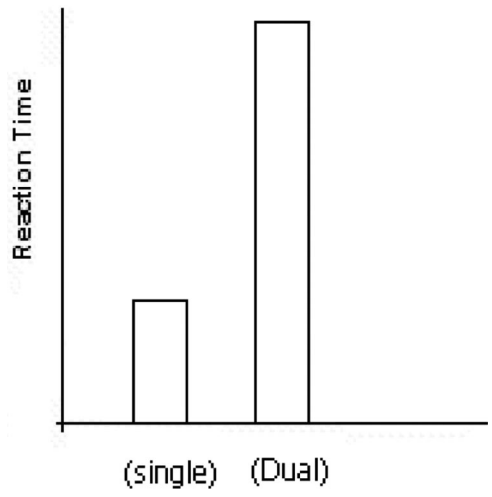

Figure 27. The expected pattern of reaction time in the single- and dual-task conditions in Ruthruff, Johnston, and Van Selst's (2001) experiment (considering the practice effect).

Routes of Entities

Similar to the route selection in the modeling of Ruthruff, Johnston, and Van Selst's (2001) experiment, the two possible routes to process the spatial working memory task are as follows:

1. 1→2/3→4→A→C→F→C→W→Y→Z→Hand.

2. 1→2/3→4→A→V→W→Y→Z→Hand.

According to the function of Server F (IPS in Server F is active for the mental calculation task), the route for the numerical operations task is

5→6/7→8→B→C→F→C→W→Y→Z→Hand.

Modeling Mechanisms

On the basis of the two possible routes in performing the spatial memory task, starting at Server A, we have Route 1 (A→C→F→C→W→Y→Z→Hand) and Route 2 (A→V→W→Y→Z→Hand). In the single-task practice condition, entities at Server A always enter Server C and then enter Server V because sojourn time at Server C is shorter than Server V (the mean processing time at Server C = 18 ms; sojourn time at Server C = 18 ms; mean processing time at Server V = 1,540 ms; see the value of these parameters in Ruthruff, Johnston, & Van Selst's, 2001, experiment; sojourn time at Server V = 1,540 ms).

Since very few entities enter Server V and its processing time does not decrease much in the single-task practice task condition, the majority of entities still take the same route throughout the practice sessions. As a result, Server F bottleneck is not bypassed by the majority of entities, the PRP effect does not disappear under the single-task practice condition, and the reduced the PRP effect is due to reduced processing time at Server F and the other servers.

In the dual-task practice condition, there is a 50% chance that sojourn time at Server C increases from the processing time to the sum of waiting time (entities maintained at Server C to wait for the previous entities to finish processing at Server F) and processing time. Therefore, similar to the modeling of Ruthruff, Johnston, and Van Selst's (2001) experiment, according to Equation 30 above, the probability of entity entering Server C decreases and the probability of entering Server V increases because of the increased sojourn time, thus decreasing the processing time at Server V further. The higher the probability of entities taking the route from Server A to Server V, the higher the probability that Server F bottleneck is bypassed and the PRP effect disappears.

Mathematical Modeling of Expected Reaction Time

Sequential Test

In both the sequential pretest and posttest, the expected RT—$E(RT_{pre\text{-}seq})$—in both the single-task practice and dual-task practice groups is the maximum of RT1 and RT2 (see introduction to their experiment, above; also see Equation 35):

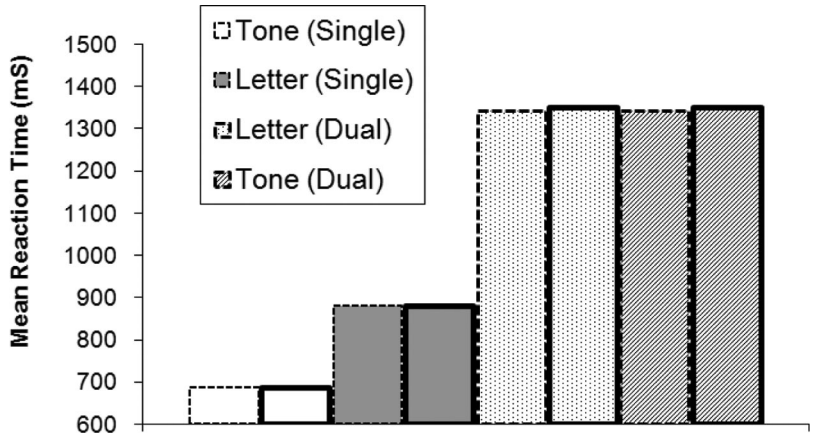

Figure 28. Mean reaction time in Ruthruff, Johnston, and Van Selst's (2001) experiment compared with modeling results (practice effect is considered). (Modeling results: columns with dashed line borders; experimental results: columns with solid line borders.) A color version of this figure is available on the Web at http://dx.doi.org/10.1037/a0013123.supp.

$$E(RT_{pre\text{-}seq}) = \max(T_{S,P} + T_{S,A} + T_{S,C} + T_{S,F} + T_{S,C} + T_{S,Y} + T_{S,W} + T_{S,Y} + T_{S,Z} + T_{S,K}, T_{T,P} + T_{T,B} + T_{T,C} + T_{T,F} + T_{T,C} + T_{T,Y} + T_{T,W} + T_{T,Y} + T_{T,Z} + T_{T,K}), \quad (35)$$

where all of the server processing times refer to the current processing times determined by Equation 31.

Simultaneous Test

Pretest RT. In the simultaneous test of the pretest, the expected RT—$E(RT_{pre\text{-}simul})$—in the two practice groups is similar to that in the basic PRP paradigm (SOA = 0); however, on the basis of the experiment design in Oberauer and Kliegl (2004), there is a 50% chance that either the spatial or the numerical operation task can be treated as T1. Hence, the expected RT in this simultaneous test for both groups is quantified as Equation 36.

$$E(RT_{pre\text{-}simul}) = 0.5[\max(T_{S,P} + T_{S,A} + T_{S,C} + T_{S,F}, T_{T,P} + T_{T,B} + T_{T,C}) + T_{T,F} + T_{T,C} + T_{T,Y} + T_{T,W} + T_{T,Z} + T_{T,K}] + 0.5[\max(T_{T,P} + T_{T,B} + T_{T,C} + T_{T,F}, T_{S,P} + T_{S,A} + T_{S,C}) + T_{S,F} + T_{S,C} + T_{S,Y} + T_{S,W} + T_{S,Z} + T_{S,K})]. \quad (36)$$

Posttest RT: Dual-task practice group. At the end of practice, there are two situations in estimating the expected RT in Oberauer and Kliegl's (2004) experiment: First, when the entities of the two tasks take two independent routes (A→V→Z and B→CμF→C→W→Y→Z), the expected RT—$E(RT_{2\text{-}route})$—is the maximum of RT of T1 and T2 (see Figure 29 and Equation 37).

$$E(RT_{2\text{-}route}) = \max(T_{S,P} + T_{S,A} + T_{S,VS} + T_{S,Z} + T_{S,K}, T_{T,P} + T_{T,B} + T_{T,C} + T_{T,F} + T_{T,C} + T_{T,Y} + T_{T,W} + T_{T,Z} + T_{T,K}). \quad (37)$$

Second, when the entities of both tasks enter Server F in the cognitive subnetwork, the expected RT—$E(RT_{1\text{-}route})$—can be quantified by Equation 38 except that the processing times of the servers change to the current processing times after practice.

$$E(RT_{1\text{-}route}) = 0.5[\max(T_{S,P} + T_{S,A} + T_{S,C} + T_{S,F}, T_{T,P} + T_{T,B} + T_{T,C}) + T_{T,F} + T_{T,C} + T_{T,Y} + T_{T,W} + T_{T,Z} + T_{T,K}] + 0.5[\max(T_{T,P} + T_{T,B} + T_{T,C} + T_{T,F}, T_{S,P} + T_{S,A} + T_{S,C}) + T_{S,F} + T_{S,C} + T_{S,Y} + T_{S,W} + T_{S,Z} + T_{S,K}]. \quad (38)$$

Therefore, similar to the quantification of RT in Ruthruff, Johnston, and Van Selst's (2001) experiment, the expected RT in Oberauer's experiment—$E(RT_{practice\text{-}dual})$—can be quantified with Equation 39, where $P_{2\text{-}route\text{-}dual}$ (determined by Equation 30) refers to the probability that entities of spatial operation task take the second route (A→V→Z) in the dual-task practice group.

$$E(RT_{practice\text{-}dual}) = P_{2\text{-}route\text{-}dual}E(RT_{2\text{-}route}) + (1 - P_{2\text{-}route\text{-}dual})E(RT_{1\text{-}route}). \quad (39)$$

Posttest RT: Single-task practice group. The expected RT of the single-task practice group—$E(RT_{practice\text{-}single})$—can also be quantified as Equation 40, where $P_{2\text{-}route\text{-}single}$ (determined by Equation 30) refers to the probability that entities of the spatial operation task take the second route (A→V→Z) in the single-task practice group.

$$E(RT_{practice\text{-}single}) = P_{2\text{-}route\text{-}single}E(RT_{2\text{-}route}) + (1 - P_{2\text{-}route\text{-}single})E(RT_{1\text{-}route}). \quad (40)$$

On the basis of the equations developed above and the modeling mechanism, Figure 30 shows the expected patterns of RT for the single-task and dual-task practice groups. The inverse relation between the probability of routing and sojourn time in Equation 30 produces a nonlinear relation between the SOA and RT, and the

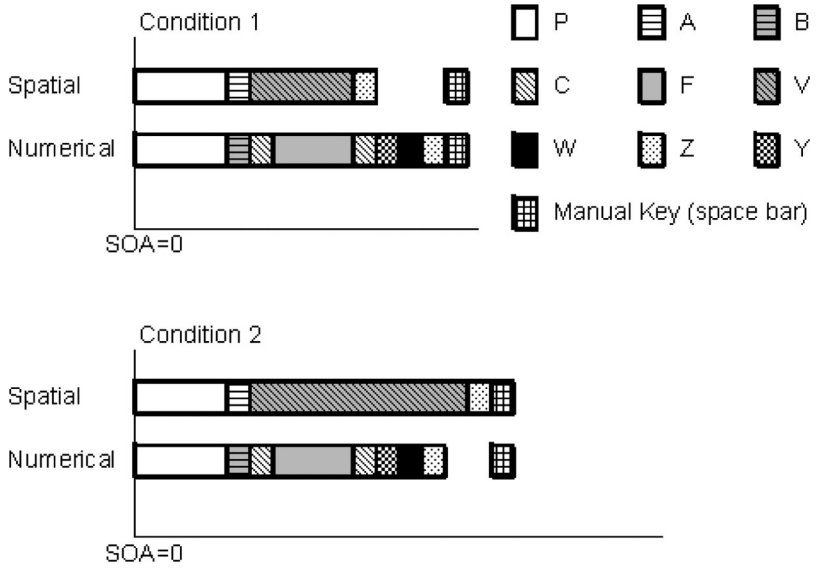

Figure 29. Two possible conditions of reaction time in the simultaneous posttest of the dual-task practice group (in both Conditions 1 and 2, the expected reaction time is the maximum of each individual task). SOA = stimulus onset asynchrony.

slope of the curve of the dual-task practice group is greater than that of single-task practice group because of the higher probability of longer sojourn times at Server C in the dual-task practice condition than the single-task practice condition (see the modeling mechanism in this section). Therefore, it is predicted that the dual-task practice group will improve their dual-task performance faster than the single-task practice group.

Parameter Setting

Only two free parameters were used in the parameter-setting process (see Appendix A, Table A9): $T_{S,F}$ and $T_{T,F}$. The values of these free parameters set for the long SOA conditions are also constrained by the task properties: The spatial working memory task involving mental updating of the current target and the numerical operation task involving mathematical addition or subtraction are more complex than the choice reaction task in the previous experimental studies in PRP, thus increasing the number of cycles at Server F compared with the processing times in regular choice reaction conditions.

Modeling Results and Their Validation

Figure 31 shows the modeling results compared with experimental results in the single- and dual-task practice groups. For the single-task practice group, the R^2 of the model is .99, and the RMS = 46.4 ms[7]; for the dual-task practice group, the R^2 of the model is .99, and the RMS = 76.7 ms.

DISCUSSION

In this article, we have described how the queuing network model is able to account for various experimental findings in PRP, including those counterexamples to the existing models. In this modeling work, we have demonstrated the important theoretical contributions and unique features of the queuing network architecture in understanding cognitive architecture and modeling multiple-task performance.

A unique theoretical position and a corresponding feature of the queuing network architecture compared with other cognitive architectures is its hybrid cognitive network structure with both serial and parallel information-processing components in its cognitive subnetwork and the concept of queuing as a coordination mechanism without the need for any executive process. First, on the basis of neuroscience findings that different brain areas (e.g., DLPFC, IPS, and ACC) serve different functions in the cognitive stage and psychological research on different cognitive modules, QN-MHP decomposes the cognitive stage into a network, and each of its servers performs a distinct role in cognitive processing. This network structure allows QN-MHP to quantify the experimental results of Schumacher et al. (1999) and Hawkins et al. (1979) showing the subadditive difficulty effect.

Second, on the basis of Byrne and Anderson's (2001) finding that humans cannot perform two arithmetic tasks at once, QN-MHP assumes that Server F is serial while other cognitive servers are parallel. As pointed out in Liu et al. (2006),

> from the theoretical point of view, although Byrne and Anderson's experiment raises serious doubts about human ability to perform two *complex* cognitive tasks at once, it does not logically imply that human cognitive system cannot perform *any* two or more activities at once at all. (Liu et al., 2006, p. 44)
>
> It is logically possible that the separate servers in the "cognitive network" work concurrently, but certain servers within this network (such as the server responsible for complex cognitive functions such

[7] Even though the absolute value of RMS is higher than the modeling results of previous studies, the relative RMS compared with the whole range of RTs (0–3,000 ms) is still small.

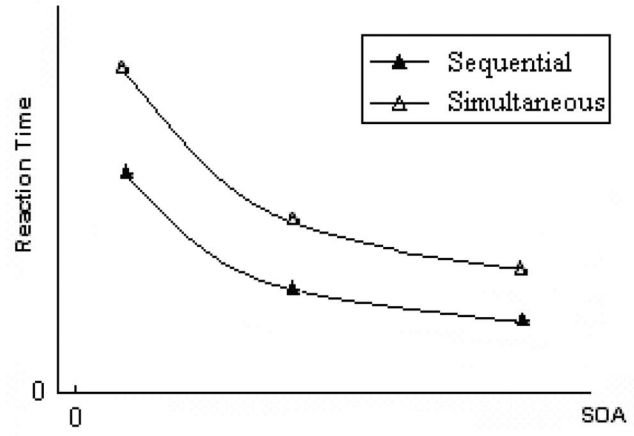

(Single-task practice group)

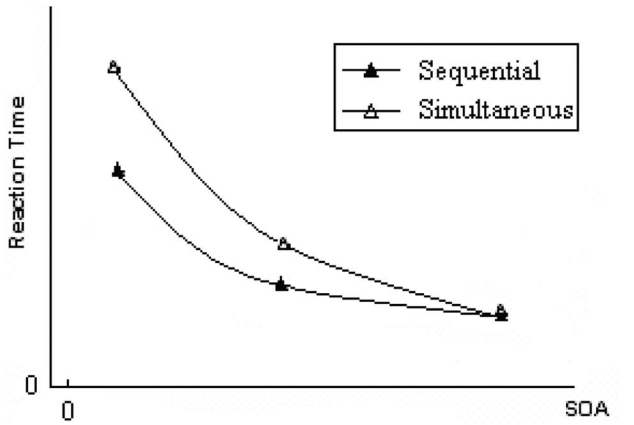

(Dual-task practice group)

Figure 30. The expected patterns of reaction time of the single- and dual-task practice groups in Oberauer and Kliegl's (2004) experiment. SOA = stimulus onset asynchrony.

> as mental arithmetic) can only process one "rule" at a time. (Liu et al., 2006, p. 45)

The current work on PRP modeling with closed-form mathematical equations offers a strong support to this theoretical position since the modeling results would not appear and the mathematical equations would break down if we did not assume F to be serial or if we assigned serial processing to any other servers.

Third, as the first word of the name of the queuing network architecture and the title of this article indicate, queuing is a unique and central theoretical concept in our work. Queuing (waiting for service) at the various servers while task entities compete for service allows multitask interference and performance patterns to emerge without the need for any executive process (Liu, 1996, 1997; Liu et al., 2006), whether a specialized (Meyer & Kieras, 1997a, 1997b) or a general one (Salvucci & Taatgen, 2008).

The hybrid cognitive structure and queuing allow QN-MHP to model a range of PRP phenomena without the need for any executive process, including the brain imaging patterns and the response grouping effect; they also explain why dual-task practice can improve human performance in two simultaneous complex mental operations (e.g., mathematical calculations) faster than single-task practice. The parallel information-processing activities in the cognitive servers other than Server F enable QN-MHP to model the disappearance of the PRP effect after extensive practice.

The overall mathematical structure of the queuing network model and entity-based information processing are also unique properties of the queuing network model. As shown in this article, these properties enable QN-MHP to mathematically quantify the interactions among the servers and to derive and predict behavior patterns and general trends without the need for simulation. In this article, all of the empirical PRP data have been modeled with closed-form mathematical equations, without any reliance on simulation. Using the mathematical structure of queuing networks and entity-based processing, the model is also able to explain why the

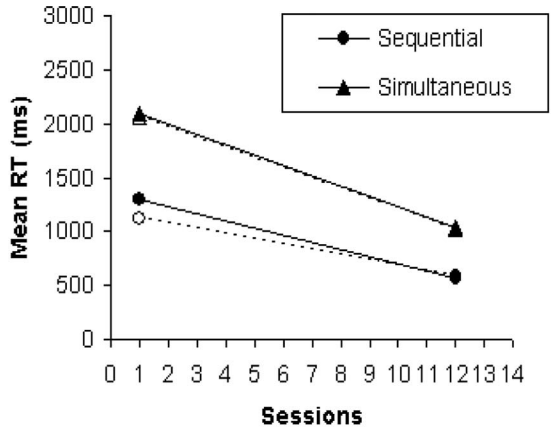

(Single-task practice group)

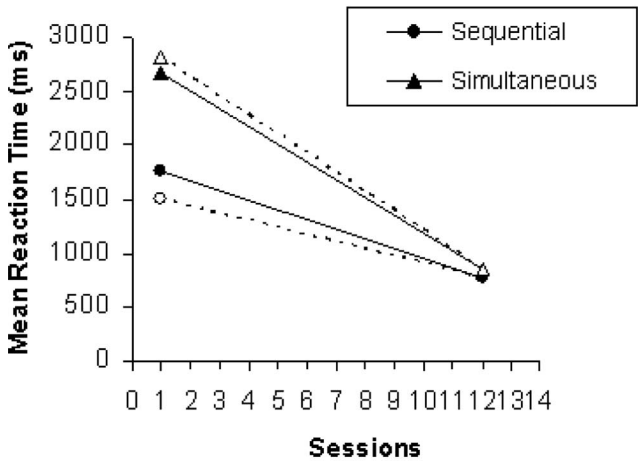

(Practice-task practice group)

Figure 31. Mean reaction time in Oberauer and Kliegl's (2004) experiment (solid lines) compared with modeling results (dashed lines). Experimental data adapted from "Simultaneous Cognitive Operations in Working Memory After Dual-Task Practice," by K. Oberauer & R. Kliegl, 2004, *Journal of Experimental Psychology: Human Perception and Performance, 30,* p. 702. Copyright 2004 by the American Psychological Association. RT = reaction time.

PRP effect disappears only via dual-task practice and how competition for service between the two streams of entities representing T1 and T2 through the network can yield the PRP effects without devising a task-specific procedure to interleave production rules into a serial program or an executive process to interactively control task processes (Liu et al., 2006).

Furthermore, these features of the queuing network model are consistent with the findings of neuroscience in dual tasks. For example, on the basis of a comprehensive review of more than 10 fMRI studies in dual tasks, Collette and Linden (2002) concluded that "no specific area could be associated with any cognitive processor for dual-task performance and that dual-task performance coordination depends mainly on the interaction between cerebral areas already activated in the single task" (pp. 117–118). McIntosh (2000) stated that

> there is no conductor in the brain. . . . [A] collection of neural ensembles that depict a memory trace, for example, may be activated through an external stimulus that evokes the memory trace or through internally initiated activity that similarly engages the trace. Such a property avoids the difficult situation of postulating a "neural conductor" or "executive" that controls the unfolding of cognition. The temporal and spatial unfolding of cognition results from the dynamic interactions among several areas of the brain (e.g., Hebb, 1949). (McIntosh, 2000, pp. 863–864)

QN-MHP modeled all of the major counterexamples to RSB, EPIC-SRD, and ACT-R/PM with fewer or the same number of free parameters, and there is no task-specific assumption in the current modeling work. It should be noted here that the settings of the entities' routes in modeling each experimental study in this modeling work are not task-specific assumptions. The routes of entities are selected on the basis of a task-independent rule—the function of brain regions (represented by the servers) determines which regions (servers) are selected in the route, and the anatomical connections among these regions determine the directions of information flow (represented by entities) in the route. This task-independent rule is consistent with the method of determining the information flow in different brain regions in neuroscience (Taylor et al., 2000). In all of the choice RT conditions, the routes of entities in the cognitive subnetwork are the same, except Server A or B, depending on the content of stimuli (phonological or visual), and their routes are changed only in the perceptual and the motor subnetworks according to the particular task setting. In the SRT and spatial working memory task conditions, the routes are determined by the findings in brain imaging studies. Even though fMRI techniques are not powerful in measuring brain activity along the time dimension, ample research shows that they can be used to determine the route of information processing in the brain with the anatomic connection of neuron pathways among these regions (Horwitz et al., 1999; McIntosh, 1999, 2000; Sporns et al., 2000; Taylor, 2003; Taylor et al., 2000).

While QN-MHP demonstrates its unique features in modeling the various PRP phenomena, a concern may be raised that if entities of T2 arrive at Server F earlier than entities of T1 in the short SOA conditions, Server F will process entities of T2 first, and the order of the responses might be reversed. We should point out that in the experimental studies modeled in this article, except for the experiment related to the response grouping effect and Hawkins et al.'s (1979) experiment, the SOAs are positive and greater than 50 ms. QN-MHP uses the same parameter value (τ_p) as MHP to represent the visual and auditory perception time, under which the chance that T2 entities arrive at Server F earlier than T1 entities is very small. Moreover, the chance that R2 is made earlier than R1 becomes even smaller since it requires two conditions to be met at the same time (entities of T2 arrive at Server F earlier than the entities of T1 and the sums of the processing times of entities of T1 in the cognitive and the motor subnetworks are greater than or equal to that of the entities of T2). Furthermore, even if R2 is made earlier than R1 on rare occasions, it is still consistent with empirical results in PRP that participants sometimes did accidentally reverse the order of their response (Pashler, 1990).

We plan to continue our QN-MHP modeling work in the future. For example, we plan to explore how QN-MHP may be used to explain and quantify the activation patterns of brain regions in various kinds of dual-task situations summarized by Collette and Linden (2002). Because the functions of the cognitive system in QN-MHP are distributed among the servers in the network and QN-MHP does not rely on a certain conductor server in coordinating or controlling the processing of other servers, we envision it possible to model these fMRI results with the natural interaction among servers. We also plan to extend our QN-MHP work of modeling task switching performance in basic psychological studies (Schneider & Logan, in press) and complex performance of dual tasks in daily life, for example, driving or flying. Liu et al. (2006) initiated the first step in modeling dual-task performance without using task-specific procedures to interleave production rules into a serial program or an executive process to interactively control task processes. In other words, once the task procedures of each individual task are implemented in the model, the model will generate dual-task performance by letting the two streams of entities representing the two individual tasks in a dual task run through the model. With this modeling approach, we have successfully modeled a range of complex tasks, including driving (Liu et al., 2006; Wu & Liu, 2007a) and transcription typing (Wu & Liu, 2008). The PRP modeling work reported in this article is one of our modeling efforts along this direction, focusing on the most basic and fundamental aspect of multitask performance and using closed-form mathematical equations as the modeling method.

In summary, this modeling work accounts for dual-task performance in PRP with fewer or equal numbers of free parameters compared with existing models and is consistent with findings in a brain imaging study (Jiang et al., 2004) and an electrophysiological study (Sommer et al., 2001) regarding the neural mechanisms involved in generating basic dual-task performance in PRP. This modeling work offers an alternative theoretical explanation for various PRP phenomena, and it also demonstrates the importance of the concepts of queuing and hybrid network structure in understanding cognitive architecture and in modeling multitask performance.

References

Aizawa, H., Inase, M., Mushiake, H., Shima, K., & Tanji, J. (1991). Reorganization of activity in the supplementary motor area associated with motor learning and functional recovery. *Experimental Brain Research, 84,* 668–671.

Anderson, J. R., Bothell, D., Byrne, M. D., Douglass, S., Lebiere, C., &

Qin, Y. (2004). An integrated theory of the mind. *Psychological Review, 111,* 1036–1060.

Anderson, J. R., & Lebiere, C. (Eds.). (1998). *The atomic components of thought.* Mahwah, NJ: Erlbaum.

Anderson, J. R., Qin, Y. L., Sohn, M. H., Stenger, V. A., & Carter, C. S. (2003). An information-processing model of the BOLD response in symbol manipulation tasks. *Psychonomic Bulletin & Review, 10,* 241–261.

Anderson, J. R., Qin, Y. L., Stenger, V. A., & Carter, C. S. (2004). The relationship of three cortical regions to an information-processing model. *Journal of Cognitive Neuroscience, 16,* 637–653.

Ashby, G., Ennis, J., & Spiering, B. (2007). A neurobiological theory of automaticity in perceptual categorization. *Psychological Review, 114,* 632–656.

Baddeley, A. D. (1992, January 31). Working memory. *Science, 255,* 556–559.

Bear, M. F., Connors, B. W., & Paradiso, M. A. (2001). *Neuroscience: Exploring the brain* (8th ed.). Baltimore: Lippincott Williams & Wilkins.

Ben-Shachar, M., Hendler, T., Kahn, I., Ben-Bashat, D., & Grodzinsky, Y. (2003). The neural reality of syntactic transformations: Evidence from functional magnetic resonance imaging. *Psychological Science, 14,* 433–440.

Black, I. B. (1999). Trophic regulation of synaptic plasticity. *Journal of Neurobiology, 41,* 108–118.

Brass, M., & Cramon, D. (2002). The role of the frontal cortex in task preparation. *Cerebral Cortex, 12,* 908–914.

Braus, D. F. (2004). Neurobiology of learning: The basis of an alteration process. *Psychiatrische Praxis, 31*(Suppl. 2), S215–S223.

Bullock, T. (1968). Representation of information in neurons and sites for molecular participation. *Proceedings of the National Academy of Sciences, USA, 60,* 1058–1068.

Burle, B., Vidal, F., Tandonnet, C., & Hasbroucq, T. (2004). Physiological evidence for response inhibition in choice reaction time tasks. *Brain and Cognition, 56,* 153–164.

Byrne, M. D., & Anderson, J. R. (1998). Perception and action. In J. R. Anderson & C. Lebiere (Eds.), *The atomic components of thought* (pp. 167–200). Mahwah, NJ: Erlbaum.

Byrne, M. D., & Anderson, J. R. (2001). Serial modules in parallel: The psychological refractory period and perfect time-sharing. *Psychological Review, 108,* 847–869.

Card, S., Moran, T. P., & Newell, A. (1983). *The psychology of human-computer interaction.* Hillsdale, NJ: Erlbaum.

Chklovskii, D. B., Mel, B. W., & Svoboda, K. (2004, October 14). Cortical rewiring and information storage. *Nature, 431,* 782–788.

Cohen, M. S. (1997). Parametric analysis of fMRI data using linear systems methods. *NeuroImage, 6,* 93–103.

Collette, F., & Linden, M. V. (2002). Brain imaging of the central executive component of working memory. *Neuroscience & Biobehavioral Review, 26,* 105–125.

Cook, A. S., & Woollacott, M. H. (1995). *Motor control: Theory and practical applications.* Baltimore: Williams & Wilkins.

Creamer, L. R. (1963). Event uncertainty, psychological refractory period, and human data processing. *Journal of Experimental Psychology, 66,* 187–203.

De Jong, R. (1993). Multiple bottlenecks in overlapping task performance. *Journal of Experimental Psychology: Human Perception and Performance, 19,* 965–980.

Eagleman, D., Jacobson, J., & Sejnowski, T. (2004, April 22). Perceived luminance depends on temporal context. *Nature, 428,* 854–856.

Eisler, H. (1975). Subjective duration and psychophysics. *Psychological Review, 82,* 429–450.

Eisler, H. (1976). Experiments on subjective duration 1968–1975: A collection of power function exponents. *Psychological Bulletin, 83,* 1154–1171.

Faw, B. (2003). Pre-frontal executive committee for perception, working memory, attention, long-term memory, motor control, and thinking: A tutorial review. *Consciousness and Cognition, 12,* 83–139.

Feyen, R. (2002). *Modeling human performance using the queuing network-model human processor (QN-MHP).* Unpublished doctoral dissertation, University of Michigan.

Fletcher, P. C., & Henson, R. N. A. (2001). Frontal lobes and human memory: Insights from functional neuroimaging. *Brain, 124,* 849–881.

Gilbert, P. F. C. (2001). An outline of brain function. *Cognitive Brain Research, 12,* 61–74.

Gordon, A. M., & Soechting, J. F. (1995). Use of tactile afferent information in sequential finger movements. *Experimental Brain Research, 107,* 281–292.

Gross, D., & Harris, C. M. (1998). *Fundamentals of queueing theory.* New York: Wiley.

Grossman, M., Smith, E. E., Koenig, P., Glosser, G., DeVita, C., Moore, P., et al. (2002). The neural basis for categorization in semantic memory. *NeuroImage, 17,* 1549–1561.

Habib, M. (2003). Rewiring the dyslexic brain. *Trends in Cognitive Sciences, 7,* 330–333.

Hawkins, H. L., Rodriguez, E., & Reicher, G. M. (1979). *Is time-sharing a general ability?* (Rep. No. 3). Eugene: University of Oregon.

Heathcote, A., Brown, S., & Mewhort, D. J. K. (2000). The power law repealed: The case for an exponential law of practice. *Psychonomic Bulletin & Review, 7,* 185–207.

Horwitz, B., Tagamets, M. A., & McIntosh, A. R. (1999). Neural modeling, functional brain imaging, and cognition. *Trends in Cognitive Sciences, 3,* 91–98.

Ilvonen, T. M., Kujala, T., Kiesilainen, A., Salonen, O., Kozou, H., Pekkonen, E., et al. (2003). Auditory discrimination after left-hemisphere stroke: A mismatch negativity follow-up study. *Stroke, 34,* 1746–1751.

Jiang, Y. H., Saxe, R., & Kanwisher, N. (2004). Functional magnetic resonance imaging provides new constraints on theories of the psychological refractory period. *Psychological Science, 15,* 390–396.

Kansaku, K., Hanakawa, T., Wu, T., & Hallett, M. (2004). A shared neural network for simple reaction time. *NeuroImage, 22,* 904–911.

Kantowitz, B. H. (1974). Double stimulation. In B. H. Kantowitz (Ed.), *Human information processing: Tutorials in performance and cognition* (pp. 83–131). Hillsdale, NJ: Erlbaum.

Karlin, L., & Kestenbaum, R. (1968). Effects of number of alternatives on the psychological refractory period. *Quarterly Journal of Experimental Psychology, 20,* 167–178.

Kaufer, D. I., & Lewis, D. A. (1999). Frontal lobe anatomy and cortical connectivity. In B. L. Miller & J. L. Cummings (Eds.), *The human frontal lobes: Functions and disorders* (pp. 27–44). New York: Guilford Press.

Kazui, H., Kitagaki, H., & Mori, E. (2000). Cortical activation during retrieval of arithmetical facts and actual calculation: A functional magnetic resonance imaging study. *Psychiatry and Clinical Neurosciences, 54,* 479–485.

Kieras, D. E., & Meyer, D. E. (1997). An overview of the EPIC architecture for cognition and performance with application to human-computer interaction. *Human–Computer Interaction, 12,* 391–438.

Koski, L., & Paus, T. (2000). Functional connectivity of the anterior cingulate cortex within the human frontal lobe: A brain-mapping meta-analysis. *Experimental Brain Research, 133,* 55–65.

Leuthold, H., & Jentzsch, I. (2001). Neural correlates of advance movement preparation: A dipole source analysis approach. *Cognitive Brain Research, 12,* 207–224.

Leuthold, H., & Jentzsch, I. (2002). Distinguishing neural sources of

movement preparation and execution: An electrophysiological analysis. *Biological Psychology, 60,* 173–198.

Liu, Y. (1996). Queueing network modeling of elementary mental processes. *Psychological Review, 103,* 116–136.

Liu, Y. (1997). Queueing network modeling of human performance of concurrent spatial and verbal tasks. *IEEE Transactions on Systems, Man, and Cybernetics: Systems and Humans, 27*(A), 195–207.

Liu, Y., Feyen, R., & Tsimhoni, O. (2006). Queueing network-model human processor (QN-MHP): A computational architecture for multitask performance in human-machine systems. *ACM Transactions on Computer-Human Interaction, 13,* 37–70.

Luce, R. D. (1986). *Response times.* New York: Oxford University Press.

Manoach, D. S., Schlaug, G., Siewert, B., Darby, D. G., Bly, B. M., Benfield, A., et al. (1997). Prefrontal cortex fMRI signal changes are correlated with working memory load. *NeuroReport, 8,* 545–549.

McCann, R., & Johnston, J. (1992). Locus of the single-channel bottleneck in dual-task interference. *Journal of Experimental Psychology: Human Perception and Performance, 18,* 471–484.

McIntosh, A. R. (1999). Mapping cognition to the brain through neural interactions. *Memory, 7,* 523–548.

McIntosh, A. R. (2000). Towards a network theory of cognition. *Neural Networks, 13,* 861–870.

Meyer, D. E., & Kieras, D. E. (1997a). A computational theory of executive cognitive processes and multiple-task performance: Part 1. Basic mechanisms. *Psychological Review, 104,* 3–65.

Meyer, D. E., & Kieras, D. E. (1997b). A computational theory of executive cognitive processes and multiple-task performance: Part 2. Accounts of psychological refractory-period phenomena. *Psychological Review, 104,* 749–791.

Meyer, D. E., & Kieras, D. E. (1999). Precis to a practical unified theory of cognition and action: Some lessons from EPIC computational models of human multiple-task performance. In D. Gopher & A. Koriat (Eds.), *Attention and Performance XVII* (pp. 17–88). Cambridge, MA: MIT Press.

Mitz, A. R., Godschalk, M., & Wise, S. P. (1991). Learning-dependent neuronal activity in the premotor cortex: Activity during the acquisition of conditional motor associations. *Journal of Neuroscience, 11,* 1855–1872.

Mustovic, H., Scheffler, K., Di Salle, F., Esposito, F., Neuhoff, J. G., Hennig, J., et al. (2003). Temporal integration of sequential auditory events: Silent period in sound pattern activates human planum temporale. *NeuroImage, 20,* 429–434.

Naatanen, R. (1971). Non-aging foreperiods and simple reaction time. *Acta Psychologica, 35,* 316–327.

Nickerson, R. S. (1965). Response time to the second of two successive signals as a function of absolute and relative duration of intersignal interval. *Perceptual and Motor Skills, 21,* 3–10.

Nickerson, R. S. (1967). Expectancy, waiting time and the psychological refractory period. *Acta Psychologica, 27,* 23–39.

Niemi, P., & Naatanen, R. (1981). Foreperiod and simple reaction time. *Psychological Bulletin, 89,* 133–162.

Oberauer, K., & Kliegl, R. (2004). Simultaneous cognitive operations in working memory after dual-task practice. *Journal of Experimental Psychology: Human Perception and Performance, 30,* 689–707.

Ohbayashi, M., Ohki, K., & Miyashita, Y. (2003, July 11). Conversion of working memory to motor sequence in the monkey premotor cortex. *Science, 301,* 233–236.

Pashler, H. (1984). Processing stages in overlapping tasks: Evidence for a central bottleneck. *Journal of Experimental Psychology: Human Perception and Performance, 10,* 358–377.

Pashler, H. (1989). Chronometric evidence for central postponement in temporally overlapping tasks. *Quarterly Journal of Experimental Psychology: Human Experimental Psychology, 41*(A), 19–45.

Pashler, H. (1990). Do response modality effects support multiprocessor models of divided attention? *Journal of Experimental Psychology: Human Perception and Performance, 16,* 826–842.

Pashler, H. (1994a). Divided attention: Storing and classifying briefly presented objects. *Psychonomic Bulletin & Review, 1,* 115–118.

Pashler, H. (1994b). Dual-task interference in simple tasks: Data and theory. *Psychological Bulletin, 116,* 220–244.

Pashler, H. (1994c). Overlapping mental operations in serial performance with preview. *Quarterly Journal of Experimental Psychology: Human Experimental Psychology, 47*(A), 161–191.

Pashler, H., & Johnston, J. C. (1989). Attentional limitations in dual-task performance. In H. Pashler (Ed.), *Attention* (pp. 155–189). Hove, England: Psychology Press.

Pashler, H., Johnston, J. C., & Ruthruff, E. (2001). Attention and performance. *Annual Review of Psychology, 52,* 629–651.

Pashler, H., Luck, S. J., Hillyard, S. A., Mangun, G. R., O'Brien, S., & Gazzaniga, M. S. (1994). Sequential operation of disconnected cerebral hemispheres in split-brain patients. *NeuroReport, 5,* 2381–2384.

Petersen, S. E., van Mier, H., Fiez, J. A., & Raichle, M. E. (1998). The effects of practice on the functional anatomy of task performance. *Proceedings of the National Academy of Sciences, USA, 95,* 853–860.

Rieke, F., Warland, D., van Steveninck, R. de R., & Bialek, W. (1997). *Spikes: Exploring the neural code.* Cambridge, MA: MIT Press.

Roland, P. E. (1993). *Brain activation.* New York: Wiley-Liss.

Rolls, E. T. (2000). Memory systems in the brain. *Annual Review of Psychology, 51,* 599–630.

Ruthruff, E., Johnston, J. C., & Van Selst, M. (2001). Why practice reduces dual-task interference. *Journal of Experimental Psychology: Human Perception and Performance, 27,* 3–21.

Ruthruff, E., Miller, J., & Lachmann, T. (1995). Does mental rotation require central mechanisms? *Journal of Experimental Psychology: Human Perception and Performance, 21,* 552–570.

Ruthruff, E., Pashler, H. E., & Klaassen, A. (2001). Processing bottlenecks in dual-task performance: Structural limitation or strategic postponement? *Psychonomic Bulletin & Review, 8,* 73–80.

Salvucci, D. D., & Taatgen, N. A. (2008). Threaded cognition: An integrated theory of concurrent multitasking. *Psychological Review, 115,* 101–130.

Schneider, D. W., & Logan, G. D. (in press). *Executive functions: Task switching.* Oxford, England: Elsevier.

Schubotz, R. I., Friederici, A. D., & von Cramon, D. Y. (2000). Time perception and motor timing: A common cortical and subcortical basis revealed by fMRI. *NeuroImage, 11,* 1–12.

Schubotz, R. I., & von Cramon, D. Y. (2001). Functional organization of the lateral premotor cortex: fMRI reveals different regions activated by anticipation of object properties, location and speed. *Cognitive Brain Research, 11,* 97–112.

Schumacher, E. H., Lauber, E. J., Glass, J. M., Zurbriggen, E. I., Gmeindl, L., Kieras, D. E., & Meyer, D. E. (1999). Concurrent response-selection processes in dual-task performance: Evidence for adaptive executive control of task scheduling. *Journal of Experimental Psychology: Human Perception and Performance, 25,* 791–814.

Shafritz, K. M., Kartheiser, P., & Belger, A. (2005). Dissociation of neural systems mediating shifts in behavioral response and cognitive set. *NeuroImage, 25,* 600–606.

Simon, S. R., Meunier, M., Piettre, L., Berardi, A. M., Segebarth, C. M., & Boussaoud, D. (2002). Spatial attention and memory versus motor preparation: Premotor cortex involvement as revealed by fMRI. *Journal of Neurophysiology, 88,* 2047–2057.

Smith, E. E., & Jonides, J. (1998). Neuroimaging analyses of human working memory. *Proceedings of the National Academy of Sciences, USA, 95,* 12061–12068.

Solomons, L. M., & Stein, G. (1896). Normal motor automatism. *Psychological Review, 3,* 492–512.

Sommer, W., Leuthold, H., & Schubert, T. (2001). Multiple bottlenecks in

information processing? An electrophysiological examination. *Psychonomic Bulletin & Review, 8,* 81–88.

Sporns, O., Tononi, G., & Edelman, G. M. (2000). Connectivity and complexity: The relationship between neuroanatomy and brain dynamics. *Neural Networks, 13,* 909–922.

Taylor, J. (2003). Paying attention to consciousness. *Progress in Neurobiology, 71,* 305–335.

Taylor, J., Horwitzc, B., Shaha, N. J., Fellenzb, W. A., Mueller-Gaertnera, H.-W., & Krausee, J. B. (2000). Decomposing memory: Functional assignments and brain traffic in paired word associate learning. *Neural Networks, 13,* 923–940.

Ulrich, R., Leuthold, H., & Sommer, W. (1998). Motor programming of response force and movement direction. *Psychophysiology, 35,* 721–728.

Ungerleider, L., & Haxby, J. V. (1994). "What" and "where" in the human brain. *Current Opinion in Neurobiology, 4,* 157–165.

van Mier, H., Tempel, L. W., Perlmutter, J. S., Raichle, M. E., & Petersen, S. E. (1998). Changes in brain activity during motor learning measured with PET: Effects of hand of performance and practice. *Journal of Neurophysiology, 80,* 2177–2199.

Van Selst, M., & Jolicoeur, P. (1997). Decision and response in dual-task interference. *Cognitive Psychology, 33,* 266–307.

Vartanian, O., & Goel, V. (2005). Task constraints modulate activation in right ventral lateral prefrontal cortex. *NeuroImage, 27,* 927–933.

Wearden, J. H., Edwards, H., Fakhri, M., & Percival, A. (1998). Why "sounds are judged longer than lights": Application of a model of the internal clock in humans. *Quarterly Journal of Experimental Psychology: Comparative and Physiological Psychology, 51*(B), 97–120.

Welch, J. (1898). On the measurement of mental activity through muscular activity and the determination of a constant of attention. *American Journal of Physiology, 1,* 288–306.

Welford, A. T. (1952). The "psychological refractory period" and timing of high speed performance: A review and a theory. *British Journal of Psychology, 43,* 2–19.

Wildgruber, D., Ackermann, H., & Grodd, W. (2001). Differential contributions of motor cortex, basal ganglia, and cerebellum to speech motor control: Effects of syllable repetition rate evaluated by fMRI. *NeuroImage, 13,* 101–109.

Wu, C., & Liu, Y. (2004a, July–August). *Modeling behavioral and brain imaging phenomena in transcription typing with queuing networks and reinforcement learning algorithms.* Paper presented at the Sixth International Conference on Cognitive Modeling, Pittsburgh, PA.

Wu, C., & Liu, Y. (2004b, July–August). *Modeling psychological refractory period (PRP) and practice effect on PRP with queuing networks and reinforcement learning algorithms.* Paper presented at the Sixth International Conference on Cognitive Modeling, Pittsburgh, PA.

Wu, C., & Liu, Y. (2007a). Queueing network modeling of driver workload and performance. *IEEE Transactions on Intelligent Transportation Systems, 8,* 528–537.

Wu, C., & Liu, Y. (2007b). A new software tool for modeling human performance and mental workload. *Ergonomics in Design, 15,* 8–14.

Wu, C., & Liu, Y. (2008). Queuing network modeling of transcription typing. *ACM Transactions on Computer-Human Interaction, 15,* 1–45.

Wu, C., Liu, Y., & Walsh, C. (in press). Queueing network modeling of a real-time psychophysiological index of mental workload: P300 in event-related potential (ERP). *IEEE Transactions on Systems, Man, and Cybernetics: Systems and Humans*.

Wu, C., Tsimhoni, O., & Liu, Y. (in press). Development of an adaptive workload management system using queueing network-model of human processor. *IEEE Intelligent Transportation Systems.*

Zysset, S., Muller, K., Lehmann, C., Thone-Otto, A. I. T., & von Cramon, D. Y. (2001). Retrieval of long and short lists from long term memory: A functional magnetic resonance imaging study with human subjects. *Neuroscience Letters, 314,* 1–4.

Appendix A

Setting of Parameters in the Model

Tables A1–A9 list the parameters (including their values, descriptions, and sources) used in modeling different psychological refractory period experimental results.

Table A1
Parameter Setting in Modeling the Basic Psychological Refractory Period (Schumacher et al., 1999, Experiment 4)

Parameter	Value (ms)	Description	Source
$T_{1,AP}$	126	Time for auditory perception time (42 ms at Servers 1,2/3, and 4; i.e., 42 × 3 = 126)	Liu et al. (2006)
$T_{2,VP}$	126	Time for visual perception time (42 ms at Servers 1, 2/3, and 4)	Liu et al. (2006)
$T_{2,A}$, $T_{2,B}$	18	Processing time at Servers A and B	Liu et al. (2006)
$T_{1,C}$, $T_{2,C}$	18	Processing time at Server C	Liu et al. (2006)
$T_{1,F}$	179	Processing time at Server F (T1)	Value estimated at long SOA conditions
$T_{2,F}$	165	Processing time at Server F (T2)	Value estimated at long SOA conditions
$T_{2,W}$	24	Processing time at Server W	Liu et al. (2006)
$T_{1,Y}$, $T_{2,Y}$	24	Processing time at Server Y	Liu et al. (2006)
$T_{1,Z}$, $T_{2,Z}$	24	Processing time at Server Z	Liu et al. (2006)
$T_{2,K}$	10	Key closure time	Byrne & Anderson (2001)
$T_{1,VO}$	100	Voice key closure time	Byrne & Anderson (2001)

Note. SOA = stimulus onset asynchrony; T1 = Task 1; T2 = Task 2.

Table A2
Parameter Setting in Modeling Experiments 3 and 4 of Schumacher et al. (1999)

Parameter	Mean value (ms)	Description	Source
		Parameters common in modeling Experiments 3 and 4 in Schumacher et al. (1999)[a]	
$T_{2,C\text{-}comp}$	18	Processing time at Server C (compatible R-S)	Liu et al. (2006)
$T_{2,C\text{-}incomp}$	36	Processing time at Server C (incompatible R-S)	Liu et al. (2006)
$T_{1,F}$	179	Processing time at Server F (T1)	Value estimated at long SOA conditions
$T_{1,W}$, $T_{2,W}$	24	Processing time at Server W	Liu et al. (2006)
$T_{1,Y}$, $T_{2,Y}$	24	Processing time at Server Y	Liu et al. (2006)
$T_{1,Z}$, $T_{2,Z}$	24	Processing time at Server Z	Liu et al. (2006)
$T_{1,K}$	10	Key closure time	Byrne & Anderson (2001)
		Parameters used in modeling Experiment 3 in Schumacher et al. (1999)	
$T_{2,F\text{-}comp}$	207	Processing time at Server F (compatible R-S, T2)	Value estimated at long SOA conditions
$T_{2,F\text{-}incomp}$	295	Processing time at Server F (incompatible R-S, T2)	Value estimated at long SOA conditions
		Parameters used in modeling Experiment 4 in Schumacher et al. (1999)	
$T_{2,F\text{-}comp}$	165	Processing time at Server F (compatible R-S, T2)	Value estimated at long SOA conditions
$T_{2,F\text{-}incomp}$	219	Processing time at Server F (incompatible R-S, T2)	Value estimated at long SOA conditions

Note. R-S = response selection; SOA = stimulus onset asynchrony; T1 = Task 1; T2 = Task 2.
[a] The values of $T_{1,AP}$, $T_{2,VP}$, $T_{2,A}$, $T_{2,B}$, $T_{1,C}$, and $T_{1,VO}$ are the same as those in Table A1.

(*Appendixes continue*)

Table A3
Parameter Setting in Modeling Experiments 1–4 of Hawkins et al. (1979)

Parameter	Mean value (ms)	Description	Source
		Parameters common in modeling Experiments 1–4 of Hawkins et al.'s (1979) study[a]	
$T_{1,C}$	18	Processing time at Server C (T1)	Liu et al. (2006)
$T_{2,C\text{-}easy}$	18	Processing time at Server C (T2, easy condition)	Liu et al. (2006)
$T_{2,C\text{-}diff}$	72	Processing time at Server C (T2, difficult condition)	Liu et al. (2006)
$T_{1,W}$, $T_{2,W}$	24	Processing time at Server W	Liu et al. (2006)
$T_{1,Y}$, $T_{2,Y}$	24	Processing time at Server Y	Liu et al. (2006)
$T_{1,Z}$, $T_{2,Z}$	24	Processing time at Server Z	Liu et al. (2006)
$T_{1,K}$	10	Key closure time	Byrne & Anderson (2001)
		Parameters used in modeling Experiment 1 in Hawkins et al. (1979; auditory–manual condition)	
$T_{1,F}$	415	Processing time at Server F (T1)	Value estimated at long SOA conditions
$T_{2,F\text{-}easy}$	270	Processing time at Server F (T2, easy condition)	Value estimated at long SOA conditions
$T_{2,F\text{-}diff}$	330	Processing time at Server F (T2, difficult condition)	Value estimated at long SOA conditions
		Parameters used in modeling Experiment 2 in Hawkins et al. (1979; auditory–vocal condition)	
$T_{1,F}$	423	Processing time at Server F (T1)	Value estimated at long SOA conditions
$T_{2,F\text{-}easy}$	280	Processing time at Server F (T2, easy condition)	Value estimated at long SOA conditions
$T_{2,F\text{-}diff}$	336	Processing time at Server F (T2, difficult condition)	Value estimated at long SOA conditions
		Parameters used in modeling Experiment 3 in Hawkins et al. (1979; visual–vocal condition)	
$T_{1,F}$	346	Processing time at Server F (T1)	Value estimated at long SOA conditions
$T_{2,F\text{-}easy}$	260	Processing time at Server F (T2, easy condition)	Value estimated at long SOA conditions
$T_{2,F\text{-}diff}$	340	Processing time at Server F (T2, difficult condition)	Value estimated at long SOA conditions
		Parameters used in modeling Experiment 4 in Hawkins et al. (1979; visual–manual condition)	
$T_{1,F}$	308	Processing time at Server F (T1)	Value estimated at long SOA conditions
$T_{2,F\text{-}easy}$	224	Processing time at Server F (T2, easy condition)	Value estimated at long SOA conditions
$T_{2,F\text{-}diff}$	280	Processing time at Server F (T2, difficult condition)	Value estimated at long SOA conditions

Note. SOA = stimulus onset asynchrony; T1 = Task 1; T2 = Task 2.
[a]The values of $T_{1,AP}$, $T_{2,VP}$, T_{2A}, $T_{2,B}$, and $T_{1,VO}$ are the same as those in Table A1.

Table A4
Parameter Setting in Modeling Karlin and Kestenbaum's (1968) Experiment

Parameter	Value (ms)	Description	Source
$T_{1,C}$, $T_{2,C}$	18	Processing time at Server C (compatible R-S)	Liu et al. (2006)
$T_{1,F}$	117	Processing time at Server F (T1)	Value estimated at long SOA conditions
$T_{2,F}$	68	Processing time at Server F (choice RT2 condition)	Value estimated at long SOA conditions
$T_{2,F}$	50	Processing time at Server F (simple RT2 condition)	Value estimated at long SOA conditions
$T_{2,V}$	140	Processing time at Server V (T2)	Value estimated at long SOA conditions
$T_{1,W}$, $T_{2,W}$	24	Processing time at Server W	Liu et al. (2006)
$T_{1,Y}$, $T_{2,Y}$	24	Processing time at Server Y	Liu et al. (2006)
$T_{1,Z}$, $T_{2,Z}$	24	Processing time at Server Z	Liu et al. (2006)
$T_{1,X}$, $T_{2,X}$	24	Processing time at Server X	Liu et al. (2006)
T_K	10	Key closure time	Byrne & Anderson (2001)
T_{perc}	350	The duration between when the anticipation process starts and the probability when participants make the motor response equal to 1	Value estimated at long SOA conditions

Note. The values of $T_{1,AP}$ and $T_{2,VP}$ are the same as those in Table A1. R-S = response selection; RT2 = reaction time to Task 2; SOA = stimulus onset asynchrony; T1 = Task 1; T2 = Task 2.

Table A5
Parameter Setting in Modeling the Study of Sommer et al. (2001)

Parameter	Value (ms)	Description	Source
$T_{1,C}$, $T_{2,C}$	18	Processing time at Server C (compatible R-S)	Liu et al. (2006)
$T_{1,F}$	338	Processing time at Server F (T1)	Value estimated at long SOA conditions
$T_{2,F}$ (choice RT)	324	Processing time at Server F (choice RT2 condition)	Value estimated at long SOA conditions
$T_{2,F}$ (simple RT)	293	Processing time at Server F (simple RT2 condition)	Value estimated at long SOA conditions
T_{perc}	570	The duration between when the anticipation process starts and the probability when participants make the motor response equal to 1	Value estimated at long SOA conditions
$T_{2,V}$	24	Processing time at Server V (T1)	Liu et al. (2006)
$T_{1,W}$, $T_{2,W}$	24	Processing time at Server W	Liu et al. (2006)
$T_{1,Y}$, $T_{2,Y}$	24	Processing time at Server Y	Liu et al. (2006)
$T_{1,Z}$, $T_{2,Z}$	24	Processing time at Server Z	Liu et al. (2006)
$T_{1,X}$, $T_{2,X}$	24	Processing time at Server X	Liu et al. (2006)

Note. The values of $T_{1,AP}$, $T_{2,VP}$, $T_{2,A}$, and $T_{2,B}$ are the same as those in Table A1. R-S = response selection; RT = reaction time; RT2 = reaction time to Task 2; SOA = stimulus onset asynchrony; T1 = Task 1.

Table A6
Parameters in Modeling Jiang et al.'s (2004) Experiment

Parameter	Value (ms)	Description	Source
$T_{1,C}$, $T_{2,C}$	18	Processing time at Server C	Liu et al. (2006)
$T_{1,F}$	408	Processing time at Server F (T1)	Value estimated
$T_{2,F}$	376	Processing time at Server F (T2)	Value estimated
$T_{1,W}$, $T_{2,W}$	24	Processing time at Server W	Liu et al. (2006)
$T_{1,Y}$, $T_{2,Y}$	24	Processing time at Server Y	Liu et al. (2006)
$T_{1,Z}$, $T_{2,Z}$	24	Processing time at Server Z	Liu et al. (2006)
$T_{1,K}$	10	Key closure time	Byrne & Anderson (2001)

Note. The values of $T_{1,AP}$, $T_{2,VP}$, $T_{2,A}$, and $T_{2,B}$ are the same as those in Table A1. T1 = Task 1; T2 = Task 2.

Table A7
Parameter Setting in Modeling Ruthruff, Pashler, and Klaassen's (2001) Experiment (Practice Effect Not Considered)

Parameter	Value (ms)	Description	Source
$T_{T,P}$	126	Time for tone detection perception	Liu et al. (2006)
$T_{S,P}$	126	Time for letter perception	Liu et al. (2006)
$T_{T,C}$, $T_{S,C}$	18	Processing time at Server C	Liu et al. (2006)
$T_{T,F}$	368	Processing time of tone counting task at Server F	Value estimated at long SOA conditions
$T_{S,F}$	600	Processing time of spatial working memory task at Server F	Value estimated at long SOA conditions
GR	21	Time to group two responses	The control experiment in Ruthruff, Pashler, & Klaassen (2001)
$T_{T,W}$, $T_{S,W}$	24	Processing time at Server W	Liu et al. (2006)
$T_{T,Z}$, $T_{S,Z}$	24	Processing time at Server Z	Liu et al. (2006)
$T_{S,K}$	10	Key closure time	Byrne & Anderson (2001)
$T_{T,VO}$	100	Voice key closure time	Byrne & Anderson (2001)

Note. SOA = stimulus onset asynchrony.

(*Appendixes continue*)

Table A8
Parameter Setting in Modeling Ruthruff, Johnston, and Van Selst's (2001) Experiment (Practice Effect Considered)

Parameter	Value in ms before extensive practice (A_i + B_i): Liu et al. (2006)	Minimal value in ms (A_i): Feyen (2002)	Description and practice process: Heathcote et al. (2000)
$T_{T,P}$	126 (42 ms mean perceptual cycle time at Servers 5, 6/7, and 8; i.e., 42 × 3 = 126 ms)	75 (25 ms minimal perceptual cycle time at Servers 5, 6/7, and 8; i.e., 25 × 3 = 75 ms)	Time for tone detection perception $A_i + B_i \times \text{Exp}(-N\xi)$
$T_{S,P}$	126 (42 ms mean perceptual cycle time at Servers 1, 2/3, and 4; i.e., 42 × 3 = 126 ms)	75 (25 ms minimal perceptual cycle time at Servers 1, 2/3, and 4; i.e., 25 × 3 = 75 ms)	Time for letter perception A $A_i + B_i \times \text{Exp}(-N\xi)$
$T_{T,C}$, $T_{S,C}$	18	6 (minimal cognitive cycle time)	Processing time at Server C $A_i + B_i \times \text{Exp}(-N\xi)$
$T_{S,VS}$[a]	1,540	10 (minimal motor cycle time)	Processing time at Server V (T1) $A_i + B_i \times \text{Exp}(-N\xi)$
$T_{T,W}$, $T_{S,W}$	24	10 (minimal motor cycle time)	Processing time at Server W $A_i + B_i \times \text{Exp}(-N\xi)$
$T_{T,Y}$, $T_{S,Y}$	24	10 (minimal motor cycle time)	Processing time at Server W $A_i + B_i \times \text{Exp}(-N\xi)$
$T_{T,Z}$, $T_{S,Z}$	24	10 (minimal motor cycle time)	Processing time at Server Z $A_i + B_i \times \text{Exp}(-N\xi)$
$T_{S,K}$	10	10	Key closure time
$T_{T,VO}$	100	100	Voice key closure time
G	21	6	Time to group two responses $A_i + B_i \times \text{Exp}(-N\xi)$
$T_{T,F}$[a]	439	6 (minimal cognitive cycle time)	Processing time of the tone counting task at Server F $A_i + B_i \times \text{Exp}(-N\xi)$
$T_{S,F}$[a]	746	6 (minimal cognitive cycle time)	Processing time of the spatial memory task at Server F $A_i + B_i \times \text{Exp}(-N\xi)$

Note. T1 = Task 1.
[a] Value estimated at long stimulus onset asynchrony conditions; ξ = .001 (Heathcote et al., 2000).

Table A9
Parameter Setting in Modeling Oberauer and Kliegl's (2004) Experiment

Parameter	Value in ms before extensive practice (A_i + B_i): Liu et al. (2006)	Minimal value in ms (A_i): Feyen (2002)	Description and practice process: Heathcote et al. (2000)
		Common parameters for both single- and dual-task groups	
$T_{T,P}$	126 (42 ms mean perceptual cycle time at Servers 5, 6/7, and 8; i.e., 42 × 3 = 126 ms)	75 (25 ms minimal perceptual cycle time at Servers 5, 6/7, and 8; i.e., 25 × 3 = 75 ms)	Time for tone detection perception $A_i + B_i \times \text{Exp}(-N\xi)$
$T_{S,P}$	126 (42 ms mean perceptual cycle time at Servers 1. 2/3, and 4; i.e., 42 × 3 = 126 ms)	75 (25 ms minimal perceptual cycle time at Servers 1, 2/3, and 4; i.e., 25 × 3 = 75 ms)	Time for letter perception $A_i + B_i \times \text{Exp}(-N\xi)$
$T_{T,C}$, $T_{S,C}$	18	6 (minimal cognitive cycle time)	Processing time at Server C $A_i + B_i \times \text{Exp}(-N\xi)$
$T_{S,VS}$	1,540 (see parameter setting in Ruthruff, Johnston, & Van Selst's 2001, experiment considering practice effect)	10 (minimal motor cycle time)	Processing time at Server V (T1) $A_i + B_i \times \text{Exp}(-N\xi)$
$T_{T,W}$, $T_{S,W}$	24	10 (minimal motor cycle time)	Processing time at Server W $A_i + B_i \times \text{Exp}(-N\xi)$
$T_{T,Y}$, $T_{S,Y}$	24	10 (minimal motor cycle time)	Processing time at Server W $A_i + B_i \times \text{Exp}(-N\xi)$
$T_{T,Z}$, $T_{S,Z}$	24	10 (minimal motor cycle time)	Processing time at Server Z $A_i + B_i \times \text{Exp}(-N\xi)$
$T_{S,K}$	10	10	Key closure time
		Parameters for single-task practice group	
$T_{S,F}$[a]	1,038	6 (minimal cognitive cycle time)	Processing time of spatial memory task at Server F $A_i + B_i \times \text{Exp}(-N\xi)$
$T_{T,F}$[a]	800	6 (minimal cognitive cycle time)	Processing time of numerical operation task at Server F $A_i + B_i \times \text{Exp}(-N\xi)$
		Parameters for dual-task practice group	
$T_{S,F}$[a]	925	6 (minimal cognitive cycle time)	Processing time of spatial memory task at Server F $A_i + B_i \times \text{Exp}(-N\xi)$
$T_{T,F}$[a]	1,498	6 (minimal cognitive cycle time)	Processing time of numerical operation task at Server F $A_i + B_i \times \text{Exp}(-N\xi)$

Note. T1 = Task 1.
[a] Value estimated at long stimulus onset asynchrony conditions; learning rate ξ = .001 (Heathcote et al. 2000).

Appendix B

Mathematical Modeling of Expected Reaction Time to Task 2 (Simple Reaction Task) in the Experiments of Karlin and Kestenbaum (1968) and Sommer, Leuthold, and Schubert (2001)

Since Task 2 (T2) in Karlin and Kestenbaum (1968) and Sommer, Leuthold, and Schubert (2001) is a simple reaction task, its mathematical modeling methods can be described in the following section.

There are two conditions in modeling the expected reaction time to T2 (RT2) at the simple reaction condition. At short stimulus onset asynchrony (SOA) conditions (entities of T2 arrive at Server F before Server F starts its anticipation process, $t_a = 0$; see Figure B1), entities of T2 have to wait until entities of Task 1 (T1) leave Server F; after entities of T1 leave Server F, entities of T2 enter Server F immediately. Since Server F is occupied by the entities of T2 (participants are busy in performing judgment of T2), the anticipation process does not occur in this condition. At long SOA conditions, Server F starts its anticipation process before entities of T2 arrive at Server F. The mathematical models of RT2 (simple reaction condition) are constructed based on these two conditions in the following sections.

Short SOA Conditions ($t_a = 0$)

Under short SOA conditions of T2 (simple reaction condition), the expected RT2 is also modeled with the same form of equation as in the choice reaction condition of RT2, except that the motor subnetwork's servers are replaced by the servers involved in the simple reaction time (see Equation B1 and Figure B1).

$$E(RT_2|t_a = 0)\ (\text{simple reaction condition}) = \max(T_{1,AP\backslash VP} + T_{1,B\backslash A} + T_{1,C} + T_{1,F} - SOA, T_{2,VP\backslash VP} + T_{1,A\backslash B} + T_{2,C}) + T_{2,F} + T_{2,C} + T_{2,V} + T_{2,Z} + T_{2,K}, \quad \text{(B1)}$$

where $T_{1,AP\backslash VP}$ is the processing time at the auditory perceptual subnetwork (Karlin & Kestenbaum's, 1968, experiment) or visual perceptual subnetwork (Sommer et al.'s, 2001, experiment) and $T_{1,B\backslash A}$ is the processing time at Server B (Karlin & Kestenbaum's, 1968, experiment) or Server A (Sommer et al.'s, 2001, experiment).

Long SOA Conditions ($t_a > 0$)

Quantification of the Anticipation Process

The anticipation process (Response 2 [R2] is made without seeing Stimulus 2 [S2]) at Server F is quantified by the following mechanisms in time perception. According to the function of Server F in anticipating a sensory event in a simple reaction task (Schubotz, Friederici, & von Cramon, 2000; Schubert & von Cramon, 2001; see the introductory section in the main text of this article), the longer Server F anticipates S2 (defined as perceived waiting time, t_{perc}), the higher the probability (defined as p) of trigging motor response without seeing S2 (anticipation process) (see Equation B2).

$$p = \frac{t_{perc}}{T_{perc}}, \quad \text{(B2)}$$

where T_{perc} is the duration between when the anticipation process starts and the probability when participants make the motor response equal to 1.

On the basis of psychophysical research in studying the relationship between perceived waiting time (t_{perc}) and actual waiting time (t_a) in very short time periods, there is considerable support for a psychophysical law for perceptual duration described by a power function following Steven's power law (Eisler, 1975, 1976). Thus,

$$t_{perc} = kt_a^{\beta}, \quad \text{(B3)}$$

where t_a is the duration between when Server F starts the anticipation process and when S2 arrives at the perceptual subnetwork. k and β are the parameters in Steven's power law (Wearden, Edwards, Fakhri, & Percival, 1998). Combining Equations B2 and B3 results in

$$p = \frac{kt_a^{\beta}}{T_{perc}}. \quad \text{(B4)}$$

We can also get

$$t_a = \left(\frac{T_{perc}}{k}p\right)^{\frac{1}{\beta}}. \quad \text{(B5)}$$

Moreover, since p is defined as the probability that the response of T2 is made with the anticipation process (R2 is made without seeing S2), there are two conditions in which expected RT2 is modeled: RT2 with or without the anticipation process.

Quantification of Expected RT2 With the Anticipation Process

On the basis of Figure B1, we can develop the expected RT2 with the anticipation process—$E(RT_{2,ANTI})$—into

$$E(RT_{2,ANTI}) = T_{Fst} + t_a + T_{2,C} + T_{2,V} + T_{2,Z} + T_{2,K} - SOA, \quad \text{(B6)}$$

where T_{Fst} is the time point when Server F starts its anticipation process (see Equation B7 and Figure B1).

$$T_{Fst} = T_{1,AP\backslash VP} + T_{1,B\backslash A} + T_{1,C} + T_{1,F}. \quad \text{(B7)}$$

(*Appendixes continue*)

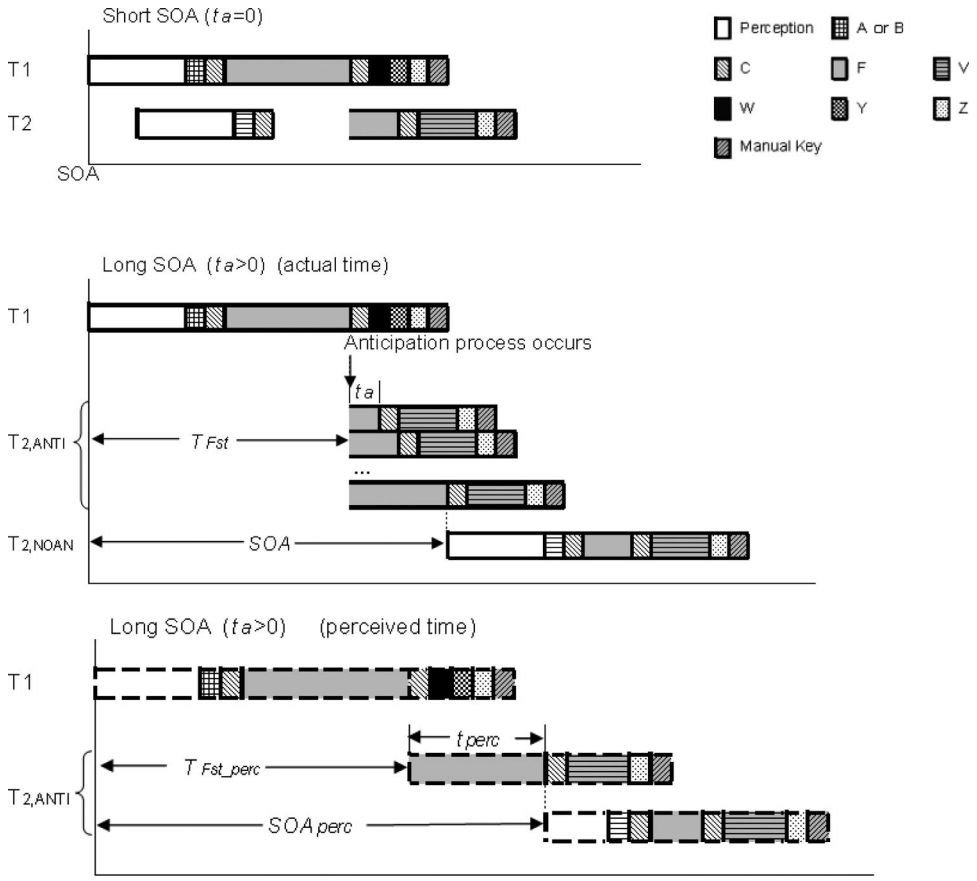

Figure B1. Mechanisms for modeling the expected reaction time to T2 (RT2) under the simple reaction condition. t_a is the duration between when Server F starts the anticipation process and when entities of Stimulus 2 arrive at the perceptual subnetwork; T_{Fst} is the time point when Server F starts its anticipation process $T_{Fst} = T_{1,AP\backslash VP} + T_{1,B\backslash A} + T_{1,C} + T_{1,F}$, where $T_{1,AP\backslash VP}$ is the processing time at the auditory perceptual subnetwork (Karlin & Kestenbaum's, 1968, experiment) or visual perceptual subnetwork (Sommer, Leuthold, & Schubert's, 2001, experiment); $T_{1,B\backslash A}$ is the processing time at Server B (Karlin & Kestenbaum's, 1968, experiment) or Server A (Sommer et al.'s, 2001, experiment). SOA = stimulus onset asynchrony; T1 = Task 1; T2 = Task 2.

From Equation B3, t_a can be rewritten into

$$t_a = (t_{perc}/k)^{1/\beta}. \quad \text{(B8)}$$

Moreover, since participants end their waiting process of S2 when they perceive the time reaches the perceived SOA, the perceived waiting time (t_{perc}) equals the perceived SOA (SOA_{perc}) minus the perceived T_{Fst} (T_{Fst_perc}), that is,

$$t_{perc} = \max(SOA_{perc} - T_{Fst\_perc}, 0), \quad \text{(B9)}$$

where SOA_{perc} and T_{Fst_perc} can be derived from Equation B3, that is, $SOA_{perc} = kSOA^{\beta}$, and $T_{Fst\_perc} = kT_{Fst}{}^{\beta}$, resulting in

$$t_{perc} = \max(kSOA^{\beta} - kT_{Fst}{}^{\beta}, 0). \quad \text{(B10)}$$

Combining Equations B4, B8, and B10 results in

$$t_a = \max[(SOA^{\beta} - T_{Fst}{}^{\beta})^{1/\beta}, 0] \quad \text{(B11)}$$

and

$$RT_{2,ANTI} = T_{Fst} + \max[(SOA^{\beta} - T_{Fst}{}^{\beta})^{1/\beta}, 0] + T_{2,C} + T_{2,V} + T_{2,Z} + T_{2,K} - SOA. \quad \text{(B12)}$$

Quantification of Expected RT2 Without the Anticipation Process

Under the condition that there is no anticipation, the expected RT2—$E(RT_{2,NOAN})$—is modeled with the same form of the equation as in the choice reaction condition, except that the motor subnetwork's servers are replaced by the servers involved in the simple reaction task (see Equation B13 and Figure B1).

$$E(RT_{2,NOAN}) \text{ (simple reaction condition)} = \max(T_{1,AP\backslash VP} + T_{1,B\backslash A} + T_{1,C} + T_{1,F} - SOA, T_{2,VP} + T_{1,A} + T_{2,C})$$

$$+ T_{2,F} + T_{2,C} + T_{2,V} + T_{2,Z} + T_{2,K}. \quad \text{(B13)}$$

Hence, the expected RT2 in long SOA conditions ($t_a > 0$) can be quantified by Equation B14:

$$E(RT_2 | t_a > 0) \text{ (simple reaction condition)} = pE(RT_{2,ANTI}) + (1 - p)E(RT_{2,NOAN}). \quad \text{(B14)}$$

In sum, the expected RT2 under the simple reaction condition is

$$E(RT2) \text{ (simple reaction)} = \begin{cases} pE(RT_{2,ANTI}) + (1 - p)E(RT_{2,NOAN}) & t_a > 0 \text{ (long SOA conditions)} \\ \max(T_{1,AP\backslash VP} + T_{1,B\backslash A} + T_{1,C} + T_{1,F} - SOA, T_{2,VP\backslash AP} + T_{1,A\backslash B} + T_{2,C}) + T_{2,F} + T_{2,C} & \\ \quad + T_{2,V} + T_{2,Z} + T_{2,K} & t_a = 0 \text{ (short SOA conditions)} \end{cases}. \quad \text{(B15)}$$

Combing Equations B4, B11, B13, and B14, Equation B15 can be rewritten into

$$E(RT2) \text{ (simple reaction)} = \begin{cases} \left(\dfrac{kSOA^{\beta} - kT_{Fst}{}^{\beta}}{T_{perc}}\right)[T_{Fst} - T_{Fst}{}^{\beta} - SOA + SOA^{\beta} & \\ \quad - (T_{2,VP\backslash AP} + T_{1,A\backslash B} + 2T_{2,C} + T_{2,F} + T_{2,V} + T_{2,Z} + T_{2,K})] & \\ \quad + (T_{2,VP\backslash AP} + T_{1,A\backslash B} + 2T_{2,C} + T_{2,F} + T_{2,V} + T_{2,Z} + T_{2,K}) & t_a > 0 \text{ (long SOA conditions)} \\ \max(T_{1,AP\backslash VP} + T_{1,B\backslash A} + T_{1,C} + T_{1,F} - SOA, T_{2,VP\backslash AP} + T_{1,A\backslash B} + T_{2,C}) & \\ \quad + T_{2,F} + T_{2,C} + T_{2,V} + T_{2,Z} + T_{2,K} & t_a = 0 \text{ (short SOA conditions)} \end{cases}. \quad \text{(B16)}$$

Appendix C

Mathematical Modeling of the Percentage of Negative Responses of Reaction Time to Task 2 (P_n)

Negative response of reaction time to Task 2 (RT2)—(RT2 < 0)—means that Response 2 (R2) occurs prior to the arrival of Stimulus 2 (S2), that is, the arrival of S2 is stimulus onset asynchrony (SOA). On the basis of Figure B1 (see Appendix B), the interval between the arrival of Stimulus 1 (time = 0) and the occurrence of R2 is $T_{Fst} + t_a + T_{2,C} + T_{2,V} + T_{2,Z} + T_{2,K}$.

Supposing $u = T_{2,C} + T_{2,V} + T_{2,Z} + T_{2,K}$ results in

$$P_n = P\{RT_2 < 0\} = P\{T_{Fst} + t_a + u < SOA\} = P\{t_a < SOA - u - T_{Fst}\}. \quad \text{(C1)}$$

Since t_a ranges from 0 to $SOA - T_{FSt}$ (t_a ends when S2 arrives according to its definition), the probability of the RT2 < 0 (P_n) is

$$P_n = \begin{cases} \displaystyle\int_0^{SOA-u-T_{Fst}} \frac{1}{SOA - T_{Fst}}\, dt_a & SOA \geq u + T_{Fst} \\ 0 & SOA < u + T_{Fst} \end{cases}. \quad \text{(C2)}$$

Solving the integral then results in

$$P_n = \begin{cases} 1 - \dfrac{T_{2,C} + T_{2,V} + T_{2,Z} + T_{2,K}}{SOA - T_{Fst}} & SOA \geq u + T_{Fst} \\ 0 & SOA < u + T_{Fst} \end{cases}. \quad \text{(C3)}$$

Appendix D

Deduction of $CB(t)$ in Modeling Jiang, Saxe, and Kanwisher's (2004) Study of the Psychological Refractory Period

Using Cohen's (1997) model, Anderson, Qin, Sohn, Stenger, and Carter (2003; Anderson, Bothell, et al., 2004; Anderson, Qin, Stenger, & Carter, 2004) proposed that the integrated BOLD signal—$CB(t)$—in a certain brain region is mainly determined by several factors: the length of time the current buffer/server occupied throughout time t ($i[x]$: at time x, if the

(*Appendixes continue*)

$$CB(t) = \begin{cases} \dfrac{kMsb}{a+1}\left(\begin{array}{l} e^{(-.5t/bs)}(t/s)^{a}(t/bs)^{-.5a}\text{WhittakerM}(.5a, .5a + .5, t/bs) - \\ e^{(-.5a\frac{t-\eta}{bs})}(\dfrac{t-\eta}{bs})^{.5a}\text{WhittakerM}(.5a, .5a + .5, \dfrac{t-\eta}{bs}) \end{array} \right) & \dfrac{t-\eta}{s} \le Y \le \dfrac{t}{s} \\ 0 & \dfrac{t-\eta}{s} > Y \text{ or } Y > \dfrac{t}{s} \end{cases}. \quad \text{(D4)}$$

current buffer/server is occupied, $i[x] = 1$; otherwise, $i[x] = 0$), latency scale s, and magnitude scale M (see Equation D1; Anderson et al., 2003; Anderson, Bothell, et al., 2004; Anderson, Qin, et al., 2004).

$$CB(t) = M\int_0^t i(x)B\left(\frac{t-x}{s}\right)dx, \quad \text{(D1)}$$

where $B(T) = kT^{a}e^{-T/b}$ (Cohen, 1997). In the queuing network model, assuming the length of time Server i is being used is η, Equation D1 can be further developed into

$$CB(t) = \begin{cases} M\int_0^{\eta} B\left(\dfrac{t-x}{s}\right)dx & 0 \le x \le \eta \Rightarrow i(x) = 1 \\ 0 & x < 0 \text{ or } x > \eta \Rightarrow i(x) = 0 \end{cases}. \quad \text{(D2)}$$

Suppose $Y = \dfrac{t-x}{s}$, and combine Equation D2 with Cohen's equation $B(T) = kT^{a}e^{-T/b}$; then, Equation D2 can be rewritten into Equation D3:

$$CB(t) = \begin{cases} skM\displaystyle\int_{\frac{t-\eta}{s}}^{\frac{t}{s}} Y^{a}e^{-Y/b}dY & \dfrac{t-\eta}{s} \le Y \le \dfrac{t}{s} \\ 0 & \dfrac{t-\eta}{s} > Y \text{ or } Y > \dfrac{t}{s} \end{cases}. \quad \text{(D3)}$$

Solving the integer above results in Equation D4, at the top of the page, where the result of the Whittaker function—WhittakerM(m, n, z)—can be obtained by solving the following differential equation: $y'' + \left(-0.25 + \dfrac{m}{z} + \dfrac{0.25 - n^2}{z^2}\right)y = 0$.

Appendix E

Derivation of Routing Probability Equation (Equation 30)

Equation 30 in the main text is derived on the basis of Black's study (1999) as well as other neuroscience findings. Brain-derived neurotrophic factor (BDNF) regulates synaptic plasticity in adults: BDNF increases the activity of N-methyl-D-aspartate receptors, increases neuron channel open probability by increasing opening frequency, and then increases the velocity of information flow travel (V) through these neuron channels. Hence, the stronger synaptic connection strength (the amount of presynaptic transmitter released and the degree of postsynaptic responsiveness) of an individual route, the greater the probability (P_i) that information flow (represented by entities) travels through that route (Ashby, Ennis, & Spiering, 2007; Black, 1999; Braus, 2004; Chklovskii, Mel, & Svoboda, 2004; Habib, 2003; see Equation E1 and Figure E1) in total U multiple routes.

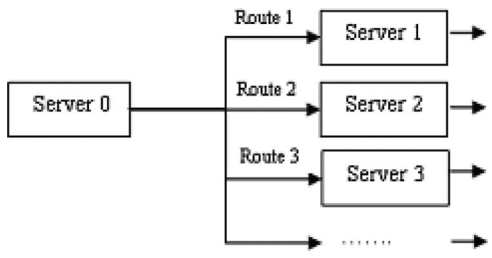

Figure E1. Multiple routes for one location in the queuing network (Server 0 has U multiple routes as output).

$$P_i = \frac{ST_i}{\sum_{j=1}^{U} ST_j}, \quad \text{(E1)}$$

where the numerator (ST_i) stands for the standardized synaptic connection strength of Route i ($ST_i \in [0, 1]$). The denominator represents the sum of the standardized synaptic connection strength of all the multiple routes starting from the original brain region (Server 0 in Figure E1). Moreover, the standardized synaptic connection strength of Route i (ST_i) is in direct proportion to the standardized velocity (V_i) that the information flow travels through that route (Black, 1999; Bullock, 1968; Chklovskii et al., 2004; see Equation E2).

$$ST_i = r_0 V_i, \quad \text{(E2)}$$

where r_0 is a parameter that stands for the ratio between ST_i and V_i.

Since the queuing network is able to capture several properties of information processing in the human brain—information flow (represented by entities) travels through different brain regions and forms brain traffic, including the possible waiting of the previous information flow to be processed (see the first assumption in

modeling the practice effect)—the travel time of the information flow (represented by entities) in Route i is composed of both waiting and processing time, and therefore, this travel time can be regarded as the sum of waiting time (W_i) and processing time (T_i) of entities, that is, sojourn time (S_i) in that route. Furthermore, this sojourn time or travel time (sum of waiting and processing time) is in inverse proportion to the standardized velocity (V_i) of the travel process (see Equation E3).

$$V_i = \gamma\left(\frac{1}{W_i + T_i}\right) = \frac{\gamma}{S_i}, \tag{E3}$$

where γ is a parameter that represents the inverse ratio between $W_i + T_i$ and Vi.

Combining Equations E1–E3, Equations E4 and E5 quantify the probability (P_i) that the information flow (entities) passes through Route i in totally U multiple routes.

$$P_i = \frac{ST_i}{\sum_{j=1}^{U} ST_j} = \frac{r_0 V_i}{\sum_{j=1}^{U} r_0 V_j} = \frac{r_0\left(\frac{\gamma}{S_i}\right)}{\sum_{j=1}^{U}\left[r_0\left(\frac{\gamma}{S_i}\right)\right]} = \frac{1/S_i}{\sum_{j=1}^{U}\frac{1}{s_j}}. \tag{E4}$$

Thus, we have

$$P_i = \frac{1/S_i}{\sum_{j=i}^{U}\frac{1}{S_j}}. \tag{E5}$$

Appendix F

Development of the Equations of Stimulus-Lateralized Readiness Potential Onset Time (Equation 23)

On the basis of Figure B1 in Appendix B, the time that entities enter Server V (V_{st}) can be estimated in two conditions depending on the value of t_a ($t_a = 0$, short stimulus onset asynchrony [SOA] conditions; $t_a > 0$, long SOA conditions; see Equation F1):

$$V_{st} = \begin{cases} \max(T_{1,AP} + T_{1,B} + T_{1,C} + T_{1,F},\ SOA \\ \quad + T_{2,VP} + T_{2,A} + T_{2,C}) + T_{2,F} + T_{2,C} & t_a = 0 \\ T_{Fst} + t_a + T_{2,C} & t_a > 0 \end{cases}. \tag{F1}$$

Since V_{st} starts from the arrival of Stimulus 1 and stimulus-lateralized readiness potential onset time (*S-LRP*) starts from the arrival of Stimulus 2 (Sommer, Leuthold, & Schubert, 2001), *S-LRP* equals $V_{st} - SOA$:

$$S\text{-}LRP = \begin{cases} \max(T_{1,AP} + T_{1,B} + T_{1,C} + T_{1,F},\ SOA \\ \quad + T_{2,VP} + T_{2,A} + T_{2,C}) + T_{2,F} + T_{2,C} - SOA & t_a = 0 \\ T_{Fst} + t_a + T_{2,C} - SOA & t_a > 0 \end{cases}. \tag{F2}$$

Since $t_a = \max[(SOA^{\beta} - T_{Fst}{}^{\beta})^{1/\beta}, 0]$, Equation F2 can be rewritten into the main text's Equation 23 (see below).

$$S\text{-}LRP = \begin{cases} T_{1,AP} + T_{1,B} + T_{1,C} + T_{1,F} + T_{2,F} + T_{2,C} - SOA & \text{If } SOA < T_{1,AP} + T_{1,B} + T_{1,C} + T_{1,F} - (T_{2,VP} + T_{2,A} + T_{2,C}) \\ T_{2,VP} + T_{2,A} + 2T_{2,C} + T_{2,F} & \text{If } T_{1,AP} + T_{1,B} + T_{1,C} + T_{1,F} - (T_{2,VP} + T_{2,A} + T_{2,C}) \le SOA \le T_{Fst} \\ T_{Fst} + (SOA^{\beta} - T_{Fst}{}^{\beta})^{1/\beta} + T_{2,C} - SOA & \text{If } SOA > T_{Fst} \end{cases}. \tag{23}$$

Appendix G

Development of the Equations of Expected Reaction Time in the Response Grouping Effect

On the basis of the five possible conditions described in Figure 23 in the main text, the following sets of equations were developed to predict the expected reaction time in the response grouping effect.

Condition 1 ($T_{1,P} + T_{1,A\text{\textbar}B} + T_{1,C} > T_{2,P} + T_{2,A\text{\textbar}B} + T_{2,C}$ and $T_{1,P} + T_{1,A\text{\textbar}B} + T_{1,C} - [T_{2,P} + T_{2,A\text{\textbar}B} + T_{2,C} + T_{2,F}] \ge 0$; i.e., $DIFF \ge T_{2,F}$):

$$E(RT_{1\text{-}route}) = E(RT_1) = E(RT_2) = T_{1,P} + T_{1,A\text{\textbar}B} + T_{1,C} + T_{1,F} + GR + \max(SF_1, SF_2), \tag{G1}$$

where $T_{1,A\text{\textbar}B}$ is the processing time at Server A or B (depending on Task 1's [T1's] route), *GR* refers to the time in grouping the two responses

(*Appendix continues*)

together, and SF_1 and SF_2 are the sum of processing time of servers after Server F (e.g., Servers Y, W, and Z) of T1 and Task 2, respectively.

Condition 2 ($T_{1,P} + T_{1,A\backslash B} + T_{1,C} > T_{2,P} + T_{2,A\backslash B} + T_{2,C}$ and $T_{1,P} + T_{1,A\backslash B} + T_{1,C} - [T_{2,P} + T_{2,A\backslash B} + T_{2,C} + T_{2,F}] < 0$; i.e., $0 < DIFF < T_{2,F}$):

$$E(RT_{1\text{-}route}) = E(RT_1) = E(RT_2) = T_{1,P} + T_{1,A\backslash B} + T_{1,C} + T_{1,F} + T_{2,F} + GR + \max(SF_1, SF_2). \quad \text{(G2)}$$

Condition 3 ($T_{2,P} + T_{2,A\backslash B} + T_{2,C} > \mathrm{T}_{1,P} + T_{1,A\backslash B} + T_{1,C}$ and $T_{2,P} + T_{2,A\backslash B} + T_{2,C} - [T_{1,P} + T_{1,A\backslash B} + T_{1,C} + T_{1,F}] > 0$; i.e., $-T_{1,F} < DIFF < 0$):

$$E(RT_{1\text{-}route}) = E(RT_1) = E(RT_2) = T_{2,P} + T_{2,A\backslash B} + T_{2,C} + T_{2,F} + GR + \max(SF_1, SF_2). \quad \text{(G3)}$$

Condition 4 ($T_{2,P} + T_{2,A\backslash B} + T_{2,C} > T_{1,P} + T_{1,A\backslash B} + T_{1,C}$ and $T_{2,P} + T_{2,A\backslash B} + T_{2,C} - [T_{1,P} + T_{1,A\backslash B} + T_{1,C} + T_{1,F}] \leq 0$; i.e., $DIFF \leq -T_{1,F}$):

$$E(RT_{1\text{-}route}) = E(RT_1) = E(RT_2) = T_{1,P} + T_{1,A\backslash B} + T_{1,C} + T_{1,F} + T_{2,F} + GR + \max(SF_1, SF_2). \quad \text{(G4)}$$

Condition 5 ($T_{2,P} + T_{2,A\backslash B} + T_{2,C} = T_{1,P} + T_{1,A\backslash B} + T_{1,C}$; i.e., $DIFF = 0$):

$$E(RT_{1\text{-}route}) = E(RT_1) = E(RT_2) = T_{1,P} + T_{1,A\backslash B} + T_{1,C} + T_{1,F} + T_{2,F} + GR + \max(SF_1, SF_2) = T_{2,P} + T_{2,A\backslash B} + T_{2,C} + T_{1,F} + T_{2,F} + GR + \max(SF_1, SF_2). \quad \text{(G5)}$$

Specifically, in Ruthruff, Pashler, and Klaassen's (2001) experimental study, $T_{1,P} = T_{S,P}$, $T_{1,A\backslash B} = T_{S,A}$, $T_{1,F} = T_{S,F}$, $SF_1 = SF_S = T_{S,C} + T_{S,W} + T_{S,Y} + T_{S,Z} + T_{S,K}$; $T_{2,P} = T_{T,P}$, $T_{2,A\backslash B} = T_{T,B}$, $T_{2,F} = T_{T,F}$, $SF_2 = SF_T = T_{T,C} + T_{T,Y} + T_{T,Z} + T_{T,VO}$. On the basis of Equations G1–G5, $RT_{1\text{-}route}$ in Ruthruff, Pashler, and Klaasen's experimental study can be estimated:

Condition 1 ($DIFF \geq T_{T,F}$):

$$E(RT_{1\text{-}route}) = E(RT_1) = E(RT_2) = T_{S,P} + T_{S,A} + T_{S,C} + T_{S,F} + GR + \max(T_{S,C} + T_{S,W} + T_{S,Y} + T_{S,Z} + T_{S,K}, T_{T,C} + T_{T,Y} + T_{T,Z} + T_{T,VO}), \quad \text{(G6)}$$

where GR refers to the time in grouping the two responses together.

Condition 2 ($0 < DIFF < T_{T,F}$):

$$E(RT_{1\text{-}route}) = E(RT_1) = E(RT_2) = T_{T,P} + T_{T,B} + T_{T,C} + T_{S,F} + T_{T,F} + GR + \max(T_{S,C} + T_{S,W} + T_{S,Y} + T_{S,Z} + T_{S,K}, T_{T,C} + T_{T,Y} + T_{T,Z} + T_{T,VO}). \quad \text{(G7)}$$

Condition 3 ($-T_{S,F} < DIFF < 0$):

$$E(RT_{1\text{-}route}) = E(RT_1) = E(RT_2) = T_{T,P} + T_{T,B} + T_{T,C} + T_{T,F} + GR + \max(T_{S,C} + T_{S,W} + T_{S,Y} + T_{S,Z} + T_{S,K}, T_{T,C} + T_{T,Y} + T_{T,Z} + T_{T,VO}). \quad \text{(G8)}$$

Condition 4 ($DIFF \leq -T_{S,F}$):

$$E(RT_{1\text{-}route}) = E(RT_1) = E(RT_2) = T_{S,P} + T_{S,A} + T_{S,C} + T_{S,F} + T_{T,F} + GR + \max(T_{S,C} + T_{S,W} + T_{S,Y} + T_{S,Z} + T_{S,K}, T_{T,C} + T_{T,Y} + T_{T,Z} + T_{T,VO}). \quad \text{(G9)}$$

Condition 5 ($DIFF = 0$):

$$E(RT_{1\text{-}route}) = E(RT_1) = E(RT_2) = T_{S,P} + T_{S,A} + T_{S,C} + T_{S,F} + T_{T,F} + GR + \max(T_{S,C} + T_{S,W} + T_{S,Y} + T_{S,Z} + T_{S,K}, T_{T,C} + T_{T,Y} + T_{T,Z} + T_{T,VO}). \quad \text{(G10)}$$

Received October 25, 2007
Revision received June 2, 2008
Accepted June 3, 2008 ■